ISOCHRON METHODS FOR LUMINESCENCE DATING IN ARCHAEOLOGY

Peter Alan Clark BTech (Hons) (Bradford)

A thesis presented in part fulfillment
of the requirements of the degree of PhD

University of Glasgow

Scottish Universities Research and Reactor Centre

1994

ABSTRACT

This work aims to contribute to the solution of a problem relevant to archaeology and microdosimetry, namely the TL dating of destratified archaeological ceramics. It is apparent that museums hold a large body of archaeological material excavated from important sites during the early part of this century. Absolute dating of this corpus of material would be extremely valuable to archaeology in allowing historic hypotheses to be tested.

The background to this problem has been presented within the context of the historical development of thermoluminescence dating and of dosimetry concepts. A critical review of previously proposed strategies for dating material from unknown gamma contexts is presented, and then a general model using an isochron approach is introduced. The isochron model is then developed explicitly and theoretical simulation is used to explore different microdosimetric systems. Two main isochron solutions have been identified, the grain size (or alpha-beta attenuation) and alpha efficiency isochrons.

An experimental approach was designed, to evaluate the validity of the grain size isochron predictions, using model matrices. Isochron behaviour was clearly observed in both cases. The first system, based on microcline feldspar grains in a high dose rate matrix, produced an age estimate consistent with the known age. The second experiment, using fluorite grains in a lower dose rate matrix, produced a highly coherent data set. However, the age estimate obtained was greater than the expected value by a factor of approximately 3. The possible reasons for this are discussed in detail. A brief experiment carried out subsequently on duplicate portion of this matrix gave results that are consistent with predicted values. Thus, it would appear that the original experimental design and method were valid and that the isochron approach does indeed deserve further investigation.

ACKNOWLEDGEMENTS

I owe the biggest debt of all to my family for their never-ending love and support that has always given me the opportunity and strength to "keep at it".

Thanks to Jenny for the happy days.

To the members of "The Group", the "Cave People", and friends old and new who have helped me cope with "the view from the hill" - THANKS and SLÀINTE MHATH !

For "musical therapy" I must thank Boots for being Darker Than Blue, and DD for the Fish - Long Live The Jester!

This research was funded by an Instant Award from the Science and Engineering Research Council.

TABLE OF CONTENTS

List of Tables

List of Figures

1.INTRODUCTION

1.1 INTRODUCTION

This thesis outlines and evaluates a general isochron formulation of thermoluminescence (TL) dating and discusses the extent to which this may contribute to overcoming some of the limitations of current techniques. An introduction to the general problem being considered is followed by a review of the basic principles and historical developments of TL dating. The manner of formation of the isochron approach is then given before the details of the experimental verification are described. A summary of the approaches employed in this research is presented with a discussion of the results obtained and their relevance to archaeological applications and dating methodologies. Areas for further research are identified.

The development of archaeological studies towards a more scientific approach has lead to diversification into a multidisciplinary subject within which there is an ever growing number of specialist areas. Subjects such as artefact analysis, the study of environmental change, social, economic, and technological development, field archaeology and many others covered by the term archaeology, or archaeological sciences, are all linked by a common interest. This is usually "How old is it?", "When did it happen?" or perhaps some other variation along these lines. This is because one of the most fundamental requirements for archaeological studies is a reliable chronological framework.

Several dating techniques, developed for the geological sciences, find some measure of application to archaeological problems. However, the great differences in the timescales involved means that, especially for radiometric methods, only the oldest periods of archaeology can be considered. There is always room for optimism, for example while dates have been obtained by conventional $^{40}K/^{40}Ar$ methods for the early hominid period (Michels, 1973) the development of an $^{40}Ar/^{39}Ar$ method may have the potential to date younger samples (Miller, 1970).

Some of the dating techniques which have been useful to geology are not generally

applicable to archaeological dating problems and so more specific methods were developed. These included dendrochronology, archaeomagnetism, radiocarbon, and hydration layer dating, for example. A useful summary of scientific dating techniques in archaeology is provided by Aitken (1990). It is not of particular relevance to discuss them in any detail here except to highlight some of the common drawbacks that they all suffer from to varying extents. These are the problems of the availability of suitable sample material (and in sufficient quantities) from the site and also the association of the sample within the archaeological context with respect to the relevance of the event being dated and the subsequent interpretation of the date.

The advantages and limitations of the TL method for dating archaeological samples will now be examined with reference to the points made above. The types of material datable by this technique, ceramics, burnt stones and sediments, are ubiquitous on many archaeological sites so the problem of insufficient amounts of material is unlikely to occur. The lifetime of use of a ceramic vessel is likely to be short compared to its archaeological age, so the event being dated, the firing of the pottery, is relevant. It must be noted, however, that the stratigraphic credentials of the context providing the samples must be ensured as there is always the possibility of residual material giving rise to conflicting dating evidence. The TL dating of burnt stone material, hearth stones for example, gives the date of the last heating of the stones and therefore the last use of the hearth. This is obviously an important event since it is very likely to signify the last date of occupation at that particular location. More recently developed applications of the technique in the area of dating unburnt sediments may allow site formation processes to be investigated. Thus the nature of materials suitable for TL dating and their archaeological interpretations within their contexts are substantial assets of the technique.

Despite these favourable aspects there are a number of limitations to TL dating. Apart from the technical challenges of efficient sample preparation and accurate measurement, a further problem is the current necessity to make on-site environmental radiation measurements although others, such as precision, cost, the possibility of hidden systematic errors (microdosimetry and fading), may also be important. The absence of

these measurements means that part of the age equation is unknown and so the dating accuracy is limited. It follows then that material that has already been removed from its original context, museum held collections for example, is also inaccessible to the method.

At this point it is worth making the distinction between destratified and unstratified samples. The former are taken as being those samples that have been deliberately removed from their archaeological contexts and as such may have some level of information pertaining to that context associated with them. Unstratified samples, however, are regarded here as being isolated, often surface, finds with no associated contextual information. They therefore normally have limited potential to provide any significant contribution to our understanding of the past. Destratified samples could include material from archaeological excavations that have already taken place that did not include a programme of TL dating in the planning of the research strategy. If this type of material became datable then it may be likely to assume increasing importance in the future since sites and funding for new archaeological excavations are both limited resources.

Similarly, if material from museum collections became accessible to reliable absolute dating this would open many interesting avenues of research. Given sufficient precision it would be possible to assess traditional age estimates, derived by archaeological means, from major ceramic assemblages without reference to traditional assumptions. On a wider scale this has implications for testing archaeological models of development of material culture, which despite increasing levels of sophistication and complexity , nonetheless retain key concepts from the nineteenth century three age system of Thomsen and Worsaae. Bintliff (1984) warns of the ever present danger "...that insufficient care is taken to validate such models against the complexities of the data; and at the worst, stage schemes of ... development are supported by reference to other theoretical work rather than constantly being tested against case studies. ". Absolute dating provides a fundamental means of conducting such case studies, and therefore can be regarded as having a significant methodological contribution to make to contemporary archaeology.

One particular area of interest here is that of the problem posed by typological sequences of pottery. The early archaeology of the nineteenth century, and earlier, was in the main carried out by antiquarian "barrow-diggers" who effectively plundered archaeological sites for their riches. Apart from recovering impressive amounts of gold and silver, these activities also removed a significant proportion of the "best" (that is, most complete) finds from their archaeological contexts. Some of this material, such as funerary urns, was arranged into typological sequences on the basis of vessel form and complexity of decoration. The intervening decades have in some cases seen these typological sequences become generally accepted as chronological sequences with little or no supporting evidence to justify such a transformation. It seems that these developments of diversity in pottery styles, for example, are often seen as only taking place in a single dimension, that of time, with the possibility of a contribution due to spatial variations receiving little attention. The validity of this type of assumption is obviously of prime importance to the interpretation of artefactual material that has been, and still is, "dated" by comparative study of these early collections held in museums. It is also a problem that could offer suitable sample material for TL dating but cannot be dated by current techniques due to the destratified nature of these sample.

The aims of this research are to investigate an isochron method of TL dating that will allow material to be dated that is currently inaccessible to routine techniques. Some areas of the possible archaeological applications have been mentioned above, but it is also important to note that this work also tests the single phase microdosimetric assumptions common to all TL dating which will be discussed in Chapter 2. A brief note on the principles of TL dating is given now followed by an account of the historical developments within the subject, leading to an introduction to TL dating.

1.2 INTRODUCTION TO THERMOLUMINESCENCE

Thermoluminescence is the emission of light from an insulator or semiconductor when it is heated. It is not the light spontaneously emitted from a substance when it is heated to incandescence. Thermoluminescence is the thermally stimulated emission of light following the previous absorption of energy from radiation.

There are three essential requirements for the production of thermoluminescence. Firstly, the material must be an insulator or a semiconductor, metals do not exhibit luminescent properties. Secondly, the material must have at some time absorbed energy during exposure to radiation. Thirdly, the luminescence emission is triggered by heating the material. Once heated to excite the light emission, the material cannot be made to emit thermoluminescence again by cooling the sample and reheating. In order to re-exhibit the luminescence the material has to be re-exposed to radiation, after which, heating the sample will again produce light.

Luminescence emission is explained by the transfer of energy from radiation to the charge carriers of the solid, exciting the electrons from a ground state to an excited state. The emission of a luminescence photon takes place when an excited electron returns to its ground state. An excited electron can also become trapped at a metastable energy level between the ground and excited states where it will remain until it is given energy to return to the excited state from where it can undergo a normal transition back to the ground-state. This excess energy required is called the trap depth. Thus, thermoluminescence is a process by which electrons are released from traps by thermal stimulation to produce light emission.

1.3 HISTORICAL DEVELOPMENTS

Investigations into luminescence and related phenomena have been reported since the seventeenth century, following on from the "observations of a diamond that shines in the dark" (Boyle, 1664). The early application of TL was largely confined to geological use as a method of mineral identification (eg Deribere, 1938). These studies were greatly facilitated by the technique of measuring the TL as glow curves, ie plots of the light output as a function of temperature, or time, during sample heating. This method was originally developed by Urbach (1930) and modified by Randall and Wilkins (1945) and used by them in studies relating phosphorescence and TL to determine the relationship between TL glow shape and trap depths.

In the following years a wide range of new applications of TL were studied, particularly

at the University of Wisconsin (Daniels *et al*, 1953). Here, the potential of TL radiation dosimetry, ie where the intensity of the TL output is proportional to the ionising radiation dose received, was being evaluated alongside the continued use in a geological context for the identification of minerals, differentiation of particular strata based on distinctive glow curve shapes, and the study of the TL from a large number of rocks. The spatial heterogeneity of the TL of rocks was demonstrated by this group by photographing samples during heating. This was also an important observation for archaeological studies as similar results were later obtained for pottery slices (Fremlin and Srirath, 1964).

At this relatively early stage of development of the subject it was thought that the prime source of the trapped electron population was the alpha particles from trace amounts of uranium and thorium and that these alpha particles were responsible for trap creation and hence the growth of TL signals and sensitivity with time. This lead the Daniels group to postulate that given certain limitations and assumptions it should be possible to estimate the date at which rocks and ancient pottery were last heated to high temperatures.

The suggestion of a method of dating ancient pottery by TL was initially followed up by the Universities of California (Kennedy and Knopff, 1960) and Bern (Grögler et al, 1960). The latter group identified, as had Daniels *et al* earlier, that the low temperature TL peaks present in the glow curve after artificial irradiation of a sample were unstable and therefore not present in the natural glow curves. It was also shown that by annealing an artificially irradiated sample before measurement the glow curve produced was of almost the same shape as the natural curve.

In the early 1960's the Oxford group critically examined the suggestion by Daniels *et al* (*op cit*) of trap creation by alpha bombardment being a suitable basis for a method of age determination and found it to be impractical on the grounds that "damage-traps" were indistinguishable from those initially present (Tite and Waine, 1962). In any case, it was later concluded that for archaeological samples the percentage increase in the number of high temperature traps since firing was less than 1% ie that over an

archaeological timescale the number of traps was effectively constant. The observations of supralinearity of TL response with beta dose and enhanced sensitivity that were originally thought to also result from trap creation were later reinterpreted as being due to competition between different types of trap (Tite, 1966, 1968, Aitken, 1968). Not only did the Oxford group identify that a dating method based on the filling of traps was the way forward but also recognised and investigated several other important factors. Despite improvements to instrumentation (eg the heating system which had been identified as a major source of inaccuracy and in the detection system where the selection of optimum filters reduced the interfering signals from blackbody radiation) an initial dating programme gave poor results suggesting that the method based on the measurement of the number of traps filled showed only a rough age dependence.

One of the most significant advances was the observation that if a sample was glowed in a nitrogen atmosphere, instead of in air, then a sample of zero age would produce zero TL, an essential requirement for a successful dating technique (Tite and Waine, 1962). This procedure had the effect of suppressing the non-radiation induced "spurious" signals that had been attributed to the effects of grinding and gas adsorption and had previously been a prime cause of concern (Tite and Waine, *op cit* , Aitken *et al*, 1963, 1968, Lewis, 1968).

Further refinements in the techniques of sample preparation were adopted after the effect of optical bleaching of the natural TL signal of stored aliquots of samples was observed (Aitken *et al*, 1963). It was found that, for the particular sample studied, all wavelengths were found to reduce the TL signal across the whole temperature of the glow curve by varying amounts. It was consequently concluded that samples should be handled in semidarkness. A second dating programme was carried out at this time incorporating the modifications noted above. The results obtained were far more encouraging with strong evidence for a linear relationship between the age of the sample and its specific TL. For the first time absolute ages could be calculated since the TL susceptibility had been measured with a calibrated beta source. In comparison to the "known" archaeological ages the TL ages were low by a factor of five.

Experimental work (Fremlin and Srirath, 1964, Fremlin, 1968, Srirath and Fremlin, 1968) regarding the spatial homogeneity of the TL characteristics of pottery showed that the main luminescence was often confined to a small or moderate number of well-defined crystals. This supported the idea that this could be one of the possible reasons for the low ages obtained by Aitken et al since it was also a possibility that the concentrations of radioactivity, as well as the luminescent regions, were non-uniformly distributed.

The situation was further complicated when, in the light of earlier work (Moorehead and Daniels, 1957), the relative efficiency at trap filling of alpha particles compared with beta and gamma radiation was considered, and found to be about an order of magnitude less effective. Taking this into account, the ages from the test programme were recalculated and although found to be in closer agreement with the archaeological ages they were not yet sufficiently close to be regarded as being accurate.

The evidence of reduced alpha efficiency increased the potential impact of the aforementioned spatial heterogeneity. The implications were not only that separated mineral fractions should be examined, but also that since the alpha contribution to the effective dose rate to the sample had been substantially reduced the beta and gamma dose rates became more important. The assumption that the sherd and soil had the same radionuclide concentrations became more significant so that the need arose for its measurement in both, rather than just the sherd. Approaches to overcome this problem of dosimetry were suggested by the results of Fleming (1966) which showed that while the radioactivity was predominantly concentrated in the clay matrix, it was the crystalline extract that gave the greater light output. The conclusion was that large quartz grains would not be affected by the short range, inefficient, alphas and hence receive only a beta plus gamma dose. Additional consideration of the ranges of betas and gammas led to the formulation of the "quartz inclusion" method which employed a separated quartz fraction of 100-200μm grains for which the alpha contribution is negligible and so the annual dose consists only of the beta dose from radioactivity within the sherd, the gamma dose from the surrounding burial soil and small contribution from cosmic rays (Aitken *et al*, 1968). A preliminary test of this method

(Fleming, *op cit*) gave absolute ages that were all within 20% of the "known" ages, thus giving strong support for the validity of the assumptions made.

An alternative approach employing the fine grains, 1-8μm, from the sherd was also suggested (Zimmerman, 1967). Grains of this size would have suffered negligible attenuation of the alpha dose and received full sherd beta and soil gamma doses. The introduction of the alpha dose into the age equation and its low efficiency to produce TL required the alpha efficiency to be measured for each sample. The results of a test programme of this method were also highly encouraging, providing further confirmation that the techniques used and the principles involved were valid (Aitken *et al*, 1968). These two approaches were soon consolidated into established dosimetric models (Fleming, 1970 and Zimmerman, 1971).

The observation of dose dependent sensitivity changes in the 110°C peak of quartz (Fleming and Thompson, 1970) led to the subsequent formulation of the "predose" method of dating (Fleming, 1973). Here the change is dependent on the previous irradiation history of the sample. The dosimetry does not involve the direct measurement of the stored TL due to the exposure dose but requires the measurement of the change in sensitivity produced by that dose. The particular advantage of this method is high sensitivity, allowing young samples (within the last 1000 years) to be dated. Its drawbacks are early saturation, a complex and poorly understood mechanism, diverse behaviour from real samples and an increasingly involved methodology. This includes additional measurements to correct for radiation quenching (Aitken and Murray, 1976; Aitken, 1979), problems caused by non-linearity due to saturation effects and investigation of the thermal activation characteristic (TAC) (Fleming and Thompson, 1970; Bailiff, 1983a). The predose method has been successfully applied to the authenticity testing of art ceramics etc. (Fleming, 1979 and Archaeometry) and promising results have been obtained from archaeological material (Bailiff, 1983b, 1985).

Another approach explored to overcome the problems associated with high temperature TL, especially when the signals are small, was that of the phototransfer technique

(Schlesinger, 1965). In this case, if a sample is illuminated with ultra-violet light prior to measurement then some of the electrons from the deeper ("donor") traps are evicted some of which become retrapped in shallower ("acceptor") traps. The method of phototransferred TL (PTTL) has also been suggested as a means to overcome anomalous (short term) fading in zircons (Bailiff, 1976). Despite the potential advantage of enabling the dating of materials such as arragonite, that changes its structure to calcite on heating during high temperature glow curve measurement, the extremely complex behaviour of PTTL (Bowman, 1979) seems likely to prevent it from becoming a routine method of dating.

Once the dosimetric models had been established, mainly by the Oxford group, their use and development spread to other laboratories. The Riso laboratory in Denmark, for example, developed feldspar inclusion methods. Their dating programme included samples of pottery sherds, bricks, burned stones, and burned clay that were measured using an automatic TL reader (Mejdahl, 1972). The development of the automatic TL system was regarded as being an essential step towards large scale routine dating programmes. The widescale acceptance of feldspar inclusions as suitable minerals for TL dating was hampered by the early observation of short term ("anomalous") fading of the TL signal of feldspars of volcanic origin (Wintle, 1973). However, a great deal of work has since been carried out (particularly in Denmark) to exploit the advantages of feldspars (greater brightness, higher internal radioactivity, greater reproducibility, etc.) over quartz (Guérin and Valladas, 1980; Mejdahl and Winther-Nielsen, 1982; Mejdahl, 1983; Sanderson *et al*, 1988). The latter work, on vitrified forts, being the first UK feldspar dates, after the quartz had been shown to have severe supralinearity of dose response. The technique of feldspar inclusion dating is now standard practice within the Riso and SURRC laboratories (Sanderson and Clark, 1987).

The seventies saw great diversification and development of methods to include non-ceramic materials of both archaeological and geological interest. A review article by Wintle (1980) provides a useful account covering burnt stones (including flint), volcanic lavas and associated burnt sediment margins, calcite, bone and shell to varying degrees of success.

Perhaps the most significant development was the potential to date unburnt sediments. Wintle and Huntley (1979) described a study of the zeroing effect of exposure to sunlight during weathering and transport, which followed on from work in the USSR (eg Morozov, 1968; Shelkoplyas, 1971 and others) and China (Li *et al*, 1977). The technique was rapidly developed to allow the direct dating of loess (wind blown sand) deposits (Hütt *et al*, 1979, Wintle, 1981). The observation of a "residual signal" (ie TL signal present in a zero age sample) that was not removed by sunlight exposure, and the fact that there maybe a sensitivity change after the first glow measurement, required modification of the methods used to determine the stored dose (Mejdahl and Wintle, 1984). These factors plus the realisation that a thermal approach to releasing the charge stored since the sunlight zeroing event may not necessarily be appropriate were the motivation behind a new research field. This was the optical dating of sediments, first reported by Huntley *et al* (1985), where the stimulating energy was provided by an argon-ion laser. The majority of this work has been carried out using monochromatic or broad band continuous light sources and there is a need for fundamental spectroscopy. However, optically stimulated luminescence had previously been reported in a dosimetry context (Rhyner and Miller, 1970) and photostimulated thermoluminescence (PSL) had been used to study the nature and properties of traps and centres in alkali halides (Fieschi and Scaramelli, 1968). Recent developments in this field include ongoing research at the SURRC laboratory involving analyses of PSL spectra and investigations of charge relaxation mechanisms through time domain studies. The use of light emitting diodes as an alternative, and cheaper, light source has also been suggested (Poolton and Bailiff, 1989, Aitken and Xie, 1991). These experimental developments have corresponding advances in the theoretical and methodological aspects and their applications. This does not mean that the interest in the more "traditional" areas of TL (archaeological/geological dating, dosimetry, models, spectral studies etc) and associated phenomena (phosphorescence and electron spin resonance etc) has waned at all. The current state of luminescence studies is readily witnessed by the breadth and depth of contributions presented at recent UK and International Specialist Seminars.

Some of the aspects introduced in the last section will be dealt with again, but in greater detail, later in the thesis. At this point, however, it is appropriate to include a concise

introduction to TL dating (with specific reference to archaeological ceramics).

1.4 TL DATING : BASIC REQUIREMENTS AND AGE EQUATION

The requirements of any absolute dating method are a measurable parameter that varies with time (preferably in a linear fashion), a start mechanism, and a means of calibrating the stored signal. These are examined below (after Wintle, 1980 and Bailiff, 1988). The phenomenon of TL provides such a basis; under the influence of ionising radiation a TL sensitive material stores a fraction of the energy imparted. The energy storage is finite and the process of energy acquisition within this storage system is cumulative. For a number of types of material (though not all) the storage is stable over archaeological time. The driving force of this particular dating mechanism is ionising radiation. This results from the decay of the naturally occurring radioelements, uranium, thorium and potassium 40, which produce a radiation field of alpha, beta, and gamma rays. The half-lives of these radioisotopes are sufficiently long that over archaeological and recent geological timescales they provide an effectively constant dose rate. This assumes that the system is in a state of radioactive equilibrium.

The start mechanism in TL dating is the zeroing event by which all previously stored energy is removed. There are a number of zeroing mechanisms for TL, eg heating to high temperatures in the case of the firing of pottery or the repeated heating of the stones of a hearth; exposure to sunlight for aeolian sediments; or crystallisation eg calcite formation. After the zeroing event has taken place the development of the TL signal recommences and (generally) continues in a linear fashion until the next zeroing event eg measurement in the laboratory. Under these conditions the basic TL age equation can be written as :-

$$\text{TL Age (yr)} = \frac{\text{Stored Dose (Gy)}}{\text{Dose Rate (Gy/yr)}} \qquad (1.1)$$

This is a very simplified view and in practice this equation has to be modified to take into account aspects of microdosimetry (Chapter 2) that will then allow practicable solutions to be achieved. The next two sections will look at the ways in which the stored dose and dose rate components of this equation can be evaluated.

1.5 STORED DOSE EVALUATION

The simplest approach to evaluation of the stored dose is to measure the natural TL signal on the first heating of an aliquot of mineral grains extracted from the sample, and to then compare it with subsequent TL response from the same aliquot after being exposed to a known radiation dose from a laboratory source. This procedure, however, is not commonly used because of possible changes in TL sensitivity associated with the first glow heating event. These can be caused by changes in the transparency of the grains due to heating or the activation of the pre-dose effect (mentioned earlier, section 1.3). An additional complication is presented by the possibility of supralinear growth of the TL response to dose in the initial low dose region.

To overcome these detrimental aspects a method of standard addition is used. Successive aliquots of the sample are given incremental calibrated radiation doses on top of their previously stored natural dose. Each aliquot is measured and the TL intensity values from the series of glow curves are used to construct an additive growth curve of the first glow response at doses above the natural level. The same aliquots can then be reirradiated, preferably in reverse order so that each will have received an equal pre-dose thereby minimising any interference from the pre-dose effect, and glowed out to give a second glow growth curve which provides the best available reconstruction in the low dose region. This method is illustrated in Figure 1.1

The stored dose is taken as the sum of the dose intercepts reconstructed from normalised plots of the first and second glow growth curves. This assumes that the supralinearity intercept obtained from the second glow measurement has not been changed by the first glow heating.

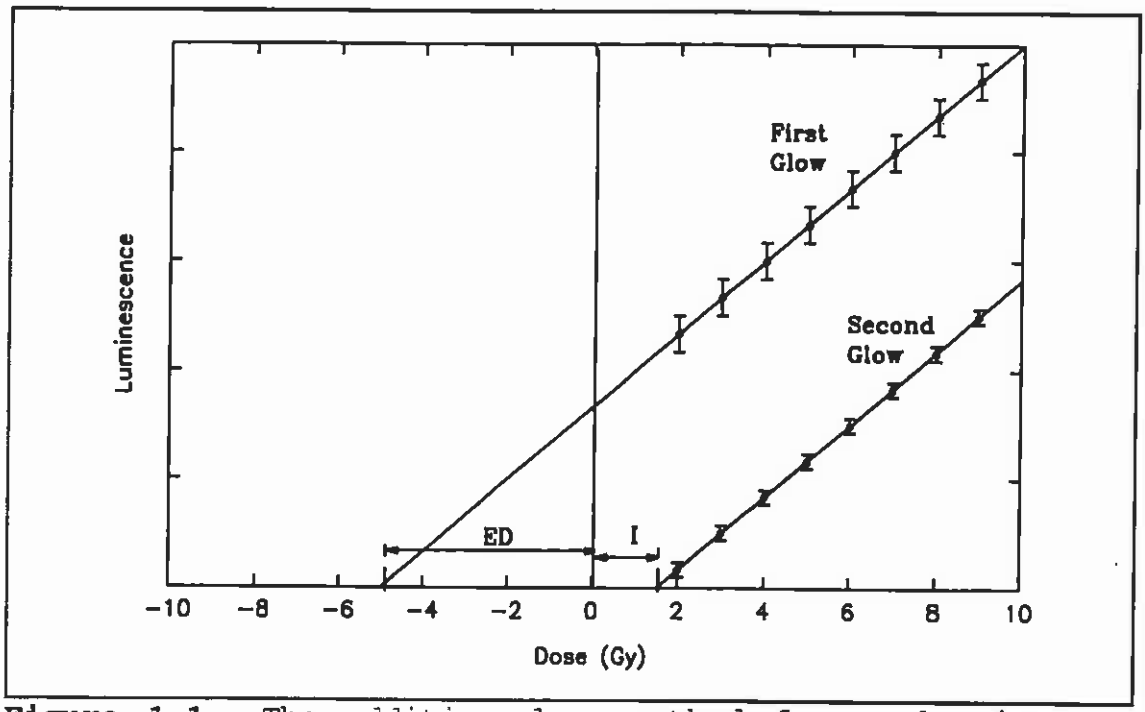

Figure 1.1 The additive dose method for evaluating the stored dose. The equivalent dose (ED) and second glow intercept (I) are evaluated by regression analysis. The stored dose is given by ED + I.

An obvious requirement for reliable stored dose evaluation is that the measurements should only consider stable signals and that these should be identifiable. This led to the development of the "plateau-test" (Aitken, 1974) in which a plot of the ratio of a natural TL curve to an artificially induced curve as a function of temperature is produced. The plateau region was then identified as being the temperature range over which the TL signals were regarded as being stable. Although desirable, the presence of a flat plateau is not an essential prerequisite for satisfactory dating. Fleming (1979) quotes such an example, where the stored dose plateau condition is not met but due to a rapid change of alpha efficiency with temperature an "age-plateau" analysis provides evidence for the validity of the TL age determination. McKeever (1985) has shown that for second-order kinetics stability can be achieved without a plateau; Sanderson (1982, 1983) has demonstrated that the presence of a plateau does not lead automatically to stability.

The observation of short term ("anomalous") fading in the high temperature regions of glow curves of some minerals (eg Wintle, 1973) and the subsequent investigations of

this phenomenon (Sutton and Zimmerman, 1978; Templer, 1985 and Visocekas, 1985) has made the inclusion of short term fading tests an essential part of any TL dating programme (Sanderson, 1988, Templer, 1986, Clark and Templer, 1988, Stoneham, 1987).

1.6 DOSE RATE EVALUATION

This section will act as an introduction to the fuller treatment of dosimetry to be found in Chapter 2. This is deemed necessary because of the large number of inter-related variables that influence the radiation dose rate that is experienced by the constituent parts of a sample. The main sources of ionising radiation that provide the dose rate to the sample are uranium and thorium with their decay products, and potassium and to a lesser extent rubidium and cosmic rays. The dose rate can be divided into alpha, beta, gamma and cosmic components for the following reasons:

(i) because variations in U, Th, K content change the relative proportions of alpha, beta and gamma from sample to sample,

(ii) because of the relative inefficiency of alpha particles for producing TL, compared to the other types of radiation,

(iii) because of their different ranges and in relation to both large and small scale inhomogeneities of radioactive content for example between soil and sample, and the clay matrix and mineral inclusions,

(iv) and because of differences in mass absorption coefficient and stopping power mean that one material may absorb more energy than another. This latter point can be usefully illustrated by consideration of the water content of the pottery and the soil since the dose received by particular grains depends on the amount of water present in the sample and its surroundings and also on the type of radiation involved (Zimmerman, 1971).

The wide range of possible techniques that can be used to evaluate dose rates is outlined here;

(i) alpha counting - this is a scintillation technique that can be used to obtain alpha,beta, and gamma dose rates based on work in the health physics field by Turner, Radley and Mayneord (1958).

(ii) beta counting - also a scintillation technique, this allows rapid and accurate beta dose rate determination, but gives no information as to the relative contributions from uranium, thorium and potassium (Sanderson, 1988).

(iii) TL dosimetry - uses very sensitive TL phosphors (CaF_2 or $CaSO_4$) to record natural beta dose rates from pottery but is labour intensive and may involve inconveniently long exposure periods (Bailiff and Aitken, 1980 and Bailiff, 1982), also extensively used to measure the *in situ* environmental gamma dose rate. The technique is not readily applicable to alpha dosimetry on account of the short range of alphas, their low efficiency for TL production, and the difficulty in matching the alpha stopping powers of phosphor and matrix.

(iv) gamma spectroscopy - two main types, firstly, laboratory based high resolution instruments that enable uranium and thorium series disequilibrium to be investigated (Murray and Aitken, 1988). The main drawbacks here are cost and potential methodological problems. The second type is the portable NaI gamma spectrometer used for on site measurement of the environmental gamma dose rate. The short measurement period could perhaps be regarded as problematical in that seasonal variations will not be taken into account as is the case for gamma TLD capsules. This should be borne in mind although each site will be different and in any case it may well be that the longer term

variations (ie over archaeological timescales) are of more significance and also more difficult to quantify. Meakins *et al* (1979) have also used NaI gamma spectrometers to measure U, Th, K for dose rate determination in sherds and soils.

(v) reactor based methods - Neutron Activation Analysis (NAA) requires access to reactor and counting facilities but is suitable for the levels of U, Th, and K commonly found in archaeological samples. The parent members of the U and Th decay series are quantified so no information is obtained regarding their state of equilibrium. Fission track mapping is useful since it can provide information about the concentration **and** the spatial distribution of uranium and thorium.

(vi) Inductively Coupled Plasma Mass Spectroscopy - ICPMS, a technique suitable for stable and long-lived isotope analysis, but not ^{40}K as this suffers interference from the carrier gas, Ar. A further complication is that usually the samples have to be presented in solution (2% HNO_3).

(vii) K analysis - in addition to those methods outlined above, flame photometry has perhaps been the traditional approach although there are also references to the use of atomic absorption and x-ray fluorescence for the same purpose.

The practical application of some of these techniques will be more fully explored in the next chapter where they will be linked with the measurement of stored dose to describe the specific strategies that have been formulated into particular TL dating methods, in relation to their dosimetric parameters.

1.7 SUMMARY

This chapter has introduced the subject of this thesis, namely the recognition of a need to able to date archaeological material that has already been removed from its burial context. Absolute dating of this corpus of material would be extremely valuable to archaeology in allowing historic hypotheses to be tested. The historical developments of luminescence dating studies have been discussed and the elements of TL dating introduced to provide a background for the subsequent chapters.

2.DOSIMETRY

2.1 INTRODUCTION

This chapter examines the sources and characteristics of the natural radiation field that provide the dose experienced by the TL sensitive mineral grains since the zeroing event. From Equation 1.1 it is clear that to be able to quantify the time elapsed since this zeroing event it is necessary to determine the radiation dose responsible for the natural TL signal and to evaluate the effective natural dose rate to the particular TL phase being measured. This more detailed account of pottery dosimetry is necessary because of its complexity and its fundamental importance, as the denominator in the age equation, to TL dating systems.

The approach will be first to introduce some dosimetry concepts and then to develop them with particular reference to pottery dosimetry. It will then be shown how routine dating techniques have been formulated to enable solutions to the TL age equation to be found, the limitations of these methods, and possible approaches to overcoming them.

2.2 BASIC DOSIMETRY DEFINITIONS

This section sets out some basic definitions of dosimetry terms that are used in this thesis (after Horowitz, 1984).

2.2.1 Energy Imparted

The energy imparted by ionising radiation to matter, E, in a volume is a stochastic quantity which is the difference between the sum of the energies (excluding rest energies) of all the directly and indirectly ionising particles that have entered the volume (ΣE_E) and the sum of the energies (excluding rest energies) of all those that left it (ΣE_L), minus any energy that is generated within the volume (ΣE_R) Unit: Joule(J)

$$E = \Sigma E_E - \Sigma E_L - \Sigma E_R \qquad (2.1)$$

2.2.2 Absorbed Dose

Absorbed dose, D, is defined as the mean energy imparted (dE) by ionising radiation per unit mass of material. Unit: $J.kg^{-1}$, the Gray, Gy.

$$D = \frac{dE}{dm} \tag{2.2}$$

2.2.3 Stopping Power

The quotient dE/dx is the linear stopping power, S, of a material for charged particles of energy, E. The energy loss has two principle components, those due to collision and those due to radiative losses.

$$S = \left(\frac{dE}{dx}\right)_{coll} + \left(\frac{dE}{dx}\right)_{rad} \tag{2.3}$$

The mass stopping power, S/ρ, is obtained by dividing the linear stopping power by the density, ρ, of the material.

2.2.4 Charged Particle Equilibrium

Charged particle equilibrium (CPE) is an important concept in gamma dosimetry. CPE is said to exist when the energy fluence of incoming and outgoing electrons at the boundary of a specified volume element is exactly equal.

2.3 INTRODUCTION TO RADIOACTIVITY

A nuclide is a particular type of atom that is specified by the total number of protons and neutrons (Atomic Mass Number, A) in its nucleus. The number of protons present

in the nucleus (Atomic Number, Z) defines the atomic element. Isotopes are different nuclides of the same element and have the same number of protons but a different number of neutrons in the nucleus.

Although most naturally occurring nuclides are stable, there are some that are not. The stability of a nucleus is determined by the numbers of neutrons and protons,their configuration and the binding energies involved. This can be seen from a plot of number of neutrons, N, against number of protons, Z, in the nucleus (a Segre chart), which shows that for $Z \leq 20$ the stable nuclides have $Z \approx N$, but at higher Z values $N > Z$. Nuclides that disintegrate, to form new nuclides, by the emission of energy are termed radionuclides. The energy released can be calculated from the difference between the masses of parent and daughter nuclides and decay products.

2.4 RADIOACTIVE DECAY LAWS

Radioactive decay is a random process. Among the atoms in a sample undergoing decay it is not possible to identify which specific atom will be the next to decay. The decay rate (the activity, A) is a measure of the number of disintegrations per unit time. The unit is s^{-1} (Becquerel, Bq).

$$A = -\frac{dN}{dt} \tag{2.4}$$

The decay rate is proportional to the number of radioactive atoms, N, present ($A \propto N$). If the number of radioactive nuclei and the number of decays per unit time are sufficiently large to allow statistical treatment, then

$$-\frac{dN}{dt} = \lambda N \tag{2.5}$$

λ is the decay constant. It represents the probability, per unit time, of radioactive decay. The general equation for simple radioactive decay can be obtained by integration.

$$N = N_0 e^{-\lambda t} \tag{2.6}$$

N_0 is the number of nuclei present at the start time, $t = 0$.

This decay is exponential and since $A \propto N$, the activity of a sample is also reduced exponentially with time.

$$A = A_0 e^{-\lambda t} \tag{2.7}$$

A_0 is the initial activity. The specific activity (activity per unit mass, A/m) of a sample is similarly time dependant and also proportional to the concentration of the radionuclides. The unit is $Bq.kg^{-1}$.

The decay constant, λ, is radionuclide specific and is essentially unaffected by pressure, temperature or chemical form. This means that radionuclides can be characterised by their period of decay. This is expressed in terms of the half-life, $t_{\frac{1}{2}}$, the time taken for the number of radioactive atoms in a sample (and therefore its activity) to decrease to half of an initial value. The relationship between the decay constant and the half-life is

$$t_{\frac{1}{2}} = \frac{\ln 2}{\lambda} \tag{2.8}$$

Series decay occurs when a parent radionuclide decays to a daughter product that is also unstable. The net rate of formation of the daughter atoms is the difference between the rate of formation of the daughter and its decay.

$$\frac{dN_2}{dt} = N_1\lambda_1 - N_2\lambda_2 \tag{2.9}$$

N_1 and N_2 are the number of parent and daughter atoms and λ_1 and λ_2 are the decay constants of the parent and daughter, respectively.

In certain cases, where the half-life of the parent is very much longer than that of the daughter, the condition of radioactive (secular) equilibrium may be achieved. This is where the rate of decay of the daughter is equal to the rate of decay of the parent.

$$N_2\lambda_2 = N_1\lambda_1 \tag{2.10}$$

2.5 MODES OF RADIOACTIVE DECAY

The principle modes of radioactive decay are alpha and beta decay with associated gamma emissions.

Alpha decay involves the release of helium nuclei, ${}_2^4He$

$$ {}^{A}_{Z}X \rightarrow {}^{A-4}_{Z-2}X + {}^{4}_{2}He + Q \tag{2.11}$$

where X is the parent nucleus, Y the daughter nucleus and Q the energy release. The alpha particles emitted are monoenergetic for a given decay and therefore they characterise the particular decay.

The term beta decay can cover a number of processes, these are outlined below.

(a) Electron, or negatron, (β^-) emission. This is equivalent to one of the neutrons in the parent nuclide becoming a proton with the emission of a negative electron, β^-, and an antineutrino, ν

$$^{A}_{Z}X \rightarrow {}^{A}_{Z+1}X + {}^{0}_{-1}\beta + \bar{\nu} \qquad (2.12)$$

(b) Positron (β^+) emission. Here a nuclear proton is transformed into a neutron with the emission of a positive electron, β^+, and a neutrino, ν

$$^{A}_{Z}X \rightarrow {}^{A}_{Z-1}X + {}^{0}_{+1}\beta + \nu \qquad (2.13)$$

(c) Electron capture. This is where an electron from the inner (K or L) orbitals of an atom is captured by the nucleus. The vacant position is subsequently filled by an outer electron with corresponding emission of K or L x-rays, or low energy (Auger) electrons.

Unlike alpha particles, beta particles are emitted with a continuous spectrum of energies up to a maximum value that is determined by the energy equivalent to the change in mass involved in the nuclear transformation. The energy released is shared between the beta particle and antineutrino (no charge and negligible mass) in varying proportions which gives rise to a continuous energy spectrum. Beta particle energy is therefore not diagnostic of the species involved.

Alpha and beta decay can leave the daughter nucleus in an excited state. The excitation energy can be removed by gamma ray emission or through internal conversion. The excited states are separated by quantised amounts of energy so that the gamma photons will have characteristic energies and probabilities of occurrence for particular transitions. Internal conversion is a process by which the energy of transition from an excited state is given to an orbital electron which is then ejected.

2.6 CALCULATION OF INFINITE MATRIX DOSE RATES

The concept of an infinite matrix provides an approach to the calculation of dose rates. For such a system, the conservation of energy requires that within a homogeneous

volume having dimensions greater than the ranges of the radiations, the rate of energy absorption is equal to the rate of energy release.

In this case, the absorbed dose rate (the rate of absorption of energy per unit mass), D, is given by the specific activity of the matrix multiplied by the energy release per decay, E.

$$\dot{D} = \frac{\lambda N}{m} \cdot E \qquad (2.14)$$

To summarise this point; -

if all the energy released by radioactive decay in a given volume is absorbed, then the dose rate is simply proportional to the radionuclide concentration.

For a volume containing more than one radionuclide then the infinite matrix dose rate can be obtained by summing the individual contributions.

Where a radioactive series is in equilibrium, so that all members of the series decay with the parent rate, the energy released per parent disintegration is the total summed over the whole series. For a series exhibiting disequilibrium, individual summations must be made.

The infinite matrix approach, although very useful as a starting point, does not fully describe those matrices typically offered by TL dating samples. This is due to the heterogeneous nature of the TL bearing minerals and the radioactivity being present on a morphological scale that is comparable with the ranges of the naturally occurring ionising radiations.

Therefore, the infinite matrix dose rate as calculated from the measured concentrations of radionuclides within a real sample needs to be modified by microdosimetric corrections before the effective dose rate applicable to that sample can be assessed.

The sources and characteristics of the radiations that provide this dose rate will be examined next.

2.7 SOURCES OF NATURAL RADIOACTIVITY

The major sources of radiation in the natural radiation environment are the alpha, beta and gamma emitting uranium and thorium decay series and the beta and gamma emitting radioisotope of potassium, ^{40}K. These are long-lived radionuclides that give rise to an effectively constant dose rate over the age span of an archaeological sample, assuming that there is radioactive equilibrium. The relevant decay schemes are shown in Tables 2.1, 2.2, 2.3 and 2.4

The calculation of dose rate conversion factors, ie the dose rate per parent concentration, requires the summation of each energy release down the decay chain. Early calculations were carried out by Bell (1976a) with later revisions (Bell, 1977, 1979) to accommodate more up to date values and in his later paper to standardise the radiation data used so as to be in line with the values adopted in geo- and cosmochronology. More recently considerable effort has been invested in the recalculation of Bell's figures (Nambi and Aitken, 1986, Sanderson, 1987). The latter author not only confirmed Bell's results but also explicitly stated the distribution of energy release at different stages of the decay chains. The recalculated values are in excellent agreement with previously published data, any differences being unimportant when considered in terms of their relative contributions within the context of dating. The dose rate conversion factors used in this work are taken from Aitken (1985) and are given in Table 2.5. The use of these conversion values can be usefully illustrated with an example of a "typical" soil, or pottery, matrix containing 3 ppm U, 10 ppm Th, 2% K (Table 2.6).

Nuclide	$T_{1/2}$	Alpha	Beta	Gamma	IC	Daughter
^{238}U	4.4683 x10^9 a	4.1849		0.00016	0.01104	^{234}Th
^{234}Th	24.10d		0.1686	0.0077	0.0263	^{234}Pa
^{234m}Pa	1.175m		2.272	0.00951	0.01491	^{234}U
^{234}Pa	6.75 h		0.560	0.001	0.0003	^{234}U
^{234}U	2.446 x10^5 a	4.7600		5x10^{-5}	0.0082	^{230}Th
^{230}Th	8.0 x10^4 a	4.753		2.5x10^{-4}	0.0111	^{226}Ra
^{226}Ra	1600 a	4.775		0.00614	0.0014	^{222}Rn
^{222}Rn	3.8235d	5.489		0.00036	---	^{218}Po
^{218}Po	3.05 m	6.002	0.256	---	---	^{214}Pb (0.9998) ^{218}At 1.85x10^{-4}
^{214}Pb	26.8 m		0.715	0.244	0.01159	^{214}Bi
^{218}At	1.5-2 s	6.693		0.0477	0.001	^{214}Bi
^{214}Bi	19.7 m		1.665	1.669	0.008	^{214}Po
^{214}Po	163.7 us	7.687		8x10^{-5}		^{210}Pb
^{210}Pb	22.26 a		0.0237	0.00186	0.029	^{210}Bi
^{210}Bi	5.012 d		1.155	---	---	^{210}Po
^{210}Po	138.4 d	5.3043		1x10^{-5}		^{206}Pb
^{206}Pb	Stable					
		Mev	MeV	MeV	MeV	

TABLE 2.1 ^{238}U Decay Scheme

Nuclide	$T_{1/2}$	Alpha	Beta	Gamma	IC	Daughter
^{235}U	7.038 x10^8a	4.394		0.14508	0.03481	^{231}Th
^{231}Th	25.52h		0.231	0.01313	0.0569	^{231}Pa
^{231}Pa	3.28 x10^4a	4.972		0.0367	0.0285	^{227}Ac
^{227}Ac	21.773a	4.933	0.0455	0.0001		^{223}Fr (1.2%) ^{227}Th (98.8%)
^{227}Th	18.17d	5.928		0.0715	0.0363	^{223}Ra
^{223}Fr	21.8m		1.135	0.05746		^{223}Ra
^{223}Ra	11.68d	5.675		0.0895	0.0003	^{219}Rn
^{219}Rn	3.92s	6.758		0.0538	0.0007	^{215}Po
^{215}Po	1.83ms	7.384		0.0002		^{211}Pb
^{211}Pb	36.1m		1.296	0.0556	0.003	^{211}Bi
^{211}Bi	2.16m	6.564		0.0446	0.0089	^{207}Tl (98.68%)
^{211}Po	0.52s	7.431	1.440	0.03508		^{211}Po (0.32%)
^{207}Tl	4.77m			0.0022		^{207}Pb
		MeV	MeV	MeV		

TABLE 2.2 ^{235}U Decay Scheme

Nuclide	$T_{1/2}$	Alpha	Beta	Gamma	IC	Daughter
^{232}Th	1.41 x10^{10}a	4.002			0.01416	^{228}Ra
^{228}Ra	5.76a		0.0292		0.06021	^{228}Ac
^{228}Ac	6.13h		1.207	0.8758	0.0489	^{228}Th
^{228}Th	1.913a	5.398		0.00249	0.0035	^{224}Ra
^{224}Ra	3.66d	5.672		0..0095		^{220}Rn
^{220}Rn	55.6s	6.288		0.00465		^{216}Po
^{216}Po	0.145s	6.779		1.4x10^{-5}	0.004	^{212}Pb
^{212}Pb	10.643h	6.090	0.3592	0.1385	0.0115	^{212}Bi
^{212}Bi	60.60m	6.050	1.738	0.0987		^{208}Tl(36%) ^{212}Po(64%)
^{212}Po	0.296us	8.784				^{208}Pb
^{208}Tl	3.05m		1.581	1.2142	0.0120	^{208}Pb
		MeV	MeV	MeV	MeV	

TABLE 2.3 ^{232}Th Decay Scheme

Nuclide	$T_{1/2}$	Alpha	Beta	Gamma	IC	Daughter
^{40}K	$1.277x10^9$ a		1.343			^{40}Ca (89.33%)
			Mean beta 0.583			
			EC	1.461		^{40}Ar (10.67%)

TABLE 2.4 ^{40}K Decay Scheme

Radionuclide	Concentration	Alpha	Beta	Gamma
U Series	1ppm ^{238}U			
No radon loss		2.779	0.1461	0.1149
100% radon loss		1.260	0.0610	0.0055
Th Series	1ppm ^{232}Th			
No thoron loss		0.739	0.0286	0.0514
100% thoron loss		0.309	0.0103	0.0208
Natural	1% K_2O	-	0.689	0.200
Potassium	1% K	-	0.830	0.241

TABLE 2.5 DOSE RATE CONVERSION FACTORS ($mGy.a^{-1}$) (FROM AITKEN, 1983)

		(Alpha)	Alpha(eff)[1]	Beta	Gamma	Total
U	3ppm	(8.337)	1.251	0.438	0.344	
Th	10ppm	(7.390)	1.109	0.286	0.514	
K	2%	-	-	1.660	0.482	
Total		(15.727)	2.360	2.384	1.341	6.085
Relative Contribution			39%	39%	22%	
Fine-grain[2]			2.444	2.370	1.341[3]	5.955
Relative Contribution			38%	40%	22%	
Inclusion[2]			0[4]	2.243	1.341[3]	3.584
Relative Contribution			-	63%	37%	

TABLE 2.6 INFINITE MATRIX DOSE RATES (mGy.a^{-1}) CALCULATED FOR A TYPICAL MATRIX AND EFFECTIVE DOSE RATES FOR FINE AND QUARTZ INCLUSION GRAINS

1. Alpha efficiency = 0.15
2. Dose rates calculated for activity free grains in a dry matrix.
3. Matrix and soil composition are the same (therefore gamma dose rate originates from the soil).
4. Alpha dose rate eliminated for inclusions by HF etching.

Other sources, providing less significant contributions to the overall dose rate, include cosmic radiation and possibly other long-lived radionuclides. Warren (1978) highlighted ^{87}Rb as one such nuclide that had previously been overlooked. He provided data regarding its calculated dose rate and also suggested values of the potassium to rubidium ratio for use with those samples for which the rubidium content had not been determined. This work was extended by Sanderson (1987) to include a number of other naturally occurring primordial nuclides, demonstrating that of all these only the rubidium beta emission was ever likely to be of any significance, and even then only to a minor extent.

The cosmic ray flux at ground level results from interactions between the upper atmosphere and a primary cosmic particle flux. It has a "soft" component of energetic electrons that is readily absorbed within 0.5 m of soil, and a "hard" component of muons which have much greater ranges in soil and therefore need to be considered here. There is a dependence on latitude due to the focusing effect of the earth's magnetic field towards the poles of the earth. There is also an altitude effect related to absorption by varying thicknesses of atmosphere. Generally speaking the relative contribution of cosmic radiation to the total dose is small (of the order of 5% for quartz inclusion dating and less for fine-grain dating). However, there are certain instances, for example where the radioactivity of the sample and its burial medium are exceptionally low or for samples originating from high altitudes, where the cosmic ray dose may become more significant.

Theoretical work (Greison, 1942) allowed an estimate of 0.13 $mGy.a^{-1}$ to be made for the lower limit of the cosmic ray contribution. Ion-chamber measurements (Shamos *et al*, 1964) suggested that the ground level cosmic radiation dose rate was of the order of 0.30 $mGy.a^{-1}$. These studies were neatly tied together, experimentally, by Aitken (1969) using thermoluminescence dosimetry (TLD) to measure the variation of cosmic ray dose rate with depth in chalk (chosen because of its low radioactivity). The results indicate a ground level dose rate of 0.28 $mGy.a^{-1}$ that is reduced to an effectively constant value of 0.14 $mGy.a^{-1}$ at a depth of approximately 1 m.

More recent work (Prescott and Stephan, 1982) recommends slightly higher values of 0.185 mGy.a^{-1} at 0.5 m and 0.150 mGy.a^{-1} at 1 m depths of standard rock (ρ = 2 g.cm^{-3}.). They also examined the effect of latitude and altitude on the cosmic ray dose rate and derived an expression for D_{cosmic}, taking these parameters into account.

2.8 DOSIMETRY

2.8.1 Introduction

The previous section described the sources of alpha, beta, and gamma radiations that together form the natural radiation fields within which samples for TL dating acquire their stored doses. The infinite matrix dose rates, as calculated from the measured radionuclide concentrations (see section 2.6), are not directly applicable as a means of determining the effective dose rates to the sample for three main reasons. The first is that alpha radiation is generally less efficient at producing TL than beta or gamma radiation. Secondly, the different ranges of alpha, beta, and gamma radiations mean that the spatial configuration of the TL sensitive minerals and the radionuclide concentrations influence the relative significance of each contribution. Thirdly, differences in stopping powers and mass absorption coefficients mean that one material may absorb more than another. These factors are fundamental to microdosimetry and will now be considered in terms of the three relevant types of radiation. The various approaches to measuring the natural radiation dose rate will then be discussed.

2.8.2 Alpha Dosimetry

Alpha particles are much heavier than electrons so they are deflected very slightly when their Coulomb fields interact with atoms to form ion-pairs and therefore travel in a straight line through matter. Compared to beta particles alpha particles have much higher specific ionisation values (number of ion-pairs formed per unit path length). The velocity of the alpha particle decreases as it loses energy in travelling through an absorber. Consequently, it will spend progressively longer times in the vicinity of any particular atom which results in an increase in the probability of interaction. This means

that there is a steady increase in the number of ion-pairs formed along the path of the particle, up to a maximum value which is close to the end of the particle's range (the Bragg Peak). Just beyond this point the kinetic energy of the particle is comparable to that of the orbital electrons of the absorber. The alpha particle can then acquire electrons becoming uncharged, and therefore incapable of causing further ionisation.

Although the particle range depends on the properties of the absorbing medium and the energy of the particle, the mean range of alpha particles resulting from natural series decay in pottery, soil and other similar media is between 20 and 30 microns (the maximum value being 45 microns from the ^{214}Po transition of 7.689 MeV). This means that for large mineral grains embedded in a radioactive medium the alpha dose from that medium is attenuated progressively within the interior of the grain. Similarly, any alpha activity within such large inclusions is unable to fully irradiate surrounding volumes. The formulation of the two routine pottery dating techniques, fine-grain and quartz inclusion, reflect this microdosimetric situation since they depend on a simplified view of the pottery matrix as having alpha activity homogeneously distributed through the clay matrix with quartz inclusions as non-radioactive spheres within it. These techniques will be discussed in more detail towards the end of this chapter.

These effects can be dealt with by introducing attenuation factors which, when multiplied by the infinite matrix dose rate for the external source give the effective dose rate. The calculation of alpha attenuation factors for the uranium and thorium series in equilibrium has been carried out for spherical grains of varying size (Fleming, 1979, Bell, 1980). The effective alpha dose rate for a grain with some alpha activity is made up of the external infinite matrix alpha dose rate multiplied by an attenuation factor plus the grain's internal infinite matrix alpha dose rate multiplied by absorbed dose fraction (1 - attenuation factor). The alpha absorbed dose fractions used in this work are those provided by Bell (*op cit*). These are presented in Table 3.1.

The contribution of alpha radiation to the natural TL signal is further reduced as a consequence of its lower efficiency for producing TL in comparison to an equivalent beta or gamma dose. This is due to the high ionisation density produced by alpha

particles, so that within the central core of the track the TL traps become saturated and so a large proportion of the alpha's energy cannot take part in trapping processes (Zimmerman, 1971). Zimmerman proposed that this efficiency factor, the k-value, should be measured as the ratio of the TL sensitivities to known doses of alpha and beta (or gamma) radiation.

$$k = \frac{\text{TL per Gy of } \alpha \text{ radiation}}{\text{TL per Gy of } \beta \text{ radiation}} \qquad (2.15)$$

The initial evaluations of k were carried out using 3.7 MeV alpha particles but this system was found to have the disadvantage of being strongly energy dependent since the ionisation density increases as the alpha particle energy decreases. This counteracted the advantage of the k-value being directly applicable to the age equation, as a prefix to the alpha dose rate term, without the need for transformation into other units. The laboratory measurement of k is therefore dependent on the particular alpha source used as well as the irradiation geometry and other experimental conditions. It also follows, then, that the amount of alpha particle TL induced over archaeological time will be dependent not only on the dose rate but also their natural energy spectrum. The latter point was compensated for by the modification of k to become k_{eff} such that for a sample with equal U and Th activities, $k_{eff} = 0.83k_{3.7}$.

Zimmerman (1972) had also observed that the TL per unit length of track was approximately independent of the alpha particle energy (up to 3.7MeV) and this was later confirmed and investigated further (up to alpha energies of 7.3MeV) by Aitken and Bowman (1975). As a result of this work they sought to redefine alpha source strengths in terms of track length delivered per unit volume of sample. This meant that the alpha efficiency was also redefined in terms of the a-value system,

$$a = \frac{\text{TL per unit } \alpha \text{ track length}}{\text{TL per unit absorbed } \beta \text{ energy (ie per Gy)}} \qquad (2.16)$$

$$a = \frac{x}{13\ S} \qquad (2.17)$$

where, x = the beta dose (in Gy) that produces the equivalent TL response as one minute's irradiation from the alpha source,

S = the alpha source strength (in $\mu m^{-2} min^{-1}$) ≡ the rate at which track length is delivered to the sample.

The numerical factor is introduced so that, for a pottery sample, the a-value will be equal to Zimmerman's k-value (for 3.7 MeV alpha particles).

Aitken and Bowman's reasoning was further developed (Bowman and Huntley, 1984) by making the assumption that the TL per unit of absorbed beta energy is also a constant that is independent of the energy of the beta particles, as well as the TL per unit alpha track length being independent of the alpha particle energy. The alpha efficiency can then be expressed in terms of the beta energy that produces the same amount of TL as one unit length of alpha track. This is then related to what is actually measured in the laboratory, where a calibrated alpha source delivers a known track length per unit volume per unit time, to a sample of thickness less than the alpha track length, and the resulting TL is compared to that induced by a known beta dose. This gives rise to a third potential measure of the alpha efficiency, the b-value

$$b = \frac{\text{TL per unit } \alpha \text{ track length per unit volume}}{\text{TL per unit absorbed } \beta \text{ dose}} \qquad (2.18)$$

b has SI units of $Gy.m^2$.

Valladas and Valladas (1982) considered the situation for coarse grains, in particular where due to uncertainties in the HF etching process (used to remove the alpha irradiated outer layer of these grains (Fleming, 1970)) this step is omitted and direct measurement is made of the alpha response. The approach is to carry out the alpha

irradiation with the coarse grains on a vibrating platform to simulate the omnidirectional alpha flux that the grains would experience within a pottery matrix and to minimise errors due to non-spherical grain shape.

Aitken (1985a, b) has also considered the case of coarse grains and has derived an expression for the relationship between the "true" effectiveness, a, as obtained by the irradiation of fine grains and the "apparent" alpha effectiveness, a', as obtained by the irradiation of coarse grains.

$$a = \frac{2\,D}{3\,\eta'\,R} \cdot a' \qquad (2.19)$$

D = grain diameter (μm)

R = alpha range for the alpha energy used

η' = ratio between the average TL per unit track length for total absorption and that for a thin layer of fine grains

Reference to Table 2.6 shows that for a relative alpha efficiency of 15%, a value that is appropriate for most dating materials, the absorbed dose for fine grains, which would otherwise have a dominant alpha contribution, will have approximately equal alpha and beta contributions. For coarse grains, however, it is possible to further reduce the effective alpha dose to a negligible level by HF acid etching of the alpha irradiated surface of the grains. These approaches have been exploited to form the basis of the routine, fine-grain and inclusion, methods of TL dating which are discussed in sections 2.12.1 and 2.12.2, respectively.

2.8.3 Beta Dosimetry

Beta particles can interact with matter through a number of mechanisms, although their energy is absorbed mainly through the processes of ionisation and atomic excitation. The process of ionisation involves the interaction of an incident beta particle with an orbital electron of an atom that leads to the ejection of the orbital electron and the scattering of the beta particle. The secondary electrons (delta rays) can have such high energies that they cause further extensive ionisation. The specific ionisation (number of ion-pairs produced per unit length of particle track) for beta particles is much lower than that of alpha particles. This is due to the much greater velocities of the beta particles that results in much longer ranges. At very high energies the beta particles have straight paths because they have a momentum much greater than that of the orbital electrons. Atomic excitation also involves the interaction of an incident beta particle with an orbital electron, but here the electron only receives sufficient energy for it to attain a higher orbit (ie an excited state) and the incident beta particle is scattered from its original path.

Of less importance are the mechanisms of radiative energy loss (Bremsstrahlung) which results from the change in velocity experienced when an incident beta particle approaches the positively charged nucleus, and Cerenkov radiation which is effectively the result of an electromagnetic shock wave. Direct interaction between electron/positron pairs is possible in which both particles are annihilated. The combined mass of the two particles is converted into electromagnetic radiation, which is emitted as two gamma photons travelling in opposite directions each having a characteristic energy of 0.511 MeV. This is called annihilation radiation and its presence in the electromagnetic spectrum of a radionuclide is strong evidence for positron emission by that nuclide.

Although beta particles have continuous energy spectra, it can be shown that most environmental betas are absorbed within 2-3 mm of their source in a quartz, or similar, matrix (Katz and Penfold, 1952). This means that for TL dating samples such as pottery which may have been buried in a medium of contrasting radioactivity, the beta

dosimetry can be confined to that of the internal activity of the sample by removing the surface layer of the sample that has been exposed to the beta radiation from the soil.

For fine-grains the beta dose rate obtained after correction for the attenuation due to water is directly applicable but for inclusion sized grains a further correction is required due to the attenuation of the beta radiation within the grains. Mejdahl (1979) has evaluated the factors by which the average beta dose to a grain of a given size is reduced from the infinite matrix dose. The model used consists of an infinite homogeneous matrix containing uniformly distributed radionuclides within which the quartz grains are regarded as being non-radioactive spheres of the same composition as the matrix. Conservation of energy requires that the attenuation of the external beta radiation by a grain must be balanced exactly by the self-dose fraction which the grain would absorb if it had the same concentration of radionuclides as the matrix. Thus for a grain of no internal radioactivity the attenuation factor is given by 1 minus the dose fraction absorbed by the cavity. Alternatively, this can be seen to be the dose fraction that would have been absorbed if the grain itself were a radioactive sphere in a non-radioactive medium.

The calculation used percentile distances, X_p, which represent the distance within which p% of the radiation is absorbed. This is achieved by using a scaling procedure (Cross, 1968) to obtain values for quartz from those given for water (Berger, 1971). This is possible because of the similarity in shape of the absorbed beta dose distributions in different media allowing scaling to be carried out on the basis of the percentile distances being proportional to density and stopping powers.

Berger (1971, 1973) produced scaled absorbed dose distributions (point kernels) for water by considering the situation for spherical regions within an infinite matrix containing uniformly distributed point beta sources. His later paper (improved point kernels) took into account the effects of energy loss by straggling and bremsstrahlung.

The absorbed dose fractions, ϕ, for quartz were calculated by Mejdahl for a large number of grain sizes for uranium and thorium series, in equilibrium, and potassium

from the expression

$$\phi = \int_0^{t_{max}} [\ 1-(3/2)\ (t/t_{max}) + (1/2)\ (t/t_{max})^3\ ]\ F(t)\,dt \qquad (2.20)$$

where $t = x/x_{90}$

x = distance from the source

x_{90} = distance within which 90% of the radiation is absorbed

$tmax = D/x_{90}$

D = grain diameter

F(t) = scaled dose distribution

These values are presented in Table 3.2 where they are used in formulating simulated isochron systems as well as being later incorporated into the experimental programme. Although the values were calculated for quartz they are also valid for feldspars, since they have stopping powers close to that of quartz. (Table 2.7)

It is also apparent from Mejdahl's calculations that the attenuation factors for uranium, thorium, and potassium are different so that the effective attenuation factor will depend on the relative abundance of these radionuclides. The self-dose fraction due to inherent potassium in alkali feldspars can be calculated from this work (Mejdahl and Winther-Nielson, 1982, Mejdahl, 1983; Sanderson, 1987; Sanderson *et al*, 1988).

2.8.4 Gamma Dosimetry

The absence of charge and rest mass for gamma photons results in little interaction with the absorbing atoms and greater penetration. Gamma photons produce only 1 - 10% of the number of ion pairs of that produced by beta particles of the same energy. As a consequence of this low specific ionisation, the ionisation is almost completely secondary 7in nature and results from the action of a few high energy primary ion pairs. The processes of interaction are outlined below.

In the photoelectric effect all of the photon's energy is absorbed by the orbital electrons of the target atom. The excited state produced is greater than the binding energy of some of the orbital electrons so that an electron can be ejected from the atom. The energy, E_e, of this emitted photoelectron is equal to the difference between the incident gamma photon, E_γ, and the binding energy, E_b, of the electron in the atom.

If the photoelectron originates from an inner electron orbital, an electron from a higher orbital moves to fill the vacancy. Here, the difference in binding energy of the higher and lower orbitals causes the emission of X-rays and low energy Auger electrons. The photoelectron as well as the Auger electrons and X-rays cause extensive secondary ionisation by interacting with absorber atoms.

	Z_{eff}	A_{eff}	Stopping power	Density ($g.cm^{-3}$)
SiO_2	10.80	21.60	0.9518	2.65
$KAlSi_3O_8$	11.81	23.92	0.9373	2.55
$NaAlSi_3O_8$	10.69	21.59	0.9450	2.60

TABLE 2.7 ELECTRON STOPPING POWERS, RELATIVE TO AIR, CALCULATED FROM CROSS (1968).

In the Compton effect an outer electron is ejected from the atom by the incident gamma photon which is deflected with a lower energy. The scattered gamma photon may have sufficient energy for further interactions to occur. The energy and scattering angles of the Compton electron and the deflected gamma photon depend on the initial energies and momentum involved.

The process of pair production involves the interaction of a gamma photon with the electromagnetic (Coulomb) field of the nucleus. The whole of the photon's energy is converted to the mass and kinetic energy of an electron and a positron. This process is not possible until the photon energy is equivalent to the rest mass of two electrons (1.02

MeV). The probability of pair production increases as the energy of the gamma photon increases above this value. The excess energy appears as the kinetic energy of the electron-positron pair and can be shared in varying proportions between the two.

A fourth, and relatively minor, process of interaction is coherent (or Bragg, or Rayleigh) scattering, where the incident photon collides with an electron that is sufficiently tightly bound to the atom for the whole atom to absorb the recoil. The energy transfer to the atom is negligible and the photon is scattered without loss of energy.

Photoelectric interactions predominate for all materials at sufficiently low photon energies, but as the energy increases the photoelectric effect falls off more rapidly than the Compton effect and the latter eventually takes over as the dominating process. With continuing increase of photon energy, although the Compton effect decreases in absolute terms, it increases still more relative to the photoelectric effect. At photon energies of several MeV the pair production process begins to make the greatest contribution to photon interactions.

As a result of the different scattering processes, mentioned above, and the wide range of gamma emission energies from the natural series, the analysis of the gamma ray dose distribution is very complex. Both primary and secondary (scattered) gamma photons contribute to the gamma dose delivered in an extended medium. Fleming (1979) estimated the gamma ray attenuation of environmental media using the approximation that the build up factor (ratio of total dose to primary dose) increases linearly with distance from the source, with the further simplifications that uranium and thorium series, in equilibrium, could be approximated by a single set of absorption coefficients and that the resulting integrated dose distributions in soil were similar to that of potassium, from which the relative contributions of soil and sherd to ceramic dating were assessed. The resulting approximation that all the gamma dose was from the soil was acceptable for small sherds.

Mejdahl (1983) has taken absorbed gamma fractions initially calculated for a soft-tissue medium from existing Health Physics results using the Monte Carlo technique and used

conversion factors to make them applicable to pottery and stone samples. These results show reasonable agreement with those of Fleming. The values used in this work are given in Table 3.3.

Aitken *et al* (1985) combined an experimental approach with computer simulation based on details of atomic compositions, cross-sections, primary emission spectra, etc. Further examination could be suggested using a more extended primary gamma list for Monte Carlo simulation and extension of the experimental work to include the thorium and potassium series.

The key questions that remain are are the uranium, thorium, and potassium build up factors really

i) the same (ie unknown U,Th,K ratios in the soil do not matter

ii) independent of complex geometries ?

Traditionally, it has been stated that one of the requirements of potential samples for TL dating is that they should come from an homogeneous layer of 30 cm radius around the sample. However, from the work stated above it is apparent that even for quartz inclusion dating, where the environmental gammas make a maximum contribution of perhaps 30% of the total dose, the situation need not be hopeless if these conditions are not met. This is because if the half of the gamma dose originating from within 8 cm of the sample can be measured accurately then the unknown part can probably be adequately estimated. It has also recently been stated (Aitken *et al*, 1985) that the practice of avoiding samples above a depth of 30 cm from the ground surface may be over cautious.

2.9 MEASUREMENT OF DOSE RATE

In this section there will be a brief overview of the main techniques available to measure the dose rate component of the TL age equation. Those techniques that have been employed during the experimental verification of the isochron model will receive fuller treatment later.

2.9.1 Alpha counting

This is a scintillation technique, based on the work of Turner, Radley and Mayneord (1958), in which a zinc sulphide screen is positioned on a photomultiplier tube (pmt), the powdered sample is then placed on the screen so that when an alpha particle hits the screen a pulse of light is emitted that is detected by the pmt and registered in a counting system. The advantages of the technique are its simplicity and that the ratio of the effective alpha dose rate to the alpha count rate is independent (to within a few percent) of whether the dose is provided by uranium or thorium (Aitken, 1978a). In order to use alpha counting to assess the beta and gamma contributions from the uranium and thorium decay series then either equal uranium and thorium activities are assumed or some attempt is made to evaluate the U/Th ratio using the 'pairs' technique. Here the counting electronics are designed so as to register pairs of counts arriving within a specified time of each other, eg. the Th chain contains the rapid pair of alpha transitions

$^{220}Rn \dashrightarrow {}^{216}Po \dashrightarrow {}^{212}Bi$ ($t_{1/2}$ = 55 and 0.145 sec, respectively) and the extremely rapid pair in the ^{235}U chain due to the 0.002 sec half-life of ^{215}Po. The main problem encountered with the pairs technique is the need for long counting times to obtain statistically meaningful results. An alternative approach to estimation of the U/Th ratio is by using energy discrimination as suggested by Sanderson (1979) and adopted by Martini *et al* (1982).

A more significant problem can be caused by the emanation of radon from a sample. This may be observed as an increase in the count rate for samples that have been stored in sealed counting cells (Aitken, 1978b).

2.9.2 Beta Counting

Sanderson (1988) described this new scintillation technique for measuring matrix beta dose rates based on thick source beta counting (TSBC) using wafers of plastic scintillator. The method is advantageous in that is direct, rapid and accurate, with a precision of ±5% quoted as being achievable in counting times as short as 15 minutes.

This is obviously beneficial for sample throughput for dating programmes that already contain certain features of automation and replication of measurements. An important feature of the beta counter is that its response is not strongly dependent on the U,Th,K composition of the sample. One disadvantage is that it does not provide any information on the relative contributions of the different source of beta radioactivity. In this respect it has been recommended that this method be used in conjunction with checks to confirm that the uranium series is a minor component (to guard against radon loss and disequilibrium) and that modern additions (from fallout or perhaps agricultural practices) are not contributing to the signal. This technique has been routinely used in this work, with neutron activation analysis being employed as the cross-check method, both of which will be discussed in terms of their experimental aspects and applications in chapter 3.

2.9.3 Thermoluminescence Dosimetry (TLD)

This method employs very sensitive TL phosphors, such as CaF_2 and $CaSO_4$, to record the dose rate directly. The possibility of using alpha TLD is complicated by many problems, replication of the alpha effectiveness appropriate to the sample, replicating grain size, and the likelihood that such low levels of TL, in relation to any spurious signals, would be obtained in a time that was practical, all combine to effectively preclude the use of the technique for alpha dosimetry.

The use of βTLD, (Bailiff and Aitken, 1980) however, is a much more promising proposition although this too is not problem free. The basic problem is the achievement of an isotope independent response - such that the relative contributions from U/Th/or K are unimportant with respect to the evaluation of the correct beta dose rate. Isotope dependence in βTLD arises partly from the need to shield the phosphor from alpha radiation, which will introduce attenuation of the beta-dose rate - that is dependent on the beta energy spectrum. There is also a gamma contribution which, despite the much lower absorption coefficients of gamma compared to beta radiation is significant. This is problematical due to the fact that the ratio of gamma to beta dose rates is strongly

isotope dependent (1.8:1 for the Th series, 0.8:1 for the U series and 0.3:1 for potassium). A number of variations of βTLD schemes have been devised of which a useful resumé is provided by Mejdahl and Wintle (1984). One of the features common to all of these systems is the need for the βTLD units to be stored for a sufficiently long period (usually 1 to 2 weeks) in a lead container to reduce the background radiation, followed by a period of labour intensive readouts (unless an automatic reader is available). Sanderson (1987) also notes that isotope independence depends on the coating thickness of each disc and varies from disc to disc, therefore individual calibrations are needed.

Gamma thermoluminescence dosimetry was the first application of TLD in TL dating since it provided a convenient way overcoming a number of problems. Firstly, the phosphor can be obtained with a radioactivity free material eg copper, stainless steel, or plastic, with a wall thickness sufficient to stop the phosphor being irradiated by beta particles. Secondly, the seasonal variations (Mejdahl, 1970) in soil water content can be averaged out by leaving the γTLD capsule buried for a year, where possible. The burial position should be as comparable as possible to that of the sample being dated so as to experience a similar gamma radiation field - this also has the advantage of automatically including the appropriate cosmic ray dose. There are disadvantages, however, of which the most significant is how well the dose rate received by the phosphor replicates that received by TL grains in a pottery matrix. This is generally not the case because of the difference in absorption coefficients for TL phosphors and TL mineral grain, particularly in the low energy region (<2.0MeV). The Oxford γTLD unit partially compensates for the over response to low energy gammas by CaF_2NAT through the use of copper shielding - wall thickness 1.5mm. The Riso laboratory uses $CaSO_4$:Dy contained in polyethylene capsules within steel tubes, a combination that has a response virtually the same as quartz (Mejdahl and Wintle, 1984). These systems are calibrated using doped concrete blocks (Oxford) or with the aid of a radioactive rock, lujavrite, in the case of Riso. Significant drawbacks of the capsule approach are that no allowance can be made for the presence of fallout (unlike gamma spectrometry methods - next section), and it is invariably the case that excavation will have removed the very context from which the pottery to be dated came from, so a compromise has to result in

measurement from a different (possibly unrepresentative) context. Fading of the TL signal during the storage period may also need to be corrected for, depending on which phosphor has been used. East (1991) describes an environmental dosimeter, designed by Sanderson at SURRC, of a "paired" type that enables both beta and gamma dose rates to be measured simultaneously. It may be said that the use of TL dosimeters to measure the environmental gamma radiation is a well-established technique.

2.9.4 Gamma Spectroscopy

The use of gamma spectroscopy falls into two main categories, the high-resolution laboratory based and the portable types. The former have the advantage of being able to analyse pottery sized samples, as well as soils, and that some information on U/Th series disequilibrium may be obtained (Murray and Aitken, 1982, 1988), although the application to small sample sizes is offset by the longer counting times required. The main disadvantage of high resolution gamma spectrometry is the expense and complexity of the equipment involved. This technique has been used at the SURRC to characterise the U, Th, K contents of a Shap granite sample that has been used as the in house standard for neutron activation analysis of TL dating samples.

Portable gamma spectrometers are generally based on a sodium iodide scintillation crystal detection system coupled to counting electronics and a rechargeable battery power supply (portable semi-conductor detectors are also available). The instrument can be used in two ways - as a spectrometer to measure individual components by utilising the characteristic gamma emissions of 2.65MeV from ^{208}Tl (Th series), 1.76 MeV from ^{214}Bi (U series) and of 1.46 MeV from ^{40}K (potassium). Alternatively, an optimum energy threshold setting may be determined so as to minimise the isotope dependence of the detector response eg 370 keV, suggested by Løvborg and Kirkegaard (1974). In this mode the total dose rate may be estimated by integrating all gamma radiation above the threshold setting. Sanderson (1987) recommended the use of two threshold settings - 350 keV and 1350 keV, the upper to determine the gamma dose rate due to U, Th and K, while the lower is a check for recent ^{137}Cs contamination (from Chernobyl fallout, etc). Concordance of the two dose rate values obtained indicates a contamination free

site. The advantages of the portable gamma spectrometer is that the measurements are rapid (~20 mins per location - so a whole site could be covered in a single day) and to some extent inhomogeneity of the soil is allowed for. The disadvantages are that a larger hole is required to accommodate the detector head in the site, and because the measurements can be made so quickly there is no allowance for seasonal variations in dose rate due to variations in soil moisture content, although Mejdahl (1970) has shown that for sufficiently deeply buried samples this may be of little significance. One practical constraint is that there is a rapid variation of count rate with threshold setting within the usual interval quoted, (0.37 - 0.45 MeV, Mejdahl and Wintle, 1984) so that the stability of the energy calibration of the instrument is crucial and should be frequently checked using a small source. The >1350 keV window is much more stable.

2.9.5 Neutron Activation Analysis (NAA)

Neutron activation analysis relies on the production of radioactive nuclides in a sample and the subsequent detection and measurement of the induced γ radiation. The technique can be readily used to determine U, Th and K concentrations at the levels typically encountered in archaeological samples, although the accuracy will be dependent on the facilities and time available. The characteristics of the method are that easy access to a reactor and suitable counting facilities is required and also that only the U and Th parents of the decay series are measured. This means that the calculated dose rates are susceptible to error if there is disequilibrium present. This can be used to advantage when the method is used in conjunction with gamma spectroscopy or beta counting. Measurement of ^{210}Po, at the end of the ^{238}U decay chain, has been suggested as an effective check on the assumption of equilibrium (Mangini *et al*, 1983). This technique of NAA has been in routine use throughout this work and will therefore be the subject of more detailed discussion in a later section (Chapter 4). Delayed neutron counting has also been shown to be capable of rapid analysis of U in pottery samples (Filberth *et al*, 1980).

2.9.6 Fission Track Analysis

This technique involves the thermal neutron irradiation of a slice of pottery, followed by the observation and counting of damage tracks, caused by the induced fission of uranium, in a mica or similar detector. It has been used to map the spatial distribution of U in a variety of archaeological samples, with a comparison of the distribution pattern of the samples TL (Malik *et al*, 1973). The technique can identify minerals of high U concentrations, eg zircon, as well as zoning of the uranium within zircon grains (Sutton and Zimmerman, 1976). Irradiation with fast neutrons is used to determine Th content of pottery, but Mejdahl and Wintle (1984) point out that it may be sufficient to irradiate once, with fast neutrons since U undergoes fission with a probability of 4.5 times that of Th. Then, since the Th/U ratio is usually ~3-4, the dose rate could be calculated from the total track density in the detector.

2.10 EFFECT OF H_2O

After the calculation of infinite matrix dose rates, from the measured concentrations of the radionuclides present in the sample and its burial context, and the application of the relevant attenuation factors to produce the effective alpha, beta and gamma dose rates to a particular grain size and mineral type, there is need of yet a further correction. This is related to the reduction of dose rate received by the mineral grains due to the presence of water in the sample and the soil. This is the case since the water reduces the radioactivity per unit mass compared to the dry situation, acting as an inert absorber of the radiation that could otherwise be involved in the production of TL within the mineral grains. Water also has different absorption coefficients for alpha, beta and gamma radiation, in comparison to a ceramic matrix. Since the infinite matrix dose rates are usually calculated for the "dry" situation these factors have to be taken into consideration. Zimmerman (1971) estimated the effect of water content, in conjunction with the relative stopping powers or absorption coefficients for water and the matrix, to allow the formulation of correction factors relevant to alpha, beta and gamma radiation. These are given by:

$$\dot{D}_{wet} = \frac{\dot{D}_{dry}}{1+R.f.w} \qquad (2.21)$$

where R = ratio of absorption coefficients between water and the matrix

for α radiation R = 1.50

for β radiation R = 1.25

for γ radiation R = 1.14

w = saturated water content expressed as a fraction of the dry weight of the sherd.

f = the fraction of the saturated water content assumed to be appropriate for the burial conditions.

Sanderson (1987) suggested that the value of 1.14 for γ is not appropriate since the ratio is energy dependent, and tentatively suggested a more suitable value to be between 1.05 and 1.10, while Rendell (1985) adopted a value of 1.00, following Bowman's suggestion (1976). The energy dependence is illustrated in Figure 2.1 (after Tyler, 1992) which shows a contrast between the ratios of absorption coefficients of a standard soil composition (after Beck, 1972) and water. The graph shows that for higher energies a value of 1.10 is appropriate although Monte Carlo simulation to take into account the effects of scattering and the calculation of a weighted average value for the ratio would be desirable.

2.11 RELATIVE DOSE CONTRIBUTIONS

Table 2.6 gives the dry infinite matrix dose rates, calculated for a "typical" matrix composition. The relative contributions of these dose rates has also been calculated for fine-grains and inclusion, both in a dry state and also with water present. This is to illustrate the effects of grain size and water content on microdosimetry. The resulting differences influence the measurements required for and the applications of specific dating techniques. These techniques are examined in the following sections.

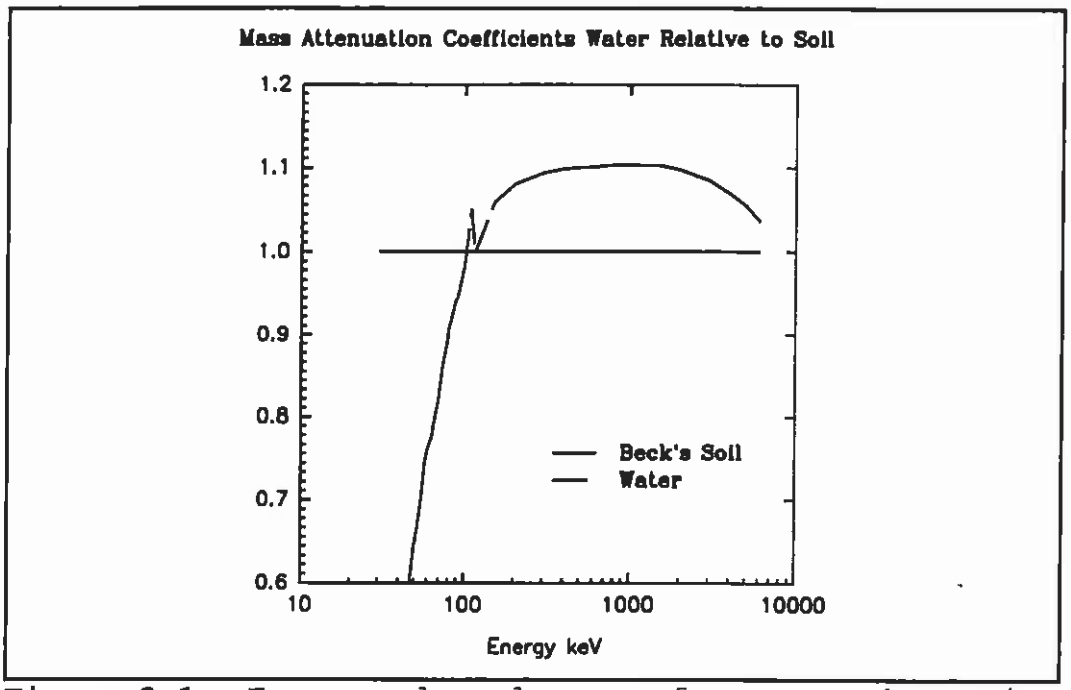

Figure 2.1 Energy dependence of mass absorption coefficients of water relative to Beck's soil.

2.12 FORMULATION OF SPECIFIC STRATEGIES FOR ROUTINE DATING OF SAMPLES FROM KNOWN GAMMA FIELDS

2.12.1 Introduction

This section will relate the microdosimetric considerations, examined earlier to the specific strategies that have been formulated for routine dating of samples from known gamma contexts. The main features of each method will be covered and in later sections that describe the experimental component of this thesis the relevant points will be expanded upon. Some aspects of sample preparation are common to all approaches, for example, the need to measure the water content (Section 2.10) and the removal of a 2-3mm layer from each surface of the pottery fragment. The reasons for this are threefold; - firstly, to remove that part of the sample that has received a beta dose from the soil which, because of the range of beta particles, will be attenuated over this region where there will be a beta dose gradient between that due to the soil and that due to the pottery itself. Secondly, the outer surfaces of the sample may well have been exposed to daylight, resulting in reduced levels of TL and thirdly, any adhering soil must be removed because of its potentially high level of geological TL. 1M HCl is used to

remove carbonates that may cause spurious TL.

2.12.2 Fine-grain dating

In the fine-grain method, developed by Zimmerman (1967, 1971), the material used for dating consists of polymineralic grains in the 1 to 8 micron range. Grains of this size are small enough not to cause very significant attenuation of the alpha dose, and will therefore experience the full dose rate due to the surrounding matrix. The sample is first disaggregated, taking care not to produce fine-grains by crushing larger inclusions. The desired grain size is obtained by suspending the 'crushed' material in acetone and then selecting the fraction that settles between times calculated from Stoke's Law. (Zimmerman's standard procedure is to collect grains that settle between 2 and 20 minutes, for a 6cm column of acetone.)

Since the grains are of a size that do not significantly reduce the alpha dose from the matrix, measurement must be made of their alpha efficiency. This can be achieved by resuspending the selected fraction in acetone and depositing it as a thin layer of a few microns onto aluminium or stainless steel discs.

A potentially advantageous aspect of the fine-grain method is that since it includes the alpha dose rate contribution it reduces the relative importance of the environmental gamma dose rate.

2.12.3 Quartz inclusion dating

An alternative approach to the fine-grain method was developed by Fleming (1966, 1970). In the quartz inclusion technique, quartz grains in the 90 to 150 micron range are selected by sieving. The dosimetry of grains of this type is such that the beta dose from the matrix will only be slightly attenuated (by less than 10%) and the alpha dose component is very significantly reduced. The small alpha dose contribution can be effectively eliminated by etching away the outer surfaces of the grains, using concentrated HF which will also remove feldspathic minerals, leaving an enriched quartz

fraction. The etching away of the outer surfaces of the quartz grains may not necessarily be isotopic and may also result in variations in grain transparency which may have implications for beta source calibrations (Bell and Mejdahl, 1981).

2.12.4 Feldspar inclusion dating

Initial observations of fading of the TL signal in volcanic feldspars (Wintle, 1973) hindered the use of these minerals for routine dating purposes. Subsequent work, however, has shown that this is not necessarily the case for all feldspars (Guérin and Valladas, 1980; Mejdahl and Winther-Nielsen, 1982; Mejdahl, 1983; Sanderson, 1987). Mineral separation is achieved by use of sodium polytungstate solutions made up to different densities eg the SURRC laboratory uses 2.51, 2.58, 2.62, 2.74 g/cc to give mineral separates of K-feldspar (2.51-2.58g/cc), Na-feldspar (2.58-2.62g/cc), quartz/plagioclase feldspar (2.62-2.74g/cc) and heavy minerals (>2.74g/cc). As in quartz inclusion dating the low alpha dose fraction can be further reduced by dilute HF acid treatment.

Contrary to the initial doubts expressed towards this group of minerals, feldspars have several advantages over quartz. The TL signal is significantly brighter 10 to 50, or more, times that of quartz and the broad glow shape often gives very long age plateaux. Mejdahl (1983) has investigated the use of large grains (>1mm) of potassium rich (>10%K) feldspars for which more than 50% of the dose is contributed by beta radiation from inherent potassium. Consequently, the errors associated with the measurement of environmental radiation and external beta radiation are considerably reduced.

2.13 PROPOSED STRATEGIES FOR DATING SAMPLES FROM UNKNOWN GAMMA FIELDS

2.13.1 Introduction

This section will describe a range of approaches towards dating samples from unknown gamma fields. These include estimation and reconstruction as well as attempts to use aspects of microdosimetry that allow alternative solutions to the age equation to be proposed.

2.13.2 Estimation

Objective authenticity testing of museum pieces and art ceramics is obviously very desirable information, but it is also readily apparent that this type of material would be extremely unlikely to have any information regarding the environmental gamma dose rate associated with it. As a consequence, the errors tend to be of the order of ± 20%, however, the qualitative nature of the question being asked of an authenticity test means that the uncertainty in the gamma dose rate generally becomes unimportant (although the possibility of old fakes should be borne in mind). Fleming (1975, 1979) has carried out extensive work in authenticity testing and through the measurement of the environmental gamma dose rate at a large number of locations has been able to derive an estimated value (within certain error limits) that can be usefully applied in many instances.

2.13.3 Reconstruction

In the case of archaeological material from old excavations there may be certain instances where some form of reconstruction of the gamma dose rate within the burial context may be possible. Some sites, for example, Pool in Orkney, exhibit remarkably little spatial variation in gamma dose rate, from which it may be possible to infer with some confidence an appropriate dose rate for areas not measured. Alternatively, it may

Examples of the use of this method can be found in Fleming (1979).

A feldspar-quartz subtraction method, based on large grains of equal size of alkali feldspar and quartz, was proposed by McKerrell and Mejdahl (1981). In this case, the two age equations are:

$$F = (env + f_1 \beta_S + f_2 \beta_F) A \quad (2.25)$$

$$Q = (env + f_1 \beta_S) A \quad (2.26)$$

where F and Q are stored doses in feldspar and quartz, β_S and β_F are infinite matrix beta dose rates in the sample and from the potassium in the feldspar grains, f_1 is the beta attenuation factor and f_2 is the absorbed of the infinite matrix beta dose in the feldspar grains.

The subtraction gives:

$$F - Q = f_2 \beta_F A \quad (2.27)$$

The age determination is based only on the beta dose rate from potassium rich feldspars and the need for information regarding environmental radiation and sample beta dose rate has been removed. The main difficulty is the measurement of large quartz grains which has hindered any widespread use of the method.

A third variation of the subtraction method has been proposed by Plachy and Sutton (1976) that has been used for dating hearths containing burnt stones of granite and quartzite/sandstone. The latter rock type is generally low in radioactivity and records

essentially the environmental dose stored over the burial period. The granites, however, usually have high radionuclide concentrations. The granite can then be dated by subtracting the environmental dose (obtained from the quartzite/sandstone) from their stored dose and then dividing by the difference in internal dose rate. This approach automatically corrects for any variation in environmental dose rate over the burial period. It should be noted, however, that the spatial arrangement of the rocks may influence the environmental dose to some extent.

2.13.5 Zircon Methods

The presence of zircon grains in ceramic matrices was noted through the observation of clusters of tracks on induced fission track maps (Zimmerman, 1971). The high density of tracks is due to the high U content of zircons (up to thousands of ppm). The resulting internal (alpha) dose rate is sufficiently high to effectively make both soil gamma and sherd beta dose rates negligible. This means that no knowledge is required of the burial environment or water content of the sherd.

Despite these favourable characteristics, there are also a number of drawbacks associated with zircons. Many grains exhibit short-term fading, and there is often zoning of their radioactivity and TL sensitivity, the two being anticorrelated. The latter point introduces practical difficulties concerning the geometry for artificial irradiation.

Sutton and Zimmerman (1976) developed a procedure for zircon dating, based on single grains in an attempt to overcome the difficulties posed by the grain to grain variability of TL sensitivity and internal radioactivity. The stored dose is determined from the ratio of the natural TL and the artificial TL induced by a pair of ^{241}Am sources positioned on either side of the grain. A correction has to be made since the grain size (approximately 60 microns or larger) is large compared to the alpha particle range. This technique is also dependent on there being no significant change in sensitivity between first and second glows. The dose rate is calculated from the U and Th concentrations obtained by induced fission methods. The results of a test programme were encouraging although the large amount of effort required, plus the number of possible problems, have

combined to give a technique that has not found widespread dating use.

An alternative approach (Sutton and Zimmerman, 1979) was investigated in which the problem of zoning was overcome by comparison of the natural TL signal with the TL signal that accumulates again after a storage period as a result of the grain's high internal radioactivity. This method removes the need for artificial irradiation and radioactivity measurements and the age equation becomes:

$$\text{Age} = \frac{\text{Natural TL}}{\text{Regrown TL}} \cdot \text{Storage Time} \qquad (2.28)$$

This method suffers from two main problems, firstly the regenerated TL signal is very low and secondly severe short term fading affects some grains. Regrowth and measurement of a much more sensitive low temperature peak (-120°C) has been attempted by Templer (1985). Here, the regrowth of the high temperature peak is inferred from measurements of the relative sensitivities. This method requires linearity over the range of the storage time up to the age of the sample (2 - 3 orders of magnitude). The current lack of accurate zircon dates suggests that these limitations are still significant.

2.13.6. Decay Methods

Charalambous and Michael (1976) claim that it is possible to obtain an artificial glow curve identical to the archaeological one, and from the experimental conditions (temperature of irradiation, and dose rate) under which the identity is achieved, it is possible to estimate the archaeological age of the sample.

The method does not require knowledge of the annual dose rate. This advantage is countered by the need to know the "equivalent" temperature of the sample over its burial time, and the assumptions that the TL sensitivity does not change after the first heating

and that the distribution of changes in traps of different depths is independent of dose rate and irradiation temperatures.

Langouet *et al* (1980) also proposed a decay method, D.A.T.E., based on minerals having two peaks - the first whose lifetime is too short for linear accumulation of trapped charges and the second, a high temperature peak with linear accumulation of trapped charges. The age can be determined by comparison of the trapped charges.

2.13.7 Mejdahl's Approach

Mejdahl (1983) described a dating programme of ceramics and burnt stones, in which a variety of minerals and grain sizes were used. Large grains (1-2mm) of potassium rich feldspar receive more than 50% of their total dose from their internal potassium, while plagioclase and quartz inclusion have progressively less internal beta activity. The age equation for grains of various size and mineral type from the same sample can be rewritten as:

$$\text{Stored Dose} = \text{Age}(\text{env} + B_M + B_G) \qquad (2.29)$$

$$\text{Stored Dose} = \text{Age}.\text{env} + \text{Age}.B \qquad (2.30)$$

B_M = Beta dose rate from matrix

B_G = Grains' internal β beta dose rate

$B = B_M + B_G$

env = environmental dose rate

A plot of the stored dose as a function of B will give a straight line of slope A and y-intercept A.E. Consequently, the age of the sample can be determined from the stored dose and beta dose, independently of the environmental dose rate.

Greater accuracy is theoretically achievable using this approach, compared to Fleming and Stoneham's "two-point" isochron, since more than two quantities are measured. However, the technique does require the sample to contain a sufficiently large variety of mineral types and grain sizes and the ability to successfully separate them.

A variation of the above approach has been described by Goedicke (1985), that utilises the effect of grain size on effective dose to provide the differences in stored dose. The approach was tested uses quartz grains (up to 750 microns) with promising results. However, it seems unlikely in practice that many samples would yield a sufficient range of quartz grain sizes with favourable TL characteristics, and that the Mejdahl approach may therefore be more readily applicable for 'routine' analyses.

2.13 SUMMARY

This chapter has introduced dosimetry concepts and aspects of radioactivity and developed them in relation to thermoluminescence dosimetry. The microdosimetry of the methods formulated to date material from known gamma contexts has been discussed, followed by a critical presentation of some proposed methods for dealing with samples from unknown gamma contexts.

The conclusion is that a **general** isochron formulation is the only real approach.
The next chapter will introduce the isochron model through the formulation of a generalised luminescence age equation. The systematic investigation of potential isochron systems through theoretical simulation of this model is then presented.

3.ISOCHRONS I - FORMULATION AND SIMULATION

3.1 INTRODUCTION

In this chapter the basic concepts of pottery microdosimetry are developed to provide a theoretical basis for the experimental work that follows in Chapters 4 and 5. The simple age equation is developed into a generalised form. It will be shown that this can lead to an isochron formulation whereby the relationships between stored dose and internal dose rates for all mineral phases may be used to estimate TL age and external dose rates. In this manner it is possible in principle to date destratified material. This has been investigated using a simulation program that makes use of attenuation factors calculated by Mejdahl (1979; 1983) and Bell (1980). The program is described and the isochron plots produced are illustrated and discussed.

3.2 GENERALISATION OF THE LINEAR AGE EQUATION

The simplest form of the TL age equation, as given in section 1.4, is

$$\text{TL Age} = \frac{\text{Stored Dose}}{\text{Dose Rate}} \qquad (3.1)$$

However, as Chapter 2 has illustrated, the dosimetry of pottery sherds is dependent on a number of factors (eg grain size, mineralogy, water content, origin of the dose components, ie from within the sherd (or grain) or from the surrounding burial environment, etc). In order to enable practicable solutions of the age equation to be produced these factors have to be taken into account and certain approximations and assumptions made. This approach to the problem has resulted in the formulation of the "fine-grain" and "quartz-inclusion" techniques which apply to specific grain sizes and mineral types. These techniques also reflect the influences of their differences in microdosimetry. The inclusion method, for example, in which the alpha contribution can be removed (or greatly reduced) by HF etching, is more sensitive to the external radiation field than the fine-grain method (unless high potassium feldspar inclusions are

used, see section 2.12.3 and Mejdahl, 1983). In the fine-grain method, the internal alpha dose contribution from the sherd (and grain) becomes significant, despite the lower efficiency for producing TL for alpha radiation.

It then follows that as a result of their microdosimetric differences, grains of different sizes and mineral types from the same sherd (and therefore of the same TL age) will also have different stored doses. It can be concluded that strictly speaking each grain size and mineral type has its own unique TL age equation. Alternatively, if the above concepts are considered for a general case by defining the absorbed dose fractions and attenuation factors in terms that apply to all grains and then, imposing the isochron constraint, the microdosimetric contrasts within each sample can be explored.

As a starting point the dry infinite matrix dose rates for the grain, G, pottery matrix, M and surrounding soil, S, are defined as:

$$\dot{D}_{\alpha}^{G} \qquad \dot{D}_{\alpha}^{M} \qquad \dot{D}_{\alpha}^{S}$$

$$\dot{D}_{\beta}^{G} \qquad \dot{D}_{\beta}^{M} \qquad \dot{D}_{\beta}^{S}$$

$$\dot{D}_{\gamma}^{G} \qquad \dot{D}_{\gamma}^{M} \qquad \dot{D}_{\gamma}^{S}$$

The mean absorbed dose fraction, Φ, summed over all nuclides, for grain species (d) is defined as

$$\Phi(d) = \frac{\Sigma f_i \phi_i(d)}{\Sigma f_i} \qquad (3.2)$$

where f_i is the fractional dose contribution for nuclide i and $\varnothing_i$ is the absorbed dose fraction for nuclide i.

It is also necessary to define and to take into account water attenuation factors, $fw^{M,S}\alpha,\beta,\gamma$, which compensate for the fact that water present within the system will act as an inert absorber of radiation that would otherwise be involved in the production of TL within the mineral grains. These correction factors have been described in Section 2.10. Similarly, the lower efficiency of alpha radiation for producing TL must also be considered, and the alpha efficiency factor, k, must be incorporated into the fully, generalised form of the TL age equation.

In its generalised form, using the following symbols for Luminescence Age (A), Stored Dose (Q) and the effective dose rate terms (Ψ) for grain species (d), the luminescence age equation can be written as

$$A(d) = \frac{Q(d)}{\Psi_\alpha(d) + \Psi_\beta(d) + \Psi_\gamma(d)} \qquad (3.3)$$

where the effective dose rate terms (Ψ) to grain species (d) are defined as

$$\begin{aligned}
\Psi_\alpha(d) &= k[\Phi_\alpha^G \dot{D}_\alpha^G + fw_\alpha^M(1-\Phi_\alpha^M)\dot{D}_\alpha^M + fw_\alpha^S(1-\Phi_\alpha^M)\dot{D}_\alpha^S) \\
\Psi_\beta(d) &= \Phi_\beta^G \dot{D}_\beta^G + fw_\beta^M(1-\Phi_\beta^M)\dot{D}_\beta^M + fw_\beta^S(1-\Phi_\beta^S)\dot{D}_\beta^S \qquad (3.4) \\
\Psi_\gamma(d) &= \Phi_\gamma^G \dot{D}_\gamma^G + fw_\gamma^M(1-\Phi_\gamma^M)\dot{D}_\gamma^M + fw_\gamma^S(1-\Phi_\gamma^S)\dot{D}_\gamma^S
\end{aligned}$$

where

$\varnothing$	=	mean absorbed dose fraction	
$(1-\varnothing)$	=	attenuation factor for a grain of diameter, d, microns	
D	=	dry infinite matrix dose rate	
fw	=	water correction factor	
G	=	mineral grain	
M	=	pottery matrix	
S	=	surrounding soil	

k = alpha efficiency

The full form of the age equation (3.3) includes terms which are negligible in practice. For example the gamma dose of the grain and matrix, and the external alpha and beta contributions will all be effectively zero in practical applications. Thus if the following approximations are made

$$\Phi_\gamma^G \dot{D}_\gamma^G \rightarrow 0 \qquad (1)$$

$$fw_\gamma^M (1-\Phi_\gamma^M) \dot{D}_\gamma^M \rightarrow 0 \qquad (2)$$

$$fw_\beta^S (1-\Phi_\beta^S) \dot{D}_\beta^S \rightarrow 0 \qquad (3)$$

$$fw_\alpha^S (1-\Phi_\alpha^S) \dot{D}_\alpha^S \rightarrow 0 \qquad (4)$$

where

(1) = gamma self dose of the grain

(2) = attenuated gamma dose from the matrix

(3) = attenuated beta dose from the soil

(4) = attenuated alpha dose from the soil

The effective internal and external dose rate components, $\Psi_{int}(j)$ and $\Psi_{ext}(j)$, can be defined as

$$\Psi_{internal}(d) = k[\Phi_\alpha^G \dot{D}_\alpha^G + fw_\alpha^M (1-\Phi_\alpha^M)\dot{D}_\alpha^M] + \Phi_\beta^G \dot{D}_\beta^G + fw_\beta^M (1-\Phi_\beta^M)\dot{D}_\beta^M \qquad (3.7)$$

$$\Psi_{external}(d) = fw_\gamma^S (1-\Phi_\gamma^S)\dot{D}_\gamma^S + (1-\Phi_{cosmic})\dot{D}_{cosmic} \qquad (3.8)$$

This reduced form of the equation for practical applications thus becomes

$$A(d) = \frac{Q(d)}{\Psi_{internal}(d) + \Psi_{external}(d)} \qquad (3.9)$$

This illustrates the possibility of resolving the dose rate term into internal components and external components with reference to the sherd.

3.3 FORMULATION OF AN ISOCHRON APPROACH

If one considers different mineral phases from within the same sample then they will experience a common external component, but their internal dose rates may differ and hence their stored doses per unit time. Equation 3. can then be rearranged into the form

$$Q(d) = A(d)\Psi_{internal}(d) + A(d)\Psi_{external}(d) \qquad (3.10)$$

For grains of common age the system is linear with stored dose and internal dose rate. These are measurable parameters and from a plot of internal dose rate versus stored dose the slope is equivalent to the TL age and the y-axis intercept is the product of the TL age and the external (gamma plus cosmic) dose rate. This is an **isochron solution.**

This approach enables the TL age of a sample to be determined independently of any knowledge of its burial environment and at the same time an estimate of this soil gamma dose rate can be obtained.

Isochron dating systems yield more information than simply an age estimation, in isotope geology studies for instance, where these systems are routinely used, the intercept gives an indication of the initial isotope ratios. In TL studies, as stated above, the extra information is a measure of the environmental γ + cosmic dose rate component. Two examples of this approach are given by Mejdahl (1983) and Goedicke (1985), and a third, using ESR, by Karakostanoglou and Schwarz (1983).

3.4 ABSORBED DOSE FRACTIONS AND ATTENUATION FACTORS

To apply this concept the microdosimetric basis of fine-grain and inclusion approaches must be extended, ie in order to be able to increase the range of grain sizes normally employed, to include intermediate and larger grains, the appropriate absorbed dose fractions (Φ) and attenuation factors ($1 - \Phi$) must be known. These values have been calculated by Mejdahl (1979) for the beta dose and Bell (1980) for the alpha dose and the attenuation factors for gamma radiation which are very small have also been determined by Mejdahl (1983) and Carriveau (1983).

These have been calculated for quartz grains and form the basis of the simulation work to follow, they are presented in Tables 3.1, 3.2 and 3.3.

Grain size (microns)	Uranium	Thorium	Potassium
1	0.010	0.009	0
5	0.053	0.045	0
10	0.108	0.093	0
15	0.166	0.141	0
20	0.228	0.193	0
30	0.372	0.310	0
40	0.498	0.433	0
50	0.586	0.529	0
60	0.650	0.598	0
70	0.697	0.651	0
80	0.734	0.692	0
90	0.762	0.725	0
100	0.785	0.752	0
120	0.813	0.784	0
150	0.856	0.833	0
200	0.892	0.874	0
250	0.913	0.899	0
300	0927	0.916	0
400	0.946	0.937	0
500	0.957	0.950	0
1000	0.978	0.975	0
2000	0.900	0.990	0
3000	1.000	1.000	0
4000	1.000	1.000	0
5000	1.000	1.000	0
6000	1.000	1.000	0
8000	1.000	1.000	0
10000	1.000	1.000	0

TABLE 3.1 ALPHA ABSORBED DOSE FRACTIONS (AFTER BELL, 1980)

Grain size (microns)	Uranium	Thorium	Potassium
1	0.002	0.002	0.002
5	0.012	0.0225	0.0018
10	0.0214	0.0366	0.0035
15	0.0296	0.0484	0.0053
20	0.0366	0.0582	0.0071
30	0.0475	0.0743	0.0106
40	0.0564	0.0875	0.0141
50	0.0642	0.0988	0.0177
60	0.0713	0.1088	0.0212
70	0.0779	0.1181	0.0248
80	0.0840	0.1269	0.0283
90	0.0901	0.1351	0.0318
100	0.0957	0.1427	0.0354
120	0.106	0.158	0.0424
150	0.124	0.165	0.053
200	0.146	0.206	0.0702
250	0.169	0.229	0.0877
300	0.189	0.251	0.1052
400	0.230	0.288	0.1402
500	0.263	0.320	0.1748
1000	0.400	0.443	0.337
2000	0.568	0.604	0.571
3000	0.667	0.701	0.696
4000	0.731	0.760	0.765
5000	0.773	0.798	0.807
6000	0.803	0.825	0.837
8000	0.842	0.859	0.873
10000	0.866	0.879	0.896

TABLE 3.2 BETA ABSORBED DOSE FRACTIONS (AFTER MEJDAHL, 1979)

Grain size (microns)	Uranium	Thorium	Potassium
1	0	0	0
5	0	0	0
10	0	0	0
15	0	0	0
20	0	0	0
30	0	0	0
40	0	0	0
50	0	0	0
60	0	0	0
70	0	0	0
80	0	0	0
90	0	0	0
100	0	0	0
120	0	0	0
150	0	0	0
200	0	0	0
250	0	0	0
300	0	0	0
400	0	0	0
500	0	0	0
1000	0.001	0.001	0.001
2000	0.002	0.002	0.002
3000	0.003	0.003	0.003
4000	0.005	0.004	0.004
5000	0.007	0.007	0.007
6000	0.008	0.008	0.008
8000	0.010	0.010	0.010
10000	0.015	0.015	0.015

TABLE 3.3 GAMMA ABSORBED DOSE FRACTIONS (AFTER MEJDAHL, 1983)

3.5 SIMULATIONS FROM THE ISOCHRON MODEL

3.5.1 Introduction

Before investigating the isochron behaviour of luminescence samples experimentally it was decided to simulate the system in a computer model to explore the extent to which measurable differences in Q(d) and $\Psi(d)_{internal}$ might be expected. A simulation model and computer program were developed and used to investigate systematically the effects of variations in grain size, alpha efficiency, and internal radioactivity on isochron systems. Sensitivity analysis and the effects of random measurement errors on isochron age determination were also undertaken.

3.5.2 The Isochron Simulation Program

The isochron simulation program uses chosen values of matrix and grain properties (radionuclide concentrations and water content for the matrix, and size, internal radioactivity and alpha efficiency for the grain) to calculate the total effective internal dose rate to the grain. These calculations are carried out as described in previous sections and use published values for dose rate conversion factors, water correction factors, and absorbed dose fractions, as noted. The program has been structured so that it can be readily modified to incorporate any recalculated values. A flow diagram of the simulation program is given in Figure 3.1.

A value for the external gamma dose rate, $D\gamma$, can be chosen and for the purpose of these simulations an age of unity assumed. In this case, the stored dose will be numerically equivalent to the internal dose rate plus $D\gamma$. A plot of the internal dose rate vs the stored dose will have a slope of 1, and a y-axis intercept equal to $D\gamma$.

The program uses a weighted regression analysis routine to determine slope and intercept values (and associated errors). This feature, combined with the option to introduce random errors into the internal dose rate and stored dose values allows the error sensitivity of the model to be investigated.

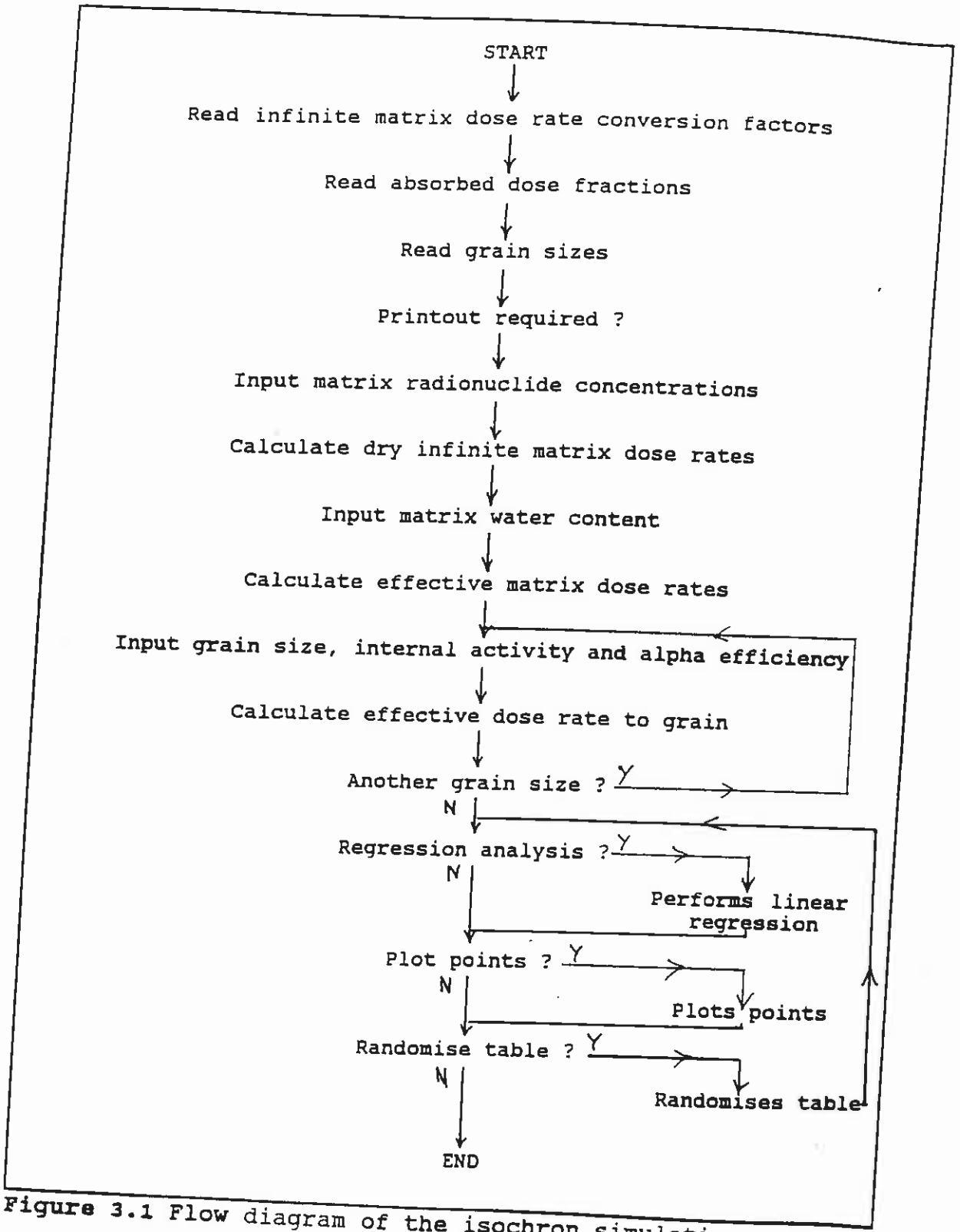

Figure 3.1 Flow diagram of the isochron simulation program.

The data can be obtained in hardcopy either as a tabulated printout of dose rate values or as an isochron plot or both.

The following section demonstrates the use of the program to investigate various isochron systems.

3.5.3 Investigation of the model: Simulated isochron plots

The simulation program described above was used to investigate systematically the characteristics of idealised isochron systems using precise values. The factors influencing microdosimetry; radionuclide content of matrix and grain, water content, grain size and alpha efficiency, as well as measurement errors were examined to assess the feasibility of practical measurement of such systems.

Initially, a simplified situation of activity free grains within a matrix of "typical" radionuclide concentrations (after Mejdahl, 1984) was examined for two cases. The first, shown in Figure 3.2, shows the influence of grain size differences on the microdosimetry (grains of 10, 30, 60, 90, 150, 500 μm were chosen). The second (Figure 3.3), illustrates a potential isochron plot based on the variation of alpha efficiency, the chosen values being 0, 0.05, 0.10, 0.15, 0.20, 0.25).

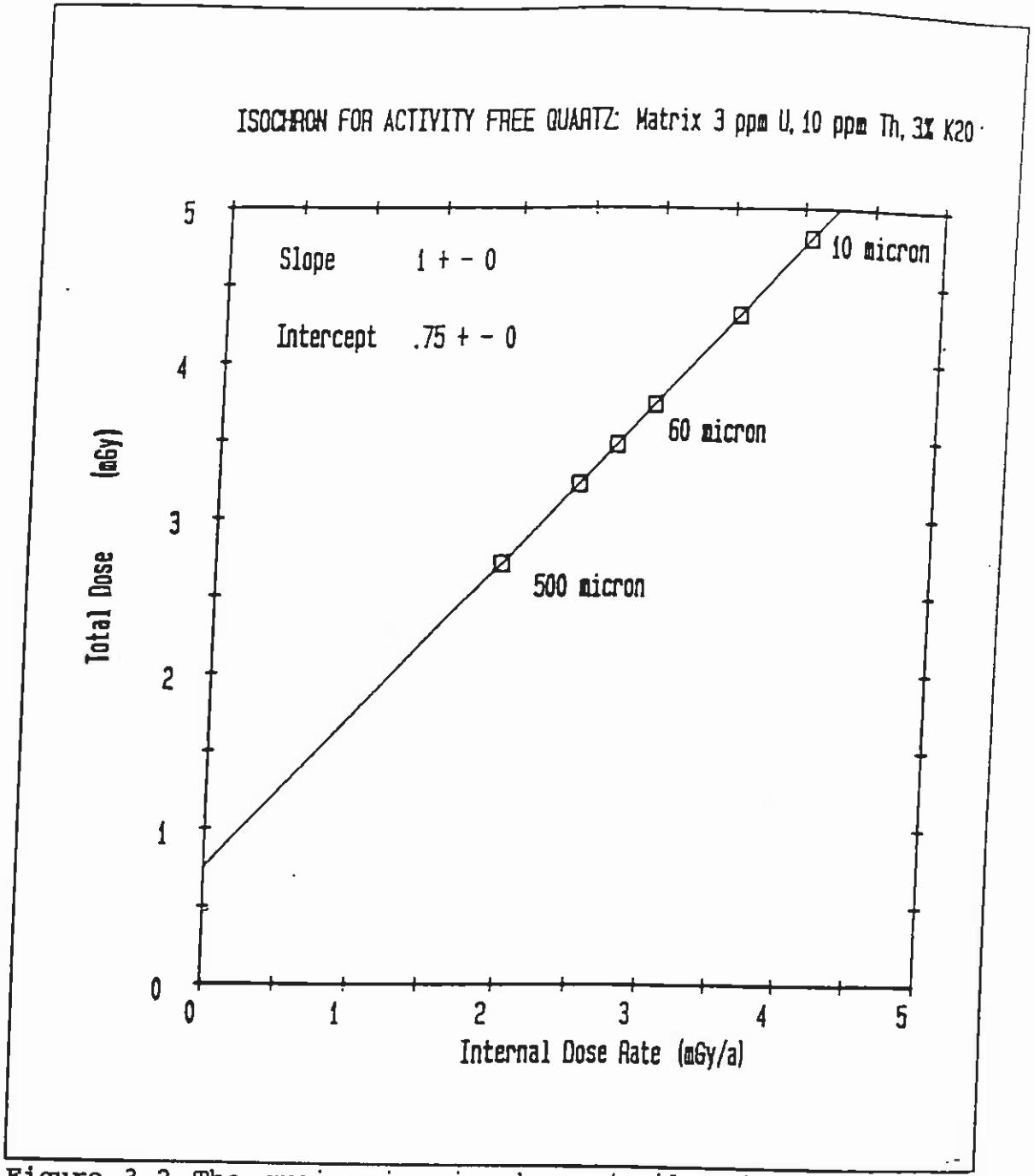

Figure 3.2 The grain size isochron (soil and matrix water content = 20%. Fixed alpha efficiency = 0.15)

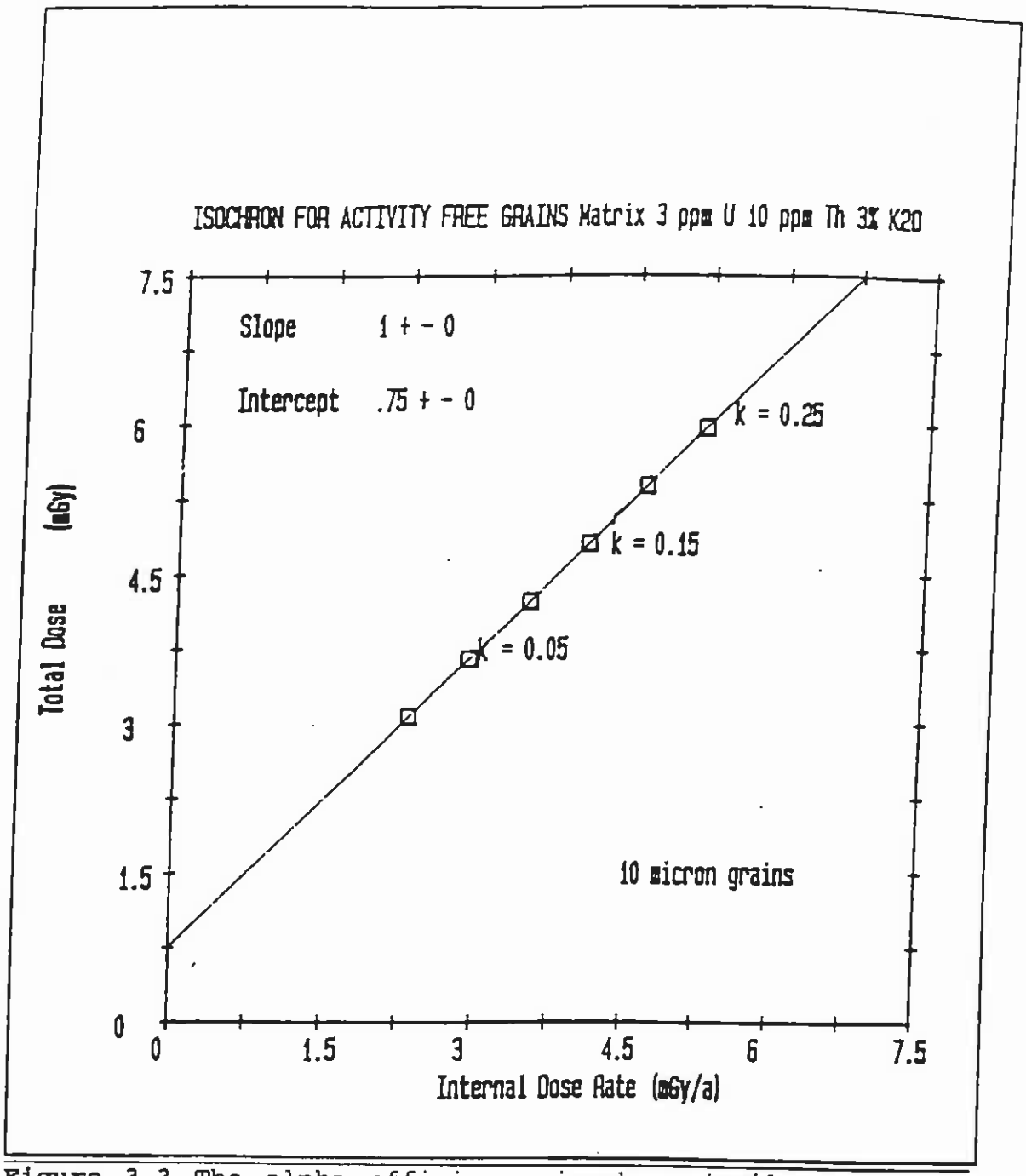

Figure 3.3 The alpha efficiency isochron.(soil and matrix water content = 20%, fixed grain size = 10 micron).

The following series of simulations, the grain size variations are the same as those used in Figure 3.2, and the alpha efficiency variations are those used in Figure 3.3.

The investigation of the effect of varying activity within mineral grains in a matrix of constant composition was based on Mejdahl's (1984) typical matrix. This allowed a systematic approach with the mineral activity being varied as a fraction of the matrix activity. These values are given in Table 3.4.

Mineral Activity (Fraction of Matrix value)	U ppm	Th ppm	K_2O %
0.05	0.15	0.5	0.15
0.10	0.30	1.0	0.30
0.25	0.75	2.5	0.75

TABLE 3.4 VALUES OF MINERAL ACTIVITY USED TO INVESTIGATE THEIR EFFECT ON THE ISOCHRON PLOTS

Fixed matrix composition

Fixed soil Dγ = 0.75 $mGy.a^{-1}$

Fixed soil H_2O = 0.20

Fixed Matrix H_2O = 0.20

Figures 3.4 (a)i to (a)iv show the effect of variation in mineral activity on the grain size isochron and Figures 3.4 (b)i to (b)iv show the effect on the alpha efficiency isochron.

The effect of matrix variations was based on data from Sanderson (1987, Table 4.3 and Figures 4.3 and 4.4) presented here as Table 3.5.

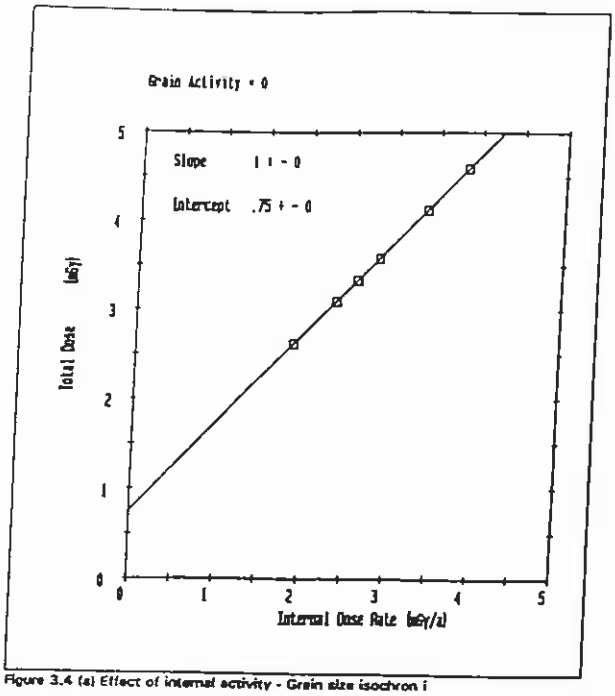

Figure 3.4 (a) Effect of internal activity - Grain size isochron i

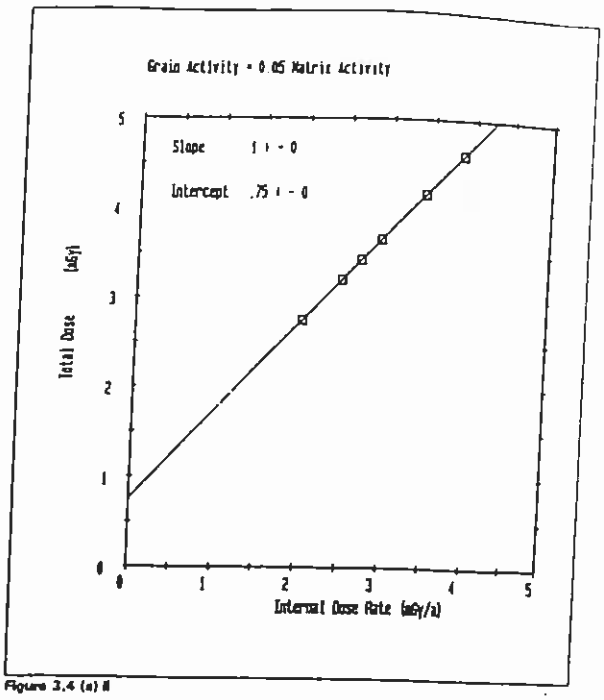

Figure 3.4 (a) ii

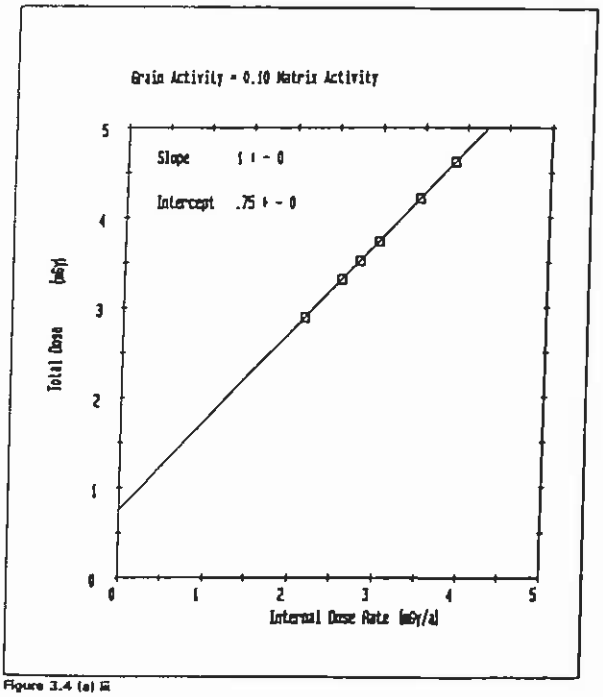

Figure 3.4 (a) iii

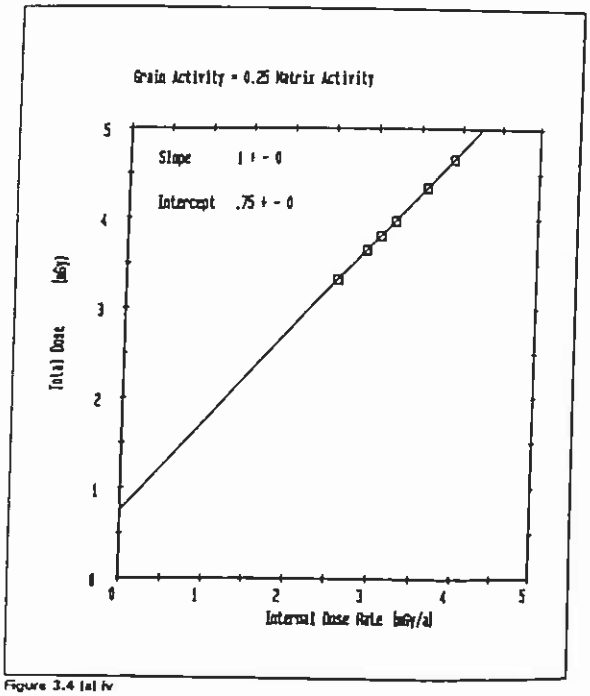

Figure 3.4 (a) iv

The series of isochron plots presented in Figure 3.4a show the effect of introducing internal radioactivity to the grains. As the internal activity of the grains increases, the coarser grains experience a greater increase in their total effective dose rate than the smaller grains. The corresponding increase in stored dose for the coarser grains, relative to the activity free case results in a shortening of the separation of the isochron points.

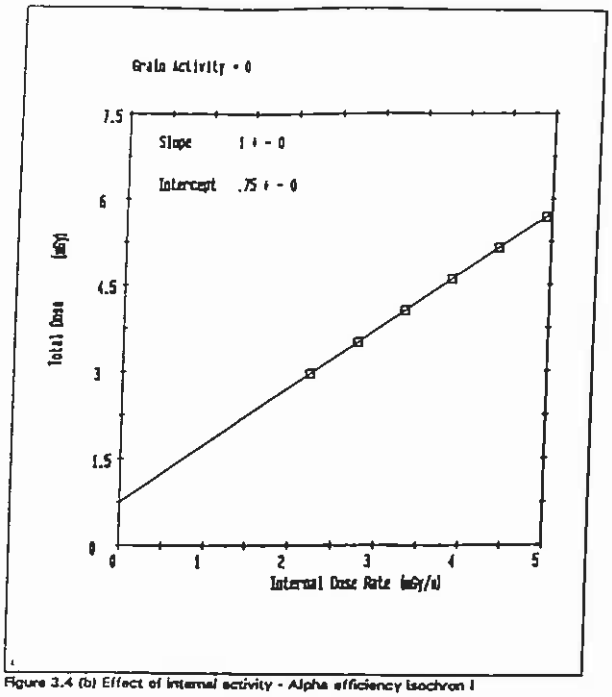

Figure 3.4 (b) Effect of internal activity - Alpha efficiency isochron I

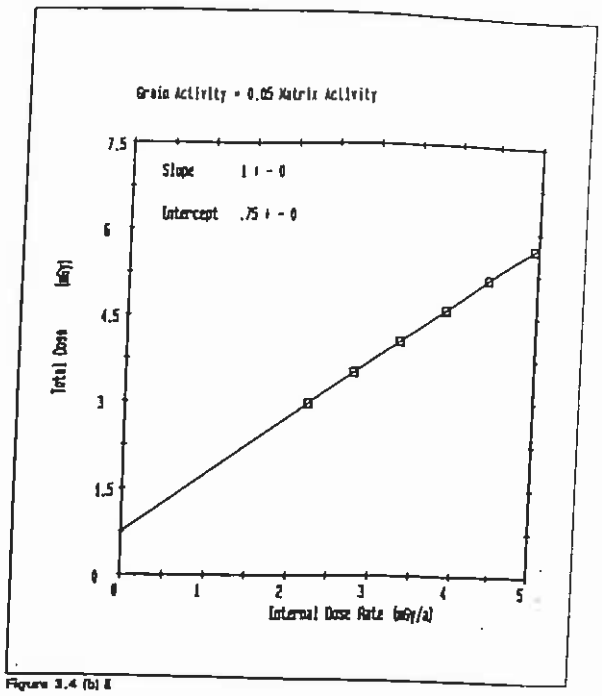

Figure 3.4 (b) ii

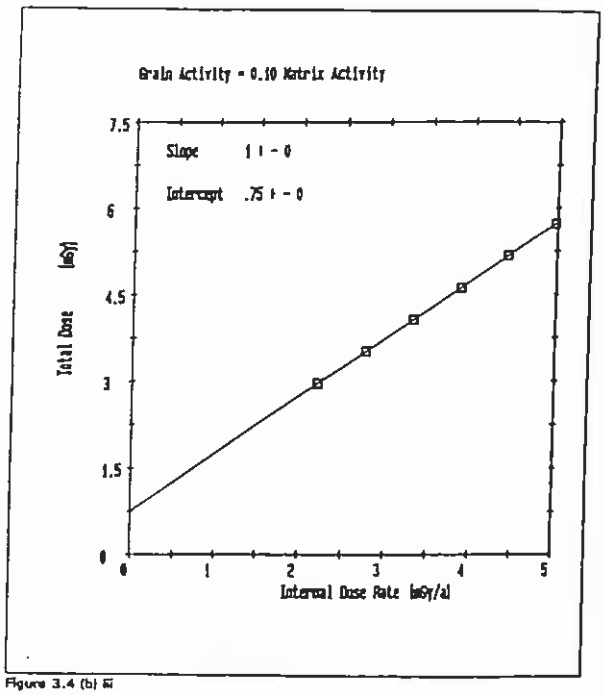

Figure 3.4 (b) iii

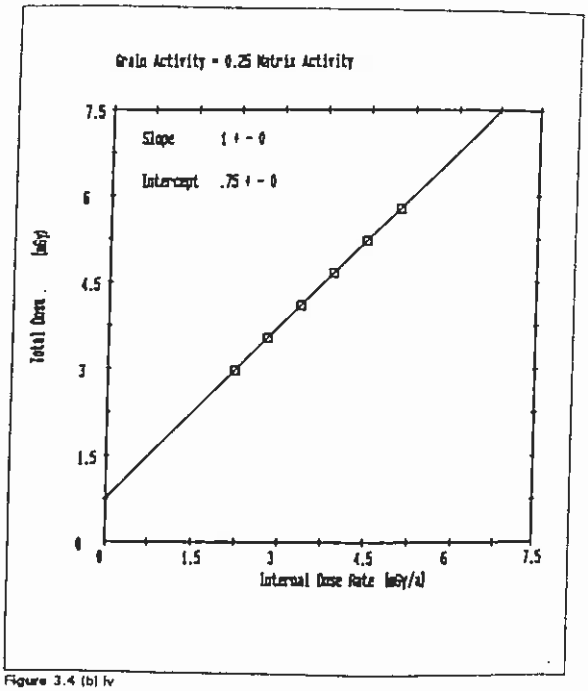

Figure 3.4 (b) iv

The series of isochron plots presented in Figure 3.4b shows the effect of introducing internal radioactivity to fine-grains (10 micron) of differing alpha efficiency. In contrast to the grain size plots, shown earlier, the effect here is to slightly increase the separation of points along the line. This results from the increased availability of an internal alpha dose component that will be preferentially recorded in the grains of higher alpha efficiency.

Site	Uppm	Thppm	Th/U ratio	$K_20\%$
Benderloch (B)	15.6	3.8	0.24	0.97
Burnt Isles (BI)	0.93	7.1	7.6	1.92
Craig Phadrig (CP)	2.2	8.8	3.96	4.33

TABLE 3.5 VALUES OF MATRIX ACTIVITY VARIATION USED TO INVESTIGATE THEIR EFFECT ON THE ISOCHRON PLOTS

Activity free grains
Fixed soil gamma = 0.75 mGy/a
Soil H_2O = 0.20
Matrix H_2O = 0.20

Figure 3.5 (a) shows the effect of matrix activity variation on the grain size isochron and Figure 3.5 (b) the effect on the alpha efficiency isochron. Figure 3.6 shows a summary of these results by plotting the difference of the end members for each data set, from which it can be concluded that the order of greatest separation of points is as follows:

B.AE > B.GS > CP.AE > CP.GS > BI.AE > BI.GS.

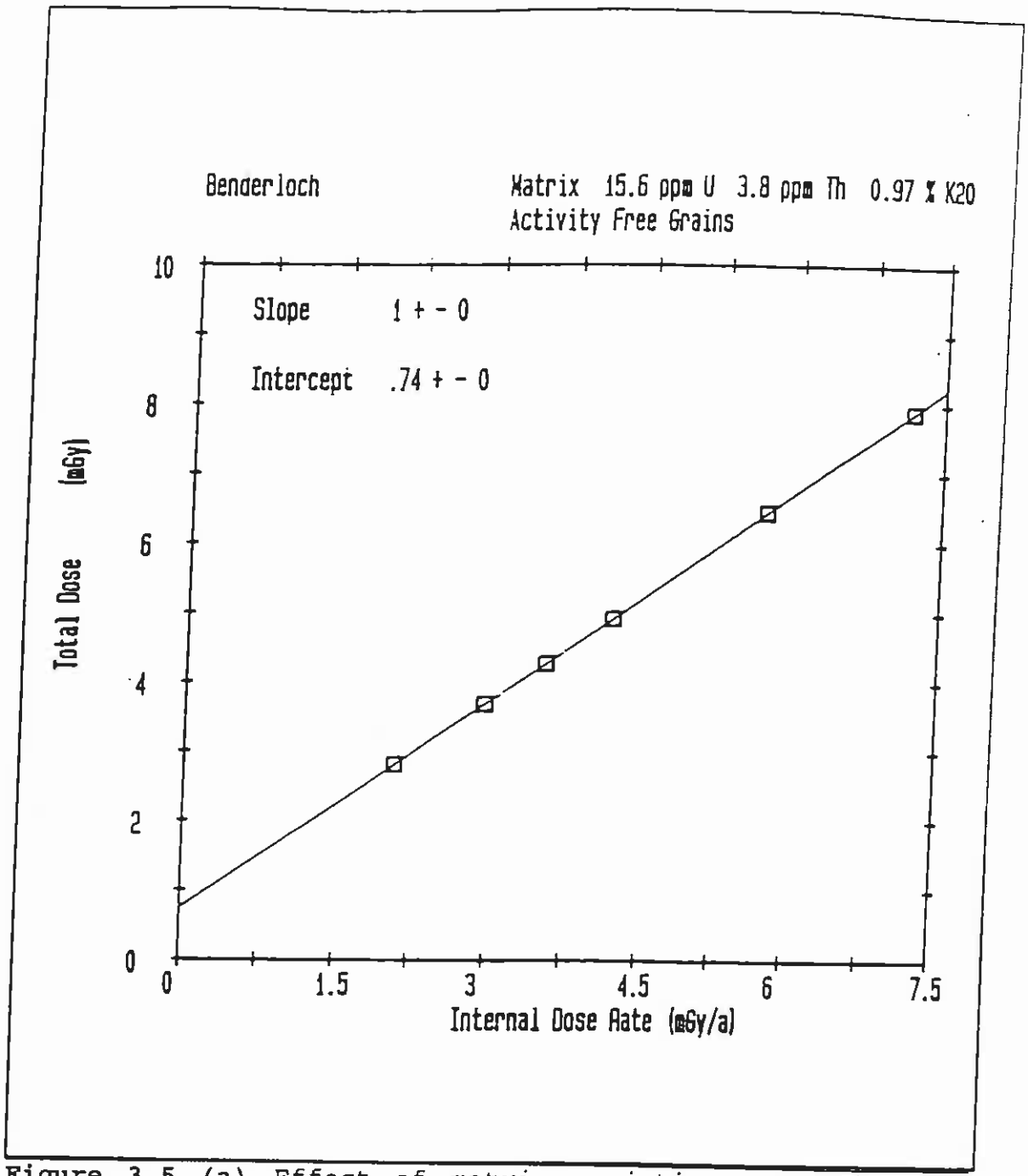

Figure 3.5 (a) Effect of matrix variations - Grain size isochron i

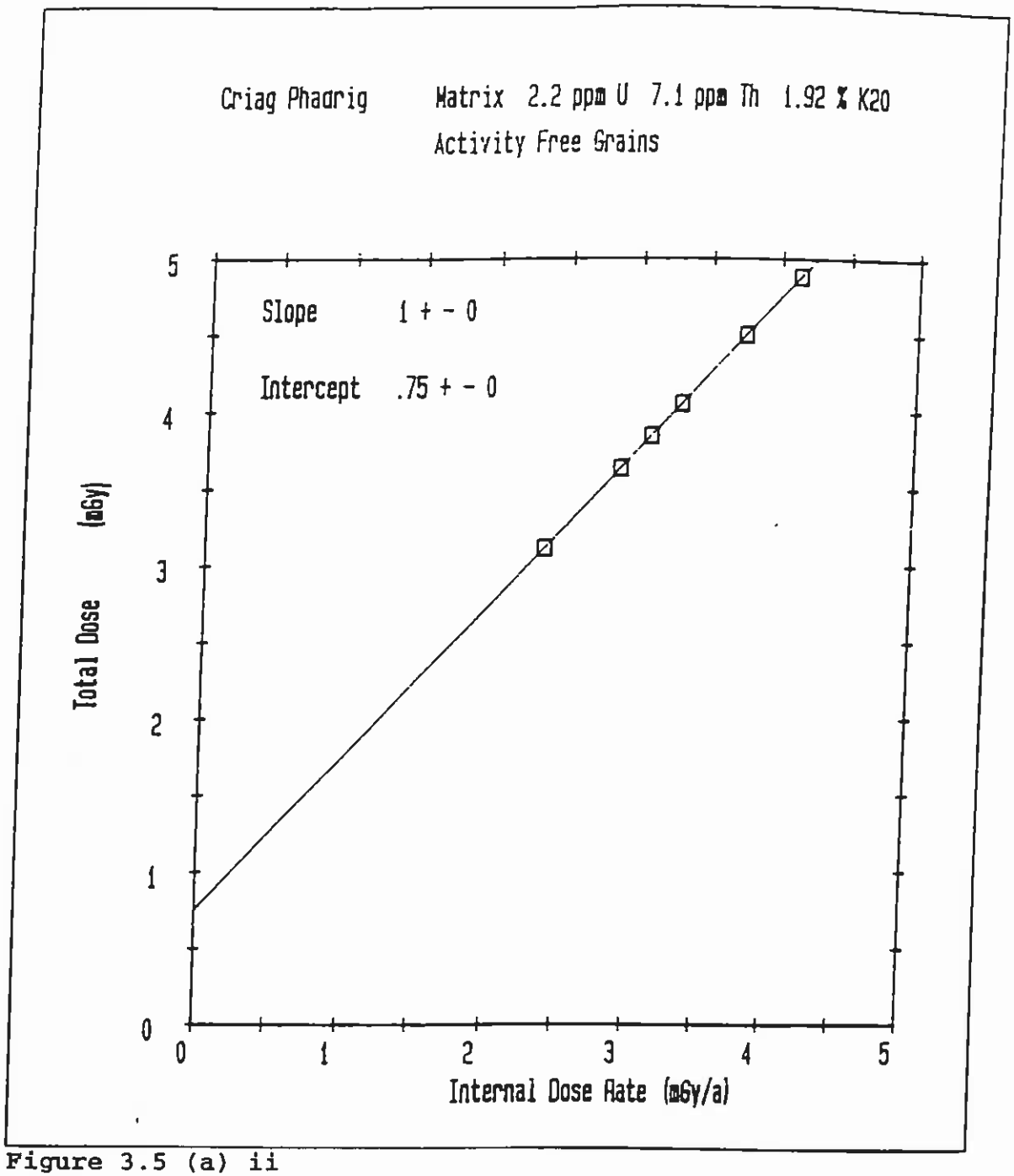

Figure 3.5 (a) ii

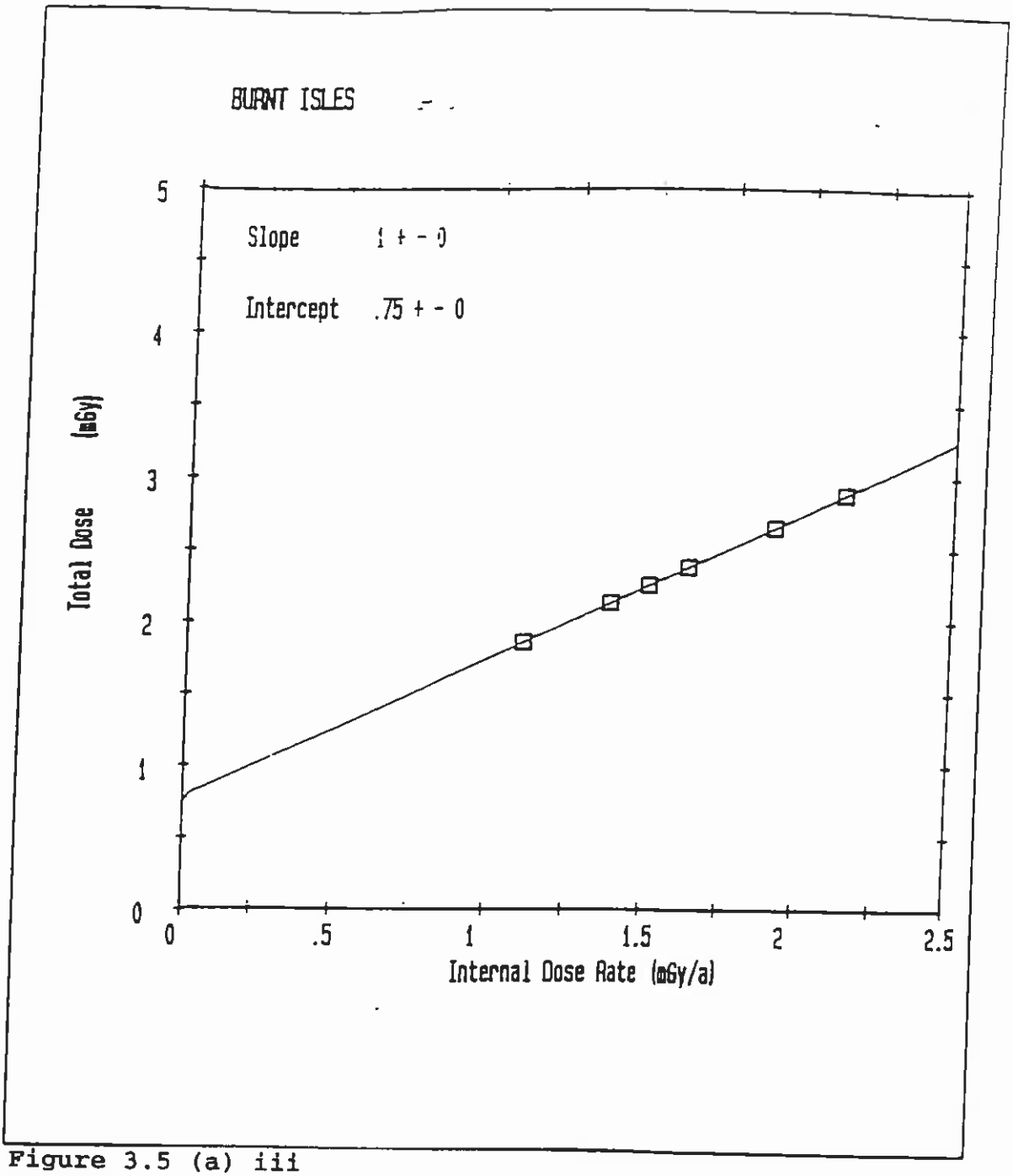

Figure 3.5 (a) iii

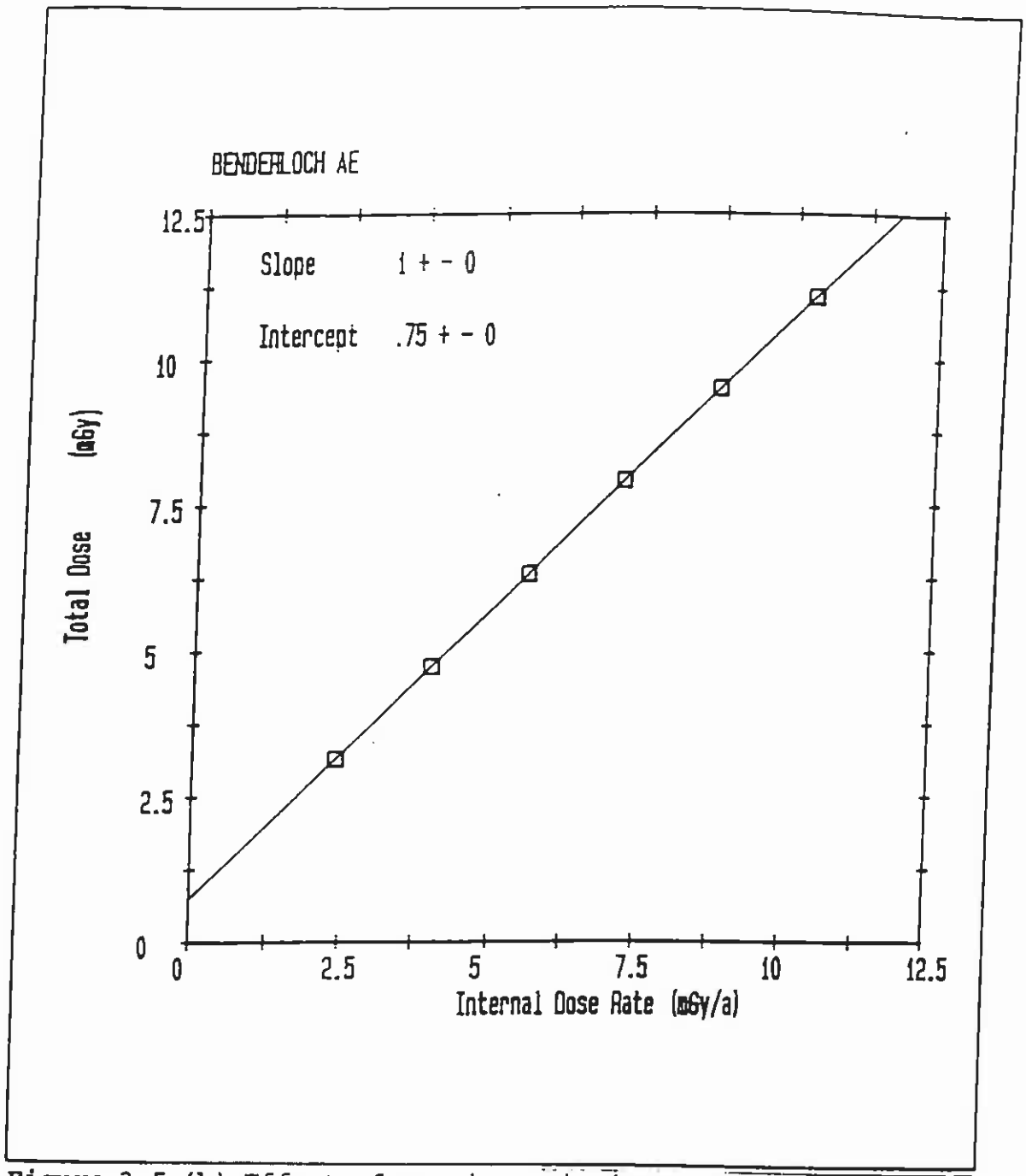

Figure 3.5 (b) Effect of matrix variations - Alpha efficiency isochron i

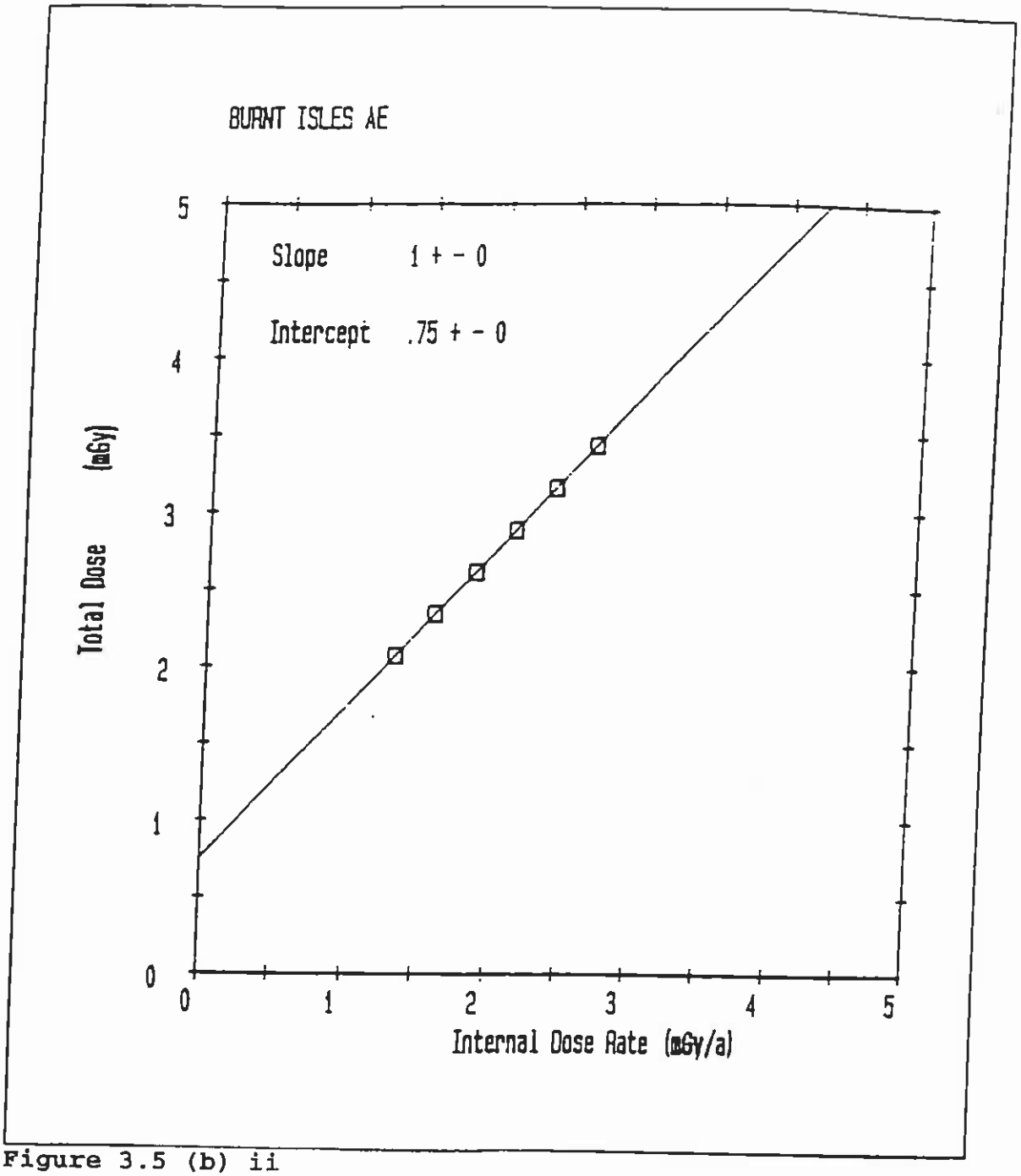

Figure 3.5 (b) ii

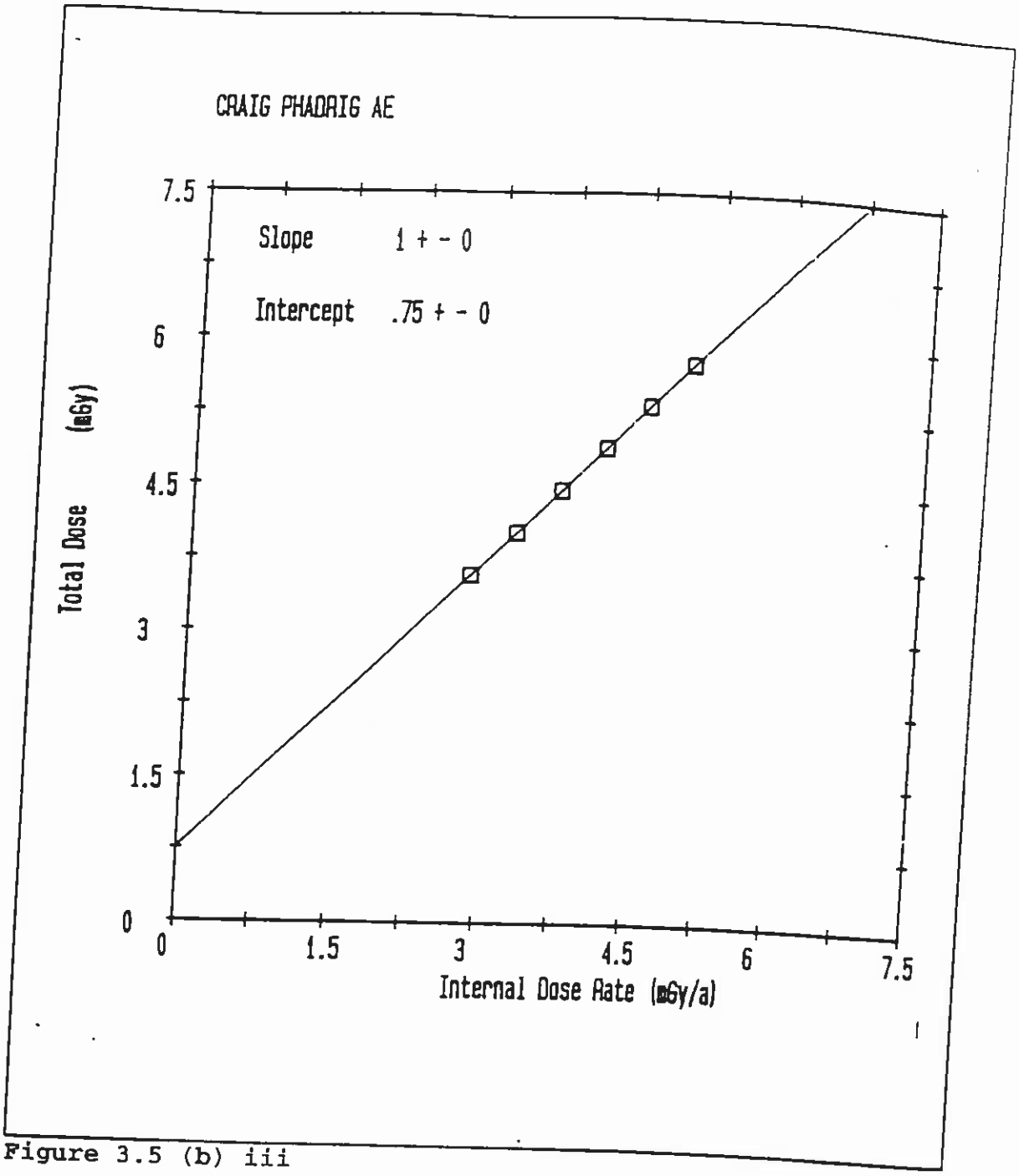

Figure 3.5 (b) iii

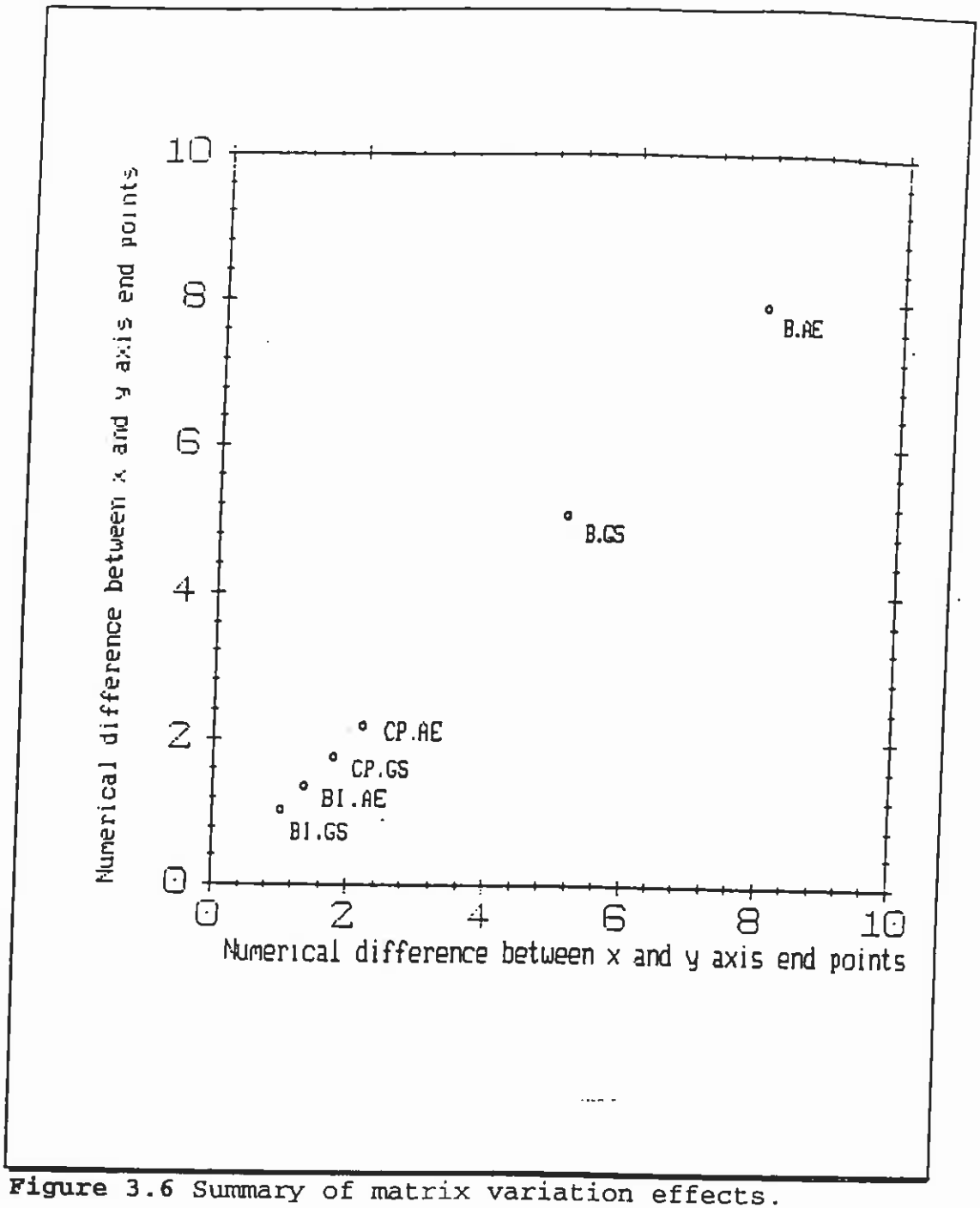

Figure 3.6 Summary of matrix variation effects.

The investigation into the possible range of isochron options was extended through examination of geochemical data to identify minerals of low, and high, internal radioactivity. Heavy mineral analyses of archaeological ceramics were studied to provide feasible mineral assemblages from ceramic matrices. The overall aim being to find isochron plots where the points were spaced as widely as possible so as to improve the regression analysis. An example of this is shown in Figures 3.7 and 3.8.

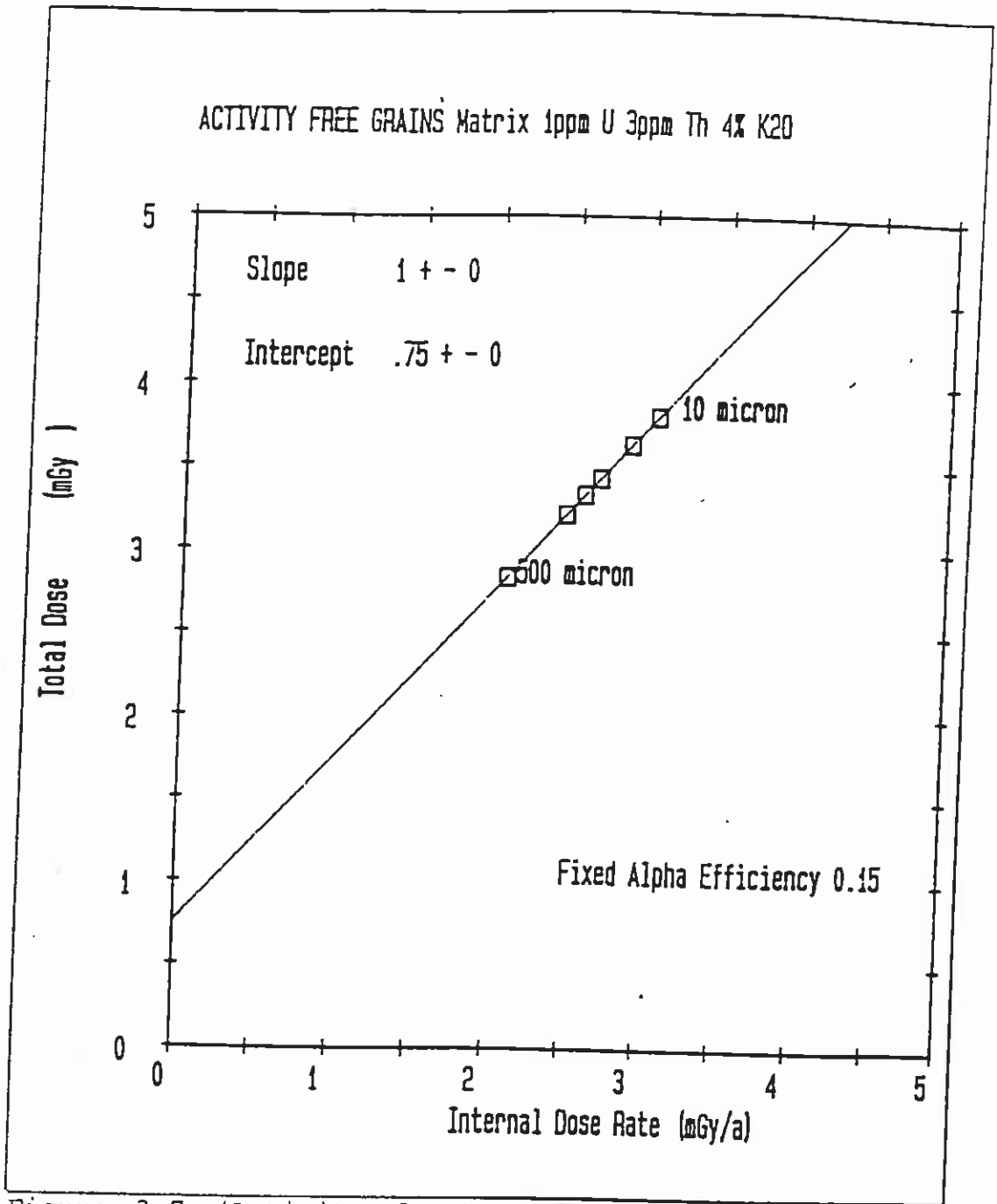

Figure 3.7 (Activity free) grain size isochron in a potassium rich matrix.

This plot shows explicitly how, in a potassium rich matrix where the dose rate is beta dominated, an (activity free) grain-size isochron plot largely reflects beta attenuation characteristics.

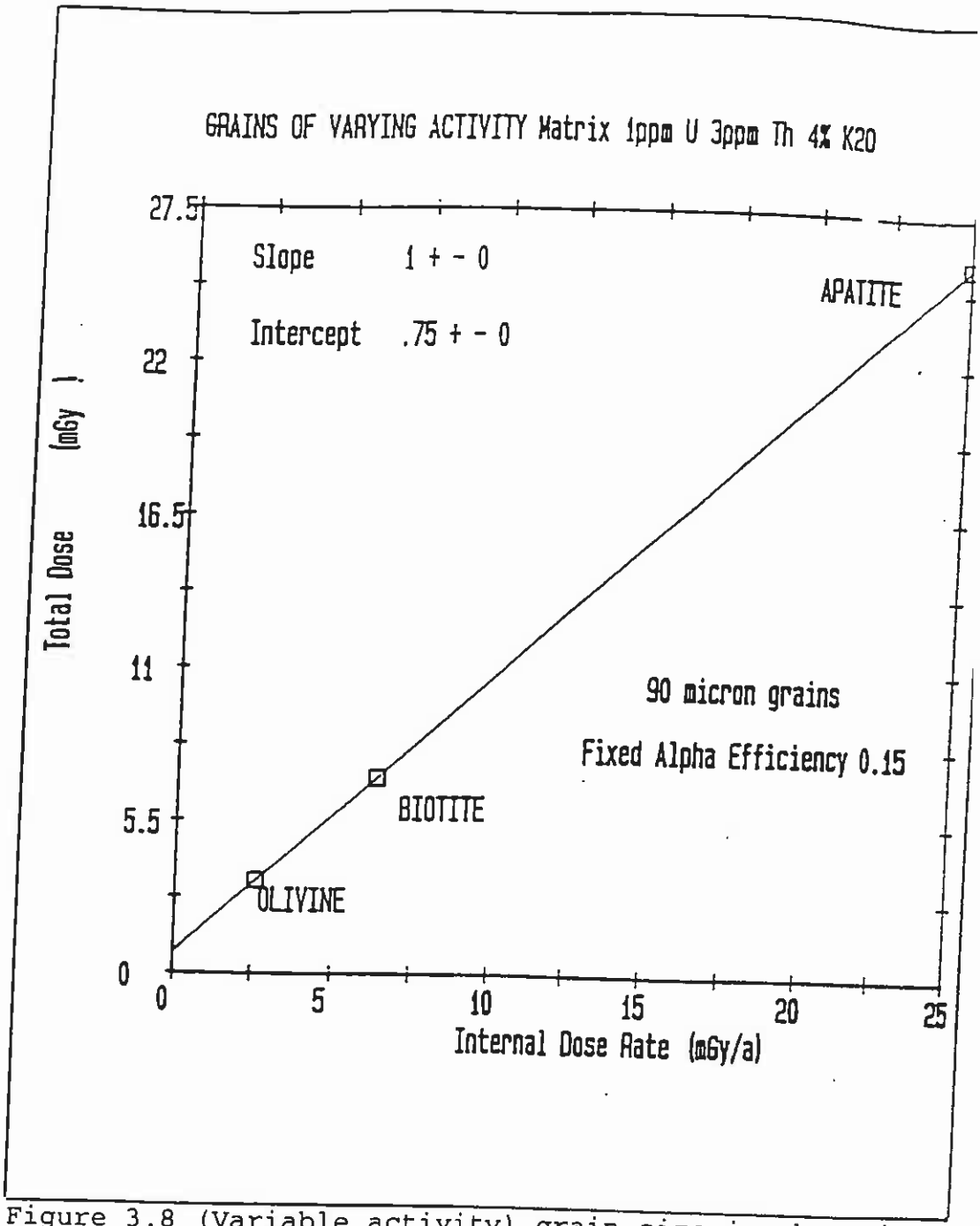

Figure 3.8 (Variable activity) grain size isochron in a potassium rich matrix.

In comparison to the previous figure, a much more promising plot may be obtained by measurement of grains of varying internal activity.

3.5.4 Investigation of the effect of matrix water content variation

This was achieved by maintaining all dosimetric parameters constant, except for the matrix water content which was varied between 0% and 100% in 25% steps. An assumption was that the soil water content was the same as that of the matrix (this is for clarity and convenience, since in practice only soil γ's would be effected by the soil H_2O, (α and β's having been eliminated).

Effective dose rates were calculated for three different values of water content. These are shown graphically in Figure 3.10 (a) for the grain size isochron and (b) for the alpha efficiency isochron.

These plots show that for both isochrons the points are more closely spaced the greater the H_2O content. For the grain-size plot the finer grains are affected to a greater extent than the coarser grains this is due to the fact that the fine grains receive a greater proportion of their dose from alphas which are attenuated by H_2O to a greater extent than betas or gammas.

The rate of change in effective dose rate also appears to be greater at the finer end of the grain size scale. Similarly, for the alpha efficiency plot, the higher efficiency points are affected more than the lower points. This may have very important implications if one considers a case where the matrix water content changes during the burial time.Here, if a sample becomes significantly wetter, or drier at some stage of the burial period then the stored dose may be composed of two (or more) periods of different effective dose rates.

Seasonal variation in H_2O content will be averaged out and it is the longer term variations that will be significant. Also, if different parts of a sherd have experienced differing water content histories, eg a thick sherd, perhaps with a dense centre and more porous outer parts then even when the outer 2mm have been removed then the is crushed for grain removal, the two different H_2O histories will be mixed.

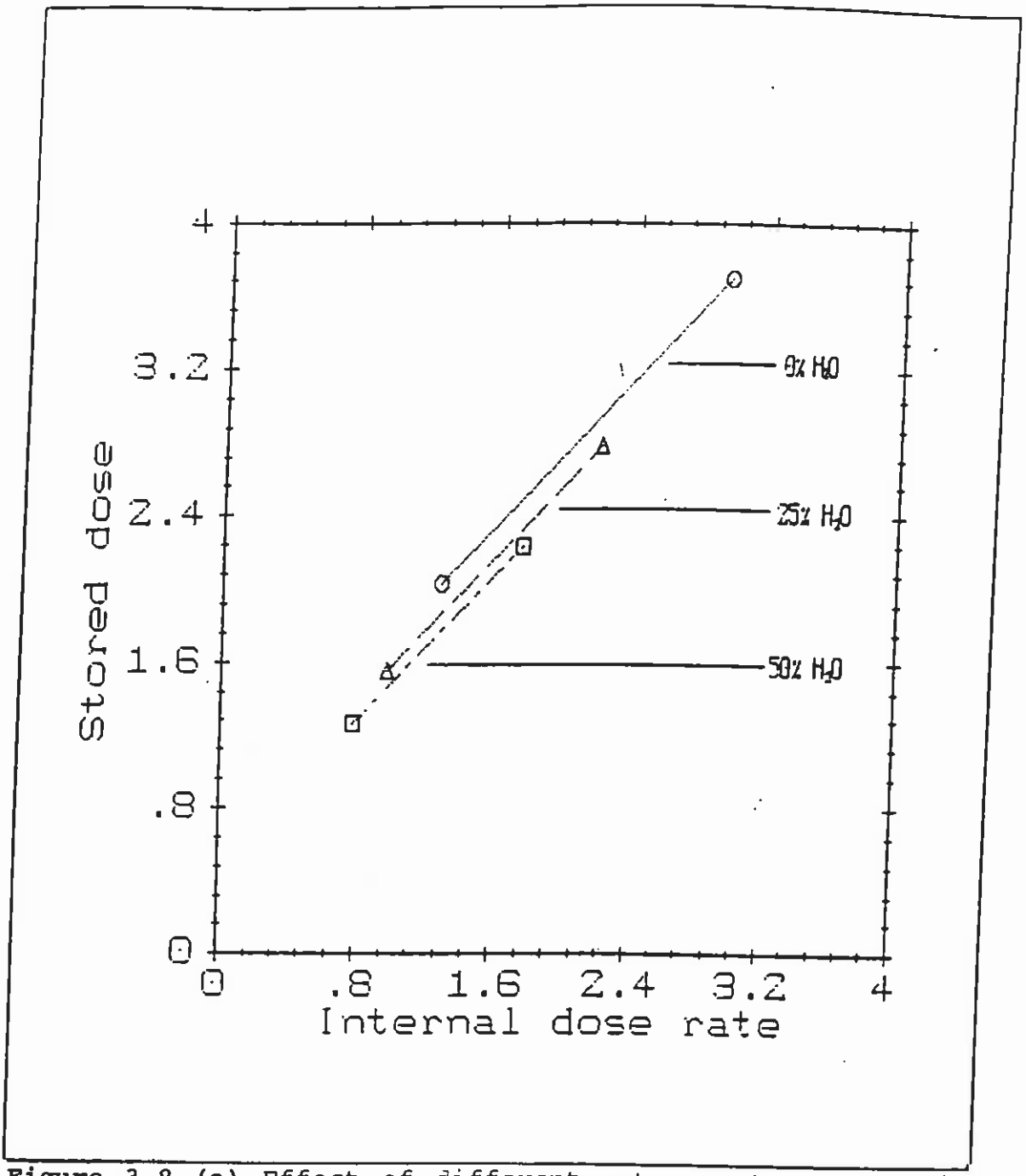

Figure 3.8 (a) Effect of different water contents - Grain size isochron.

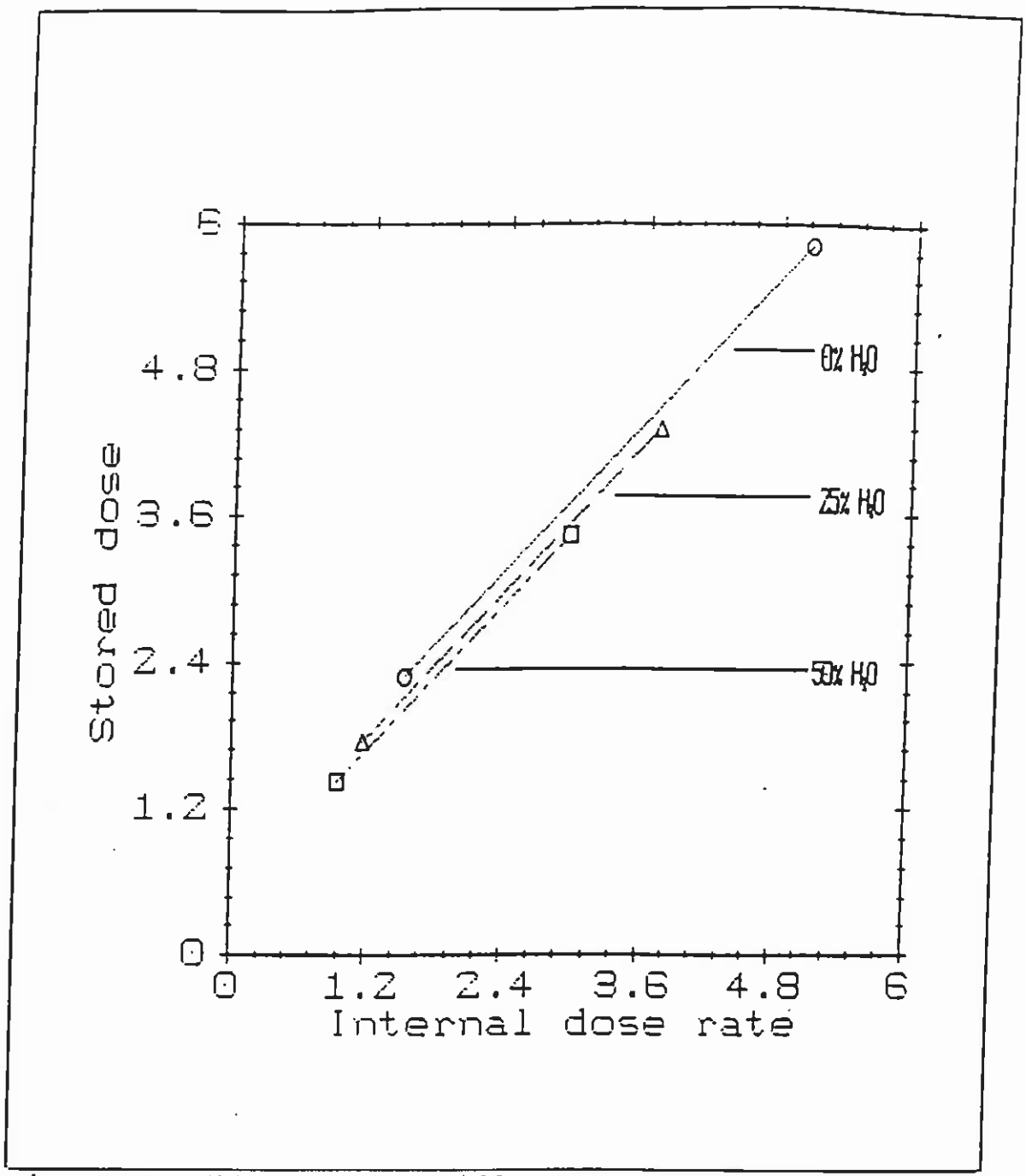

Figure 3.8 (b) Effect of different water contents - Alpha efficiency isochron.

3.6 ERROR SENSITIVITY OF THE MODEL

One of the options available in the isochron simulation program was to be able to introduce random errors into the data prior to regression analysis. This was achieved by generating two independent normal 0-1 variables, X1 and X2, from two independent uniform 0-1 random variables, U1 and U2 obtained from the RND function of the Apple computer, using the following expressions supplied by Scott (pers comm 1988).

$$X1 = \sqrt{-2.\log_e U1} \;.\; \cos 2\pi U2 \qquad (3.11)$$

$$X1 = \sqrt{-2.\log_e U1} \;.\; \sin 2\pi U2 \qquad (3.12)$$

The chosen percentage variations in the x and y axes, P1 and P2 respectively are then used to calculate the new values of x and y from the equation.

$$x = x+(x+p1.X1/100) \qquad (3.13)$$

The calculation is performed on each x and y value in the data set and then regression analysis calculate the slope and intercept and their associated errors. The program was also modified so as to read in the data points for the perfect line plot (Figures 3.2 and 3.3) from a separate file and to then carry out repeated randomisation of that file. The printout provides a record of the slope and intercept values with their errors which could be saved on disc. Their mean and standard deviation and the maximum and minimum values. A simple histogramming program was also included to produce a frequency table of the results. A further modification was to produce a version that performed the same function but with a printout restricted to the mean values, standard deviation, maximum and minimum values and the frequency table. The screen display was also reduced so as to reduce the calculation time for large numbers of runs. Histograms of the results of 500 repeated randomisation routines on the perfect line data are presented in Figures 3.9 (a) and 3.9 (b) for various percentage random variations in the x and y axes.

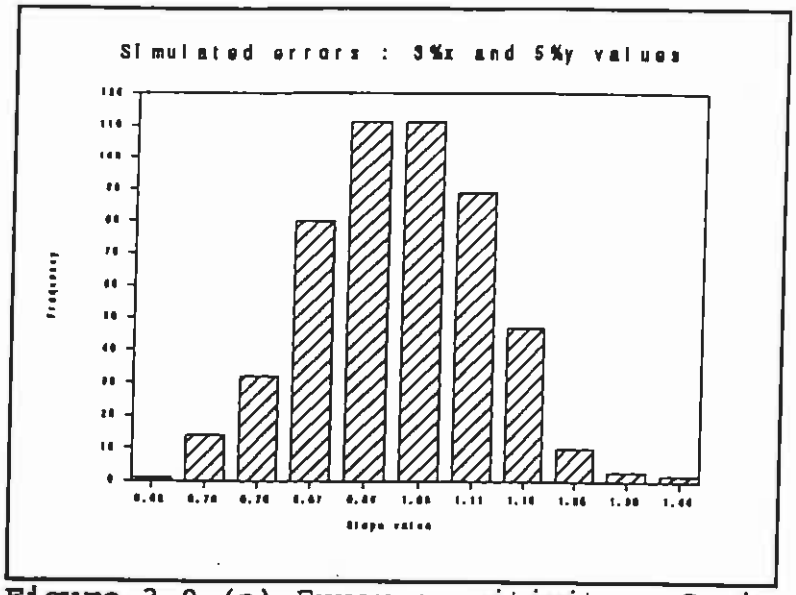

Figure 3.9 (a) Error sensitivity - Grain size isochron i

Mean = 1.00 std.dev. = 0.13

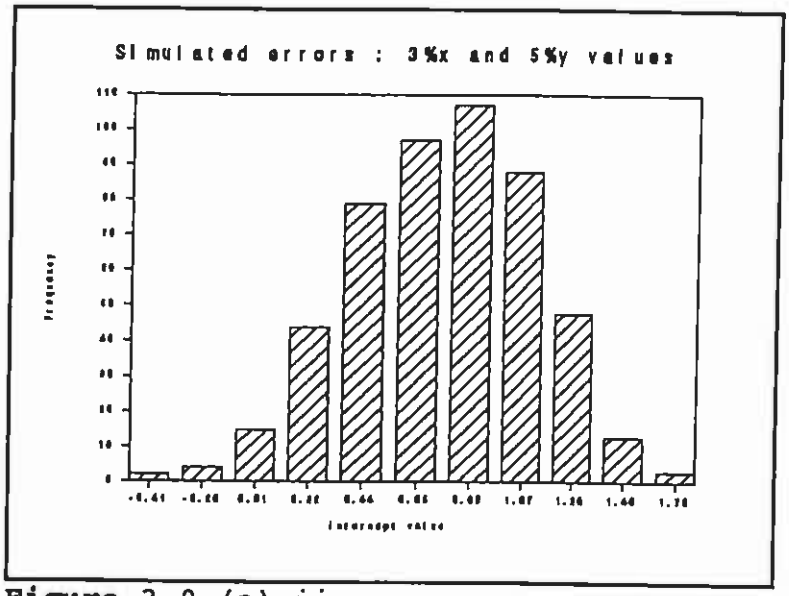

Figure 3.9 (a) ii

Mean = 0.76 std.dev. 0.37

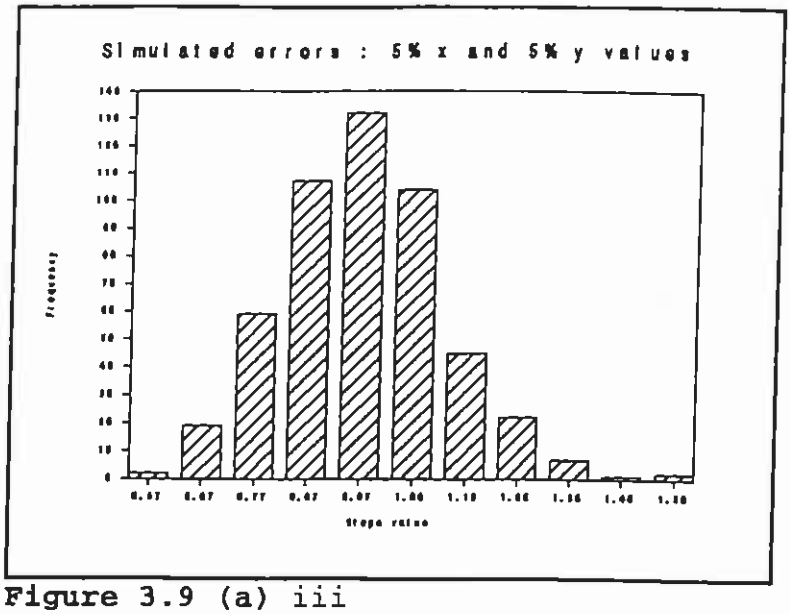

Figure 3.9 (a) iii

Mean = 0.98 std.dev. = 0.16

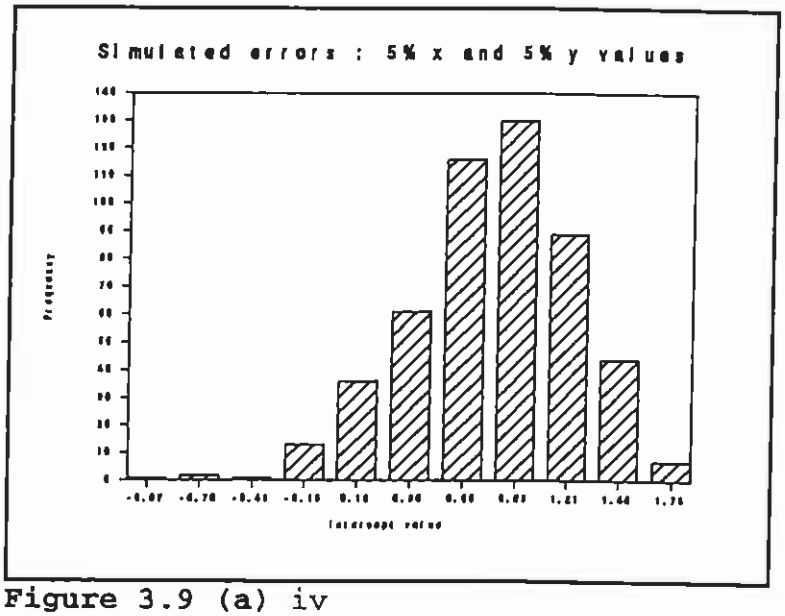

Figure 3.9 (a) iv

Mean = 0.81 std.dev. = 0.43

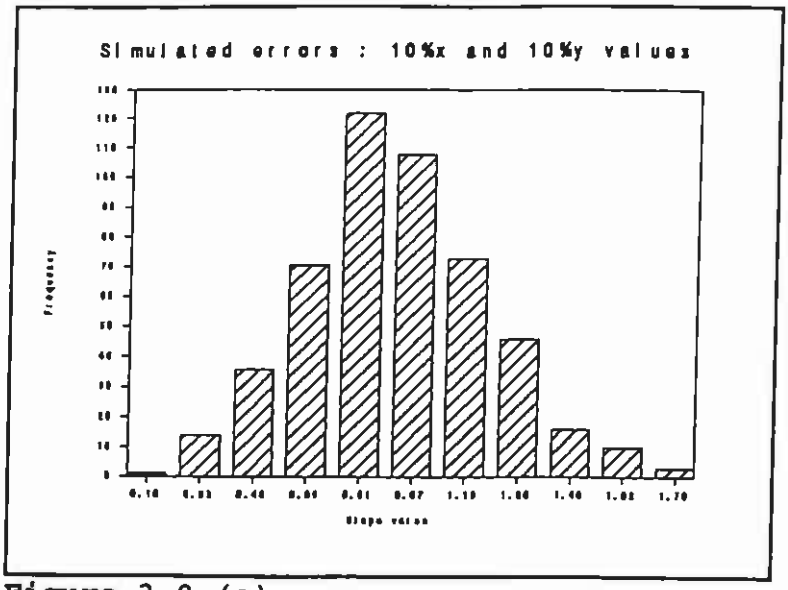

Figure 3.9 (a) v

Mean = 0.92 std.dev. = .28

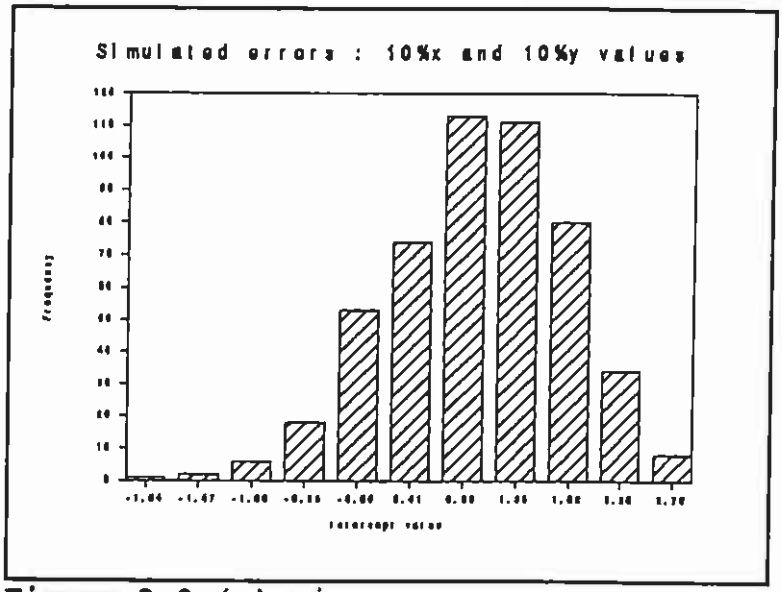

Figure 3.9 (a) vi

Mean = 1.00 std.dev. = 0.79

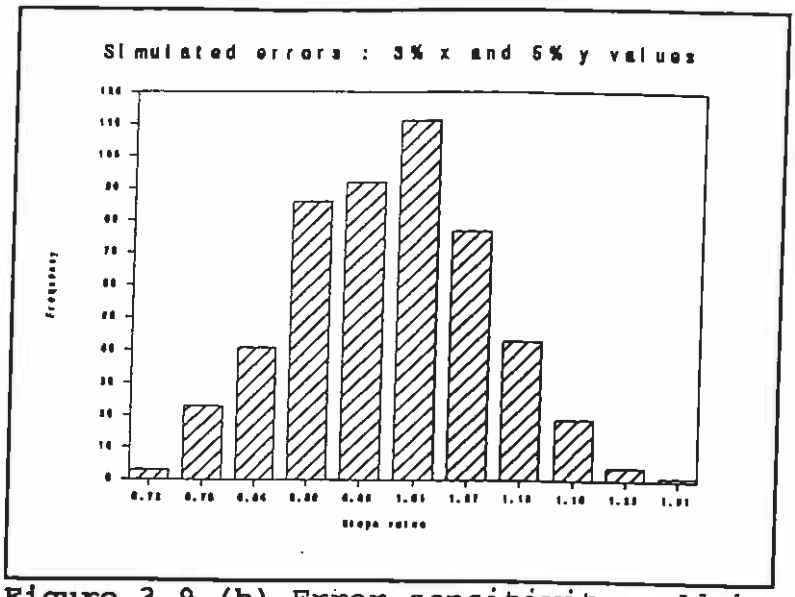

Figure 3.9 (b) Error sensitivity - Alpha efficiency isochron i

Mean = 0.98 std.dev. = 0.11

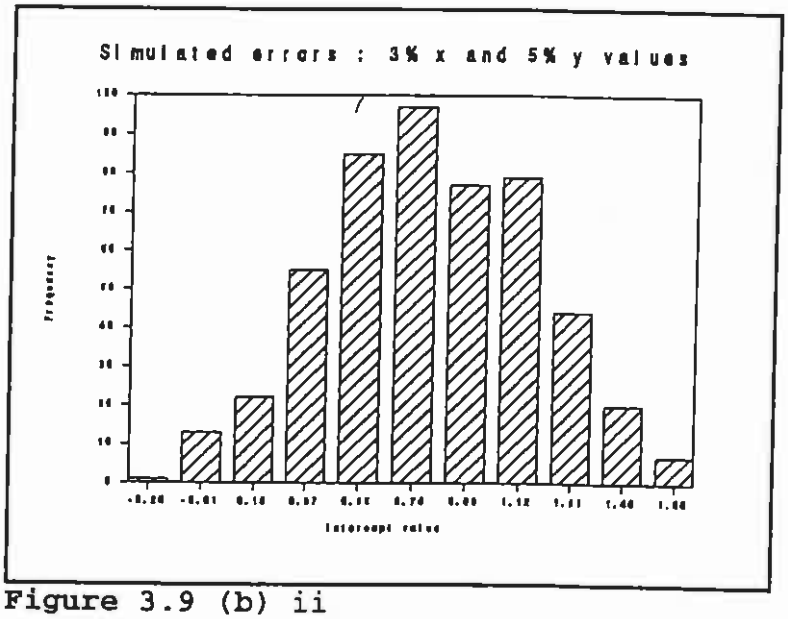

Figure 3.9 (b) ii

Mean = 0.80 std.dev. = 0.37

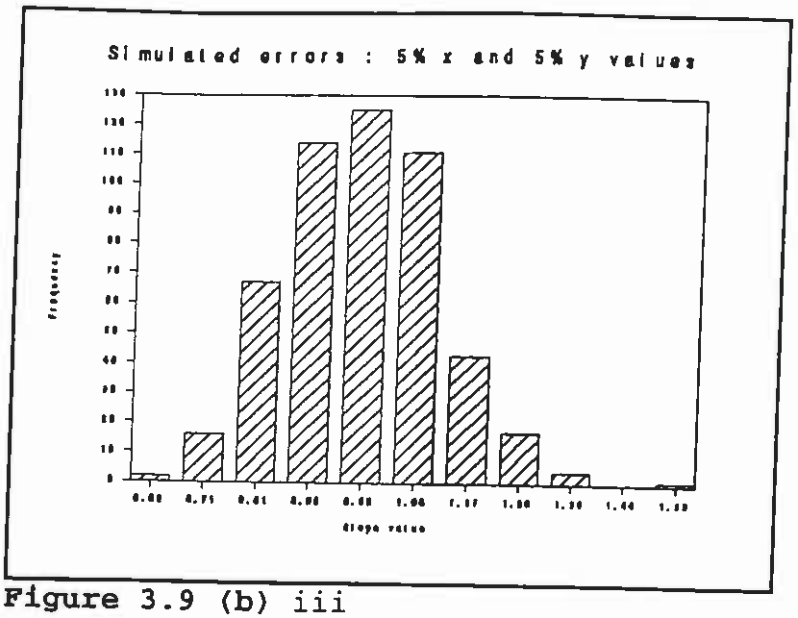

Figure 3.9 (b) iii

Mean = 0.98 std.dev. = 0.13

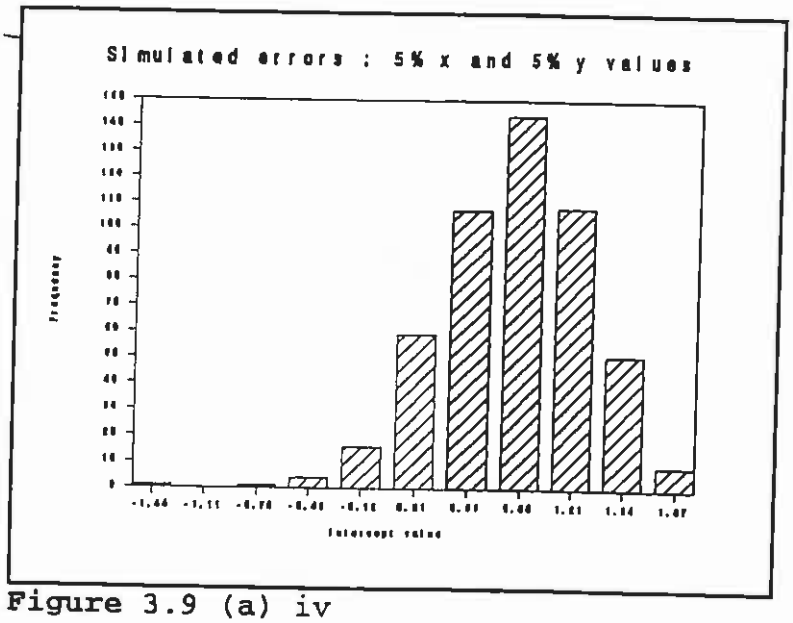

Figure 3.9 (a) iv

Mean = 0.83 std.dev. = 0.46

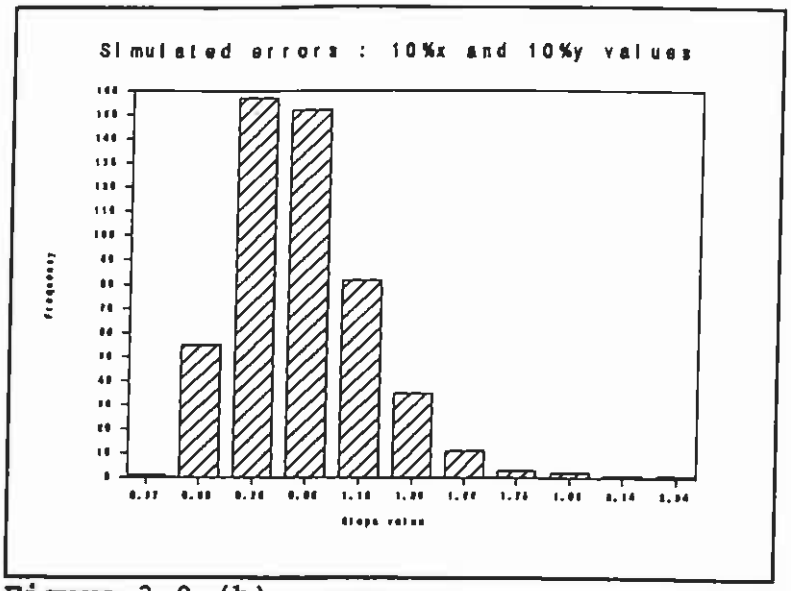

Figure 3.9 (b) v

Mean = 0.94 std.dev. = 0.26

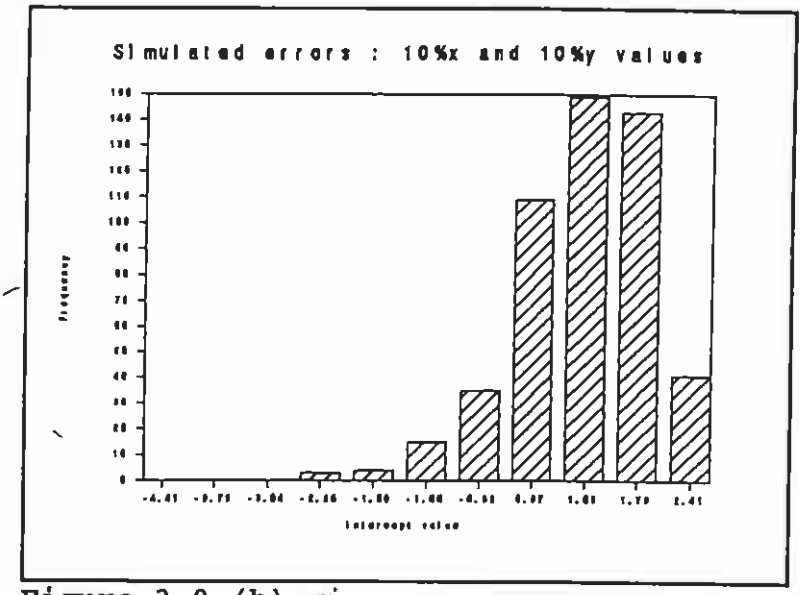

Figure 3.9 (b) vi

Mean = 0.99 std.dev. = 0.90

3.7 SUMMARY

The theoretical consideration of aspects microdosimetry have led to the formulation of an isochron model which is based on a generalised form of the TL age equation. This allows solutions to be evaluated for this equation without knowledge of the environmental γ dose contribution.

A computer program has been used to simulate the general microdosimetric model. This has been used to investigate the effect of the variation of particular microdosimetric parameters. The program uses values of absorbed dose fractions and attenuation factors that have been published for spherical grains of quartz. However, the structure of the program would allow different values, perhaps based on different grain shapes, to be readily incorporated. Two main isochron solutions have been identified the alpha efficiency and grain-size (or alpha-beta-attenuation) isochrons.

The effects of mineral and matrix activity variations and water content variation have been systematically explored. An investigation into the error sensitivity of the model has been presented and suggests that the value of the slope (the age) is more robust to scatter than the intercept (measure of the external gamma dose rate).

The next chapter describes an experimental investigation of isochron systems using model matrices to evaluate the validity of the grain size isochron predictions.

Promising isochrons do exist in principle. They have the potential to deal with destratified samples but require lots of measurements.

The next chapter explores isochron systems experimentally, using model matrices loaded with grains of known characteristics. This represents a logical step between the theoretical approach just described and the application to real samples.

4. ISOCHRONS II - EXPERIMENTAL VERIFICATION

'RODUCTION

It has been shown by simulation that isochrons for grain size graduation, alpha efficiency variation and internal activity contrast in particular appear to be sufficiently promising to warrant experimental investigation.

In this chapter, a series of model matrix experiments designed to investigate the predictions of the isochron model is described. This represents a logical step towards the development of isochron methodologies suitable for archaeological application. As stated earlier the TL characteristics of archaeological samples are not only complex, but also involve many different natural variables associated with both dosimetry and luminescence properties. The control of some of these parameters, particularly knowledge of sample radioactivity, control of age, and selection of favourable luminescence characteristics, within a model experiment provides a practical test for underlying isochron behaviour without introducing a need to characterise all possible variables which might influence real samples. These experiments were designed so that the precision required (section 3) to observe isochron behaviour should be readily achievable with available techniques. They also provide an explicit test of the microdosimetric assumptions that are fundamental to routine TL dating. The principle adopted was to prepare well-characterised matrices, derived from international secondary reference standards for equilibriated uranium and thorium series activities. These matrices were loaded with TL materials which had previously been shown to have good dosimetric properties, and exposed in a low background lead shield for accurately known periods. Recovery of the TL phosphors, using sample preparation techniques which would be needed to examine real archaeological samples, was followed by a series of TL and radioactivity measurements and an isochron analysis.

The simulation work had identified several possible isochron systems, based on dosimetric differences resulting from variations in grain size and alpha efficiency. The feasibility of preparing model matrices containing suitable TL mineral grains was first considered. It was concluded that two separate matrices were required to examine grain-size isochrons. The first used microcline feldspar embedded in an enriched radioactive

silicate matrix containing higher than normal proportions of U and Th series radioactivity; the second used CaF_2 phosphor embedded in a more typical matrix of slightly enriched natural radioactivity. To conduct this investigation of grain size isochrons, conventional inclusion separation methods (sieving, followed by density separation and acid treatment) had to be extended to extract grains of many size fractions between 1 and 200 μm. It was decided to implement these two experimental systems, which are described in this chapter. The design requirements of alpha efficiency isochron model experiments were also considered, based on the use of dosimetry phosphors with known and contrasting alpha efficiency. While it was decided not to pursue these schemes experimentally, work was undertaken to develop methods for density separation of fine grain samples with a view to exploiting any variations between alpha efficiency of the various alkali and plagioclase feldspar fractions, and quartz.

Here, the details of the preparation, storage, measurement and results of the two matrices investigating the grain size isochron system are presented.

4.2 DESIGN CONSIDERATIONS FOR EXPERIMENTAL MATRICES

4.2.1 Objective

The aim was to design a set of experiments with a high probability of observing isochron behaviour, if it exists. These experiments were to be as realistic a simulation of dating systems as possible, while nonetheless controlling the number of experimental variables to minimise the probability of the underlying trends being masked by experimental artefacts.

The approach taken was to prepare a series of model systems whereby zeroed luminescence materials were incorporated into matrices containing known radioactivity and stored for known periods of time before extraction and luminescence measurement. Measurement of stored doses and evaluation of effective dose rates for each extract could then be used to assemble isochron plots for age estimation. By comparison with

the known age the performance of the isochron system could be assessed. To maintain realism the matrices and TL minerals should represent natural systems. To control experimental variability, reference materials and well characterised TL materials were used.

4.2.2 Materials and constraints

To fulfil these experimental aims several aspects of matrix composition had to be considered. One requirement was that a sufficiently high dose rate could be achieved so that a measurable TL signal would be accumulated within the proposed storage period. The choice of dosimetry materials was also an important consideration. Natural potassium feldspars have been shown to be capable of detecting doses in the mGy region (see Section 4.2.4) so a matrix capable of delivering a dose-rate of the order of 100-200mGy per month would be appropriate. However, at the enhanced levels of radionuclide concentrations required for this, the enrichment of the ^{40}K component required to maintain typical U:Th:K proportions would be extremely difficult due to its very low natural abundance (0.0117%). One approach, to overcome this problem, would be to undertake the production of an enriched source of ^{40}K using neutron activation of a spectroscopically pure potassium salt e.g. KCl. This would have taken up to one year to irradiate in the SURRC UTR thermal column and was not pursued further during this study.

The limitation presented by the readily achievable level of ^{40}K enrichment lead to a decision to use two different radioactive matrices to investigate the grain-size isochron system. To record a measurable stored dose from a natural mineral commonly found in ceramic matrices, such as potassium feldspar, within the available experimental time it was necessary to raise the matrix dose rate to a level which required predominance of U and Th series radionuclides. Within this constraint, however, it was also felt that as realistic as possible a U:Th ratio should be maintained, so that typical alpha spectra were generated.

It was also felt necessary to simulate a matrix that did have a more typical isotopic

composition so that a more representative spectrum of ionising radiation would be present. The problem of ^{40}K enrichment, mentioned above, acts as a restraint on the levels of U and Th enrichment available, whilst keeping radionuclide proportions within typical natural limits; high potassium enrichment also leads to modification of the bulk matrix composition. The dose rate achievable under these conditions is significantly lower than available on the basis of U and Th concentration, and consequently dictates the use of a different dosimetry material. Environmental dosimetry work (Sanderson and Postlethwaite in East, 1991) had previously identified CaF_2.nat as being able to detect doses in the μGy region using SURRC TL readers, making it a suitable phosphor for this particular matrix (see section 4.2.4).

The matrices themselves were prepared from a series of IAEA gamma ray spectroscopy standard reference materials and Canmet standards whose values are given in Table 4.1.

The compositions of the planned matrices are described in section 4.2.5 and detailed descriptions of their preparation are given in section 4.3.2 and 4.4.2.

A literature search was carried out to assess the variation of reported values of alpha efficiency. This was to give an insight into the feasibility of exploiting the differences within an isochron approach. Several limitations were apparent as discussed below. As previously stated, section 2.8.2, alpha efficiency varies with alpha particle energy and hence alpha efficiencies measured by straightforward comparison of TL per Gy alpha to TL per Gy beta will be dependent on the particular alpha source used. Measured alpha efficiencies given as 'a-values' do not suffer from this problem; however this system has not been widely adopted outside the TL dating literature, and many literature sources for dosimetry phosphor specify neither the alpha source used nor the efficiency system. Thus comparisons must only be tentative at this stage. Another problem common to most papers is that the quotation of the associated error term is missing or where an error has been evaluated, its method of calculation is not presented. The dating literature, based on polymineral fine grain samples shows evidence of sample to sample variation by a factor of up to two. Since both mineral composition and pure mineral alpha efficiencies are varying within these bulk samples, there is a possibility that

greater contrast may occur within certain samples due to variations between pure fine grain silicate phases. Lack of clear knowledge of this possible variation precluded the design of a fine grain alpha-efficiency contrast model experiment. A limited investigation that attempted to separate, or at least enrich, particular mineral phases within the fine grain fraction from ceramics did not produce evidence of marked differences in their measured alpha efficiency. An alternative approach could be to look at the alpha efficiency as measured for fine grain samples prepared from crystals of different mineral types.

The observation that some TL phosphors do exhibit a much greater range of alpha efficiencies offered the possibility of constructing an alpha efficiency isochron model matrix experiment. (For example, quoted (Aitken, 1978) alpha efficiencies for CaF_2:nat = 0.10, $CaSO_4$:Dy = 0.30, CaF_2:Dy = 0.50). At this stage, however, it was felt inappropriate since this would require the use of minerals not commonly found in ceramic matrices and therefore not representative of a likely microdosimetric situation.

4.2.3 Matrix Effects

The previous section described possible grain/matrix combinations. Here, potential complicating factors are identified and briefly discussed with a more detailed treatment in the results and discussion sections.

Firstly, the matrix composition has a bearing on both experiments. The proposed microcline/model matrix composition was of a silicate base with enriched uranium and thorium levels. This means that the ^{40}K part of the energy spectrum would be missing. In the case of the fluorite/model matrix, the radionuclide proportions used would reflect more closely the natural ionising radiation energy spectrum. However, to achieve this and a useful dose rate required the matrix to be approximately 75% K_2SO_4 ie it is not a silicate based matrix and therefore has a different stopping power. The use of fluorite grains in this matrix also requires consideration of its stopping powers for alpha and beta radiation, compared to those for quartz (for which the self-dose fractions and attenuation factors have been calculated).

One possible option to overcome the non-silicate nature of the matrix and to maintain the potassium dose contribution would be to use a high potassium silicate. This would be one of the potassium rich feldspars, sanidine, orthoclase or microcline. This in itself would introduce drawbacks since the highest potassium content of these feldspars is of order of the one quarter that of potassium sulphate, so that lower dose rates would be achievable and therefore longer exposure times would be required.

Standard	Uppm	Thppm	K%
RGU-1	400 ± 2	-	-
RGTh-1	6.3 ± 0.4	800 ± 16	0.02 ± 0.01
RGk-1	-	-	44.8 ± 0.3
S16	445 ±	16,800 ±	-
BL3	10,200 ±	-	-

TABLE 4.1 IAEA AND CANMET STANDARD REFERENCE VALUES

(NB Certified values were obtained from Report - IAEA/RL/148, 1987 which accompanied the standards.)

It is worth noting that Sanderson's (1987) observation of the effect on the thick source beta counting of reducing sample size for KCl (z_{eff} = 18.06) was found to be very similar for the fluorite/model matrix (βstd(II)) (z = 13.6) which suggests that for this particular parameter the variation of z for the matrix has very little effect.

Secondly, the configuration of the matrix and grains was considered. The possibilities were for the grains to be separated from the matrix by a thin foil containment but surrounded by the matrix for the exposure period. This would then make the separation of the grains from the matrix extremely straightforward. However, the problems introduced by this approach, attenuation of the alpha dose and possibly the same effect for the low energy end of the beta spectrum, and, depending on the geometry there would be the possibility of self-shielding by the grains, were felt to outweigh its advantages. The decision was therefore taken to mix the grains intimately with the matrix since this is the configuration found in ceramic matrices.

Another important factor in deciding on the volume of container to use is the significance of any edge effects, due to the finite size of the matrix, ie the dose will be lower at the edges of the matrix volume. Large radii containers would have the smallest volumes experiencing the edge effect. Large volumes could present problems in the quantity of material required to make sufficient matrix to fill them, and the possibility of a gamma self-dose may no longer be negligible. The limiting factor for the minimum size is the maximum beta particle range of 2-3mm which would therefore require a radius of material of at least 3mm to ensure infinite matrix conditions.

Alternatively, an inner container of <"β thick" plastic sheet could be used to make a container for matrix plus grains, ~2mm in radius less than the outer container the space between the two could be filled with matrix only. However, this is likely to produce further edge effects, almost certainly for α's and probably to lesser extent for β's too (especially lower energy ones).

The third approach would be to have the matrix/grains mixture in a smaller container and to allow them to accumulate their dose in a configuration with no inner boundary. Once the storage period is over a cylindrical sleeve, of radius 2-3mm less than the storage container could be inserted into the mixture.

In this way it was hoped that it would be possible to exclude that part of the matrix/grain mixture that contain grains from the boundary layer, thereby ensuring that the majority of grains collected (if not all) would have experienced the full alpha and beta infinite matrix dose rates of the matrix. This was the adopted approach, the matrix container was 36mm diameter x 58mm height.

The advantage of this last approach is that it mimics the real dosimetry situation as closely as possible. The consideration of these factors has suggested possible disadvantages of βTLD (Bailiff, 1982). Here, phosphor grains are not mixed within the pottery matrix so that the contributions from beta particles of different energies is unlikely to be the same as for mineral grains within the pottery matrix.

4.2.4 Grain Requirements

Once the limitation of ^{40}K enrichment had been identified and circumvented by the proposed preparation of two model matrices of different radionuclide concentration, the next requirement was to match suitable phosphor grains with matrices. The desirable properties of the phosphor were that it should possess good TL characteristics, ie it should have bright (ie high TL sensitivity) reproducible TL signals with little or no short term fading, and that it should be as straightforward as possible to recover from the matrix.

An experimental investigation into sensitivity ranges and minimum detectable doses in alkali feldspars (Sanderson *et al*, 1989) had identified a microcline feldspar (MC1 as having a linear growth characteristic from 1 to 200 mGy (and beyond) with no evidence of supralinearity (Figure 4.1)). This feldspar was from a graphic granite (Chiapaval pegmatite) from South Harris and was kindly provided by J Jocelyn (Geol. Dept., SURRC) as a pre-separated mineral fraction of approximately 160-210 μm grains.

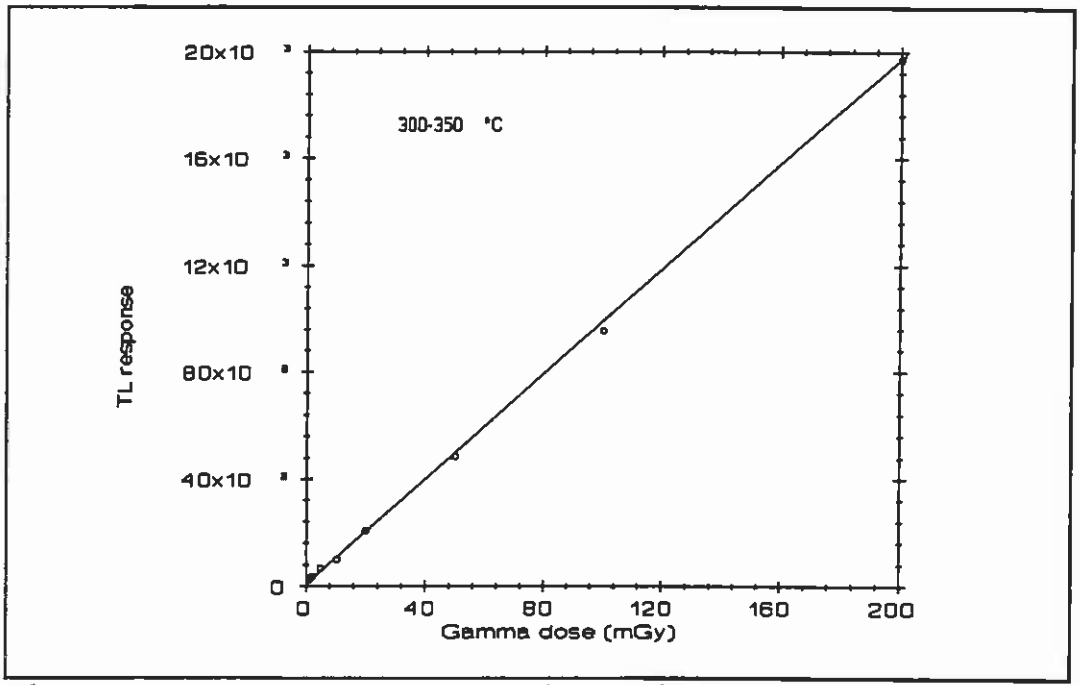

Figure 4.1 TL response of microcline (MC1) feldspar in the mGy dose region.

Extensive practical experience of advanced mineral separation techniques using solutions of sodium polytungstate and centrifugation developed from those of Mejdahl (1983) and Sanderson (1987) coupled with the observation that the predominant constituent of RGU-1 and RGTh-1 was quartz, (ρ = 2.65g.cm^{-3}) (99.43% and 97.23%, respectively) meant that the recovery of the relatively "light" microcline feldspar (ρ = 2.54 - 2.57g.cm^{-3}) ought to be readily achievable. This mineral was therefore chosen as the dosimetry material suitable for use with the matrix providing the higher of the two dose-rates. It also has the favourable characteristic of being a common rock-forming mineral and therefore a frequent constituent of ceramic matrices.

The less active matrix required a much more sensitive dosimetry material, capable of measuring stored doses in the low tens of mGy region. Natural calcium fluoride is one such material - its use in thermoluminescence dosimetry eg in medical radiotherapy and radiation protection, is an obvious testimony to its high sensitivity. It is also advantageous in that it exhibits negligible fading, 1-2% per year (Aitken, 1985) and that it has a density of 3.18 g.cm^{-3} - offering the potential for very efficient recovery from the matrix. There are disadvantages, however, the high sensitivity (six orders of magnitude higher than most of the minerals routinely encountered in the TL dating laboratory) means that there is a very significant risk of cross-contamination, unless great care is taken, which could be potentially disastrous for a laboratory such as that at SURRC working not only with archaeological material but also very low dose environmental dosimetry (Sanderson and Postlethwaite, in East (1991)) and high dose measurements (~200kGy) using glass microscope cover slips (Ward, 1988). The fact that there was no evidence for any cross-contamination during this work was the result of the implementation of strict procedures to ensure cleanliness within the preparation and measurement laboratories.

Natural CaF_2 has been shown to contain radioactive impurities that can provide a "self-dose" of the order of 100μGy.a^{-1} (Aitken, 1985). Although this would not be significant at the dose levels envisaged here investigation was made of the radionuclide concentrations within both the CaF_2 and microcline phosphors.

The most significant disadvantage of using CaF_2 results from the difference in α, β

stopping powers and gamma absorption coefficients compared to the usual dating minerals. This will be discussed in a later section and at this stage it was felt to be a suitable dosimetry material for this model matrix.

4.2.5 Planned Matrices

After consideration of the points raised earlier in this chapter - the problem of ^{40}K enrichment, the resulting decision to employ two matrices of differing radionuclide concentrations, and the identification of two suitable phosphors, the following matrix compositions were planned:

		Dα	Dβ	Dγ	Total
U	739.27ppm	(2054.4)	108.00	84.94	
Th	2840ppm	(2098.8)	81.22	145.98	
K%	$8x10^{-3}$%	-	Neg	Neg	
	TOTALS	(4153.2)	189.22	230.92	1043.11
U:Th	1:3.84	rel. contrib	18%	22%	

TABLE 4.2 MODEL MATRIX I: MICROCLINE GRAIN SIZE ISOCHRON

Based on a matrix composed of 40% RGU-1, 40% RGTh-1, 15% S16, 5% BL3, by mass.

Here, as elsewhere in this thesis, D is used to denote dose rate. Hence, D_α represents alpha dose rate.

		Dα	Dβ	Dγ	
U	36.15ppm	(100.5)	5.28	4.15	
Th	120.00ppm	(88.7)	3.43	6.17	
K	34.14%	-	28.35	8.23	
	TOTALS	(189.2)	37.06	18.55	83.98
U:Th	1:3.32	rel.contrib	44%	22%	

TABLE 4.3 MODEL MATRIX II: CAF_2 GRAIN SIZE ISOCHRON

*NB D values are in $mGy.a^{-1}$.

Based on a matrix composed of 76.20% RGK-1, 8.80%, RGU-1, 15% RGTh-1, by mass. Model Matrix II represents an approximate ten fold increase in the radionuclide concentrations typically found in ceramic matrices.

4.3 EXPERIMENTAL PROCEDURES AND DEVELOPMENTS

4.3.1 Introduction

The following sections describe the experimental procedures that were followed to prepare the model matrices and their grains. This required the development of established grain size and mineral separation techniques to apply to intermediate grain sizes. A routine designed for the measurement of the apparent alpha efficiency of these phases is described.

4.3.2 Matrix Preparation

The raw materials for the model matrices were radioactive standard reference materials obtained from IAEA and CANMET. The certified radionuclide concentrations are given in section 4.2.2 (Table 4.1). These were used to characterise the response of the laboratory thick source beta counter (T.S.B.C., Sanderson, 1988) to determine the threshold setting for isotope independence, (where the sensitivity, or dose rate conversion factor, was the same for all three radionuclides). The use of an in-house beta

standard also enabled the comparison of the observed and expected dose rates from the proposed model matrix constituents. The in-house beta calibration standard refers back to CANMET standards that are certified independently of IAEA materials to ± 2%. Table 4.4 shows potassium sources consistently measured to ± 1% of the certified values, thorium series to within 4% and uranium series to within 7%. IAEA materials are only certified to ± 5% therefore this agreement is satisfactory. The radon loss probably explains the slight under-response. Therefore the materials used can be shown to be traceable to international dose rate standards at high precision.

Standard	Dβ exp $mGy.a^{-1}$	Dβ obs $mGy.a^{-1}$	Dβ obs/Dβ exp
KCl (analar)	43.49	43.09	0.99
RGU-1 (IAEA)	58.47	54.37	0.93
RGTh-1 (IAEA)	23.82	22.82	0.96
RGK-1 (IAEA)	37.20	37.68	1.01

TABLE 4.4 OBSERVED AND EXPECTED BETA DOSE RATES FROM STANDARD REFERENCE MATERIALS

Having successfully measured the beta dose rates from the individual standards a secondary, mixed, beta standard, βstd(II), was prepared. This was designed to have $D\beta K = 0.78D\beta_{TOTAL}$, $D\beta U = 0.13D\beta_{TOTAL}$ and $D\beta Th = 0.09D\beta_{TOTAL}$. The weighting factors were included to take into account the typical relative contributions of K, U and Th in natural matrices. This corresponds to a mixture composed of 76.20% RGK-1, 8.80% RGU-1 and 14.96% RGTh-1, by mass, with a calculated beta dose rate of $37.06mGy.a^{-1}$. The mixing procedure was to place the main constituent (RGK-1) into a 150ml gamma counting geometry, to which the RGTh-1 was gradually added as a number of separate aliquots, with thorough mixing of each aliquot. The RGU-1 was added similarly. The mixture was then transferred to a ball mill (Fritsch "analysette

3"/"pulversette 0") and mixed for 25 minutes (intermittent mode), then allowed to stand for approx 5 minutes to allow all dust particles to settle and so reduce any inhalation risk.

Two independent quality control checks were performed to confirm the matrix compositions, β-counting and neutron activation analysis. A 30g subsample of this βstd(II) mixture was removed for β-counting - the measured β dose rate was 36.55 ± 0.42 $mGya^{-1}$, which is 0.99 of the expected value (37.05$mGya^{-1}$). This was a very encouraging result since it confirmed the validity of the methods used to calculate and prepare the secondary βstd(II) mixture and that they could be justifiably applied to the production of the model matrices.

The second method employed was neutron activation analysis (NAA). This utilised the reactor facility at SURRC and the close proximity of gamma detectors allowed the analysis of short-lived isotopes. The quantitative analysis of the amounts of uranium, thorium and potassium present in a sample requires comparison with a standard of known concentration of these elements. An homogenised Shap granite sample had previously been used for this purpose and was chosen for this study. The working values of the uranium, thorium and potassium contents were derived from high resolution gamma spectrometry of sealed samples relative to Canmet standards and are believed to be correct to better than ± 3%. The values were 12ppm U, 28 ppm Th, 4.43% K.

The samples and standards were contained as accurately measured masses, usually 20 or 50mg for the grains and 100mg for matrix samples, in individual silica vials (O.D. = 5mm, I. D. = 3mm, length = 40-50mm) flame sealed by Mr F Cornwallis. For rapid uranium analysis, the pneumatic transfer ("large rabbit") system was used to irradiate the samples. The irradiation time varied depending on the reactor power, but was typically of the order of five to ten minutes, followed by an approximately ten minute cooling period during which time very short-lived activity (eg $^{28}_{13}Al$, t½ = 2.24mins) would decay and therefore reduce the dead time of the detector. The sample vials were also cleaned during this period to remove any activated dust particles that could

contaminate the detector. The reaction being exploited here is:

$$^{238}_{92}U \ (n,\gamma) \ ^{239}_{92}U \quad t_{\frac{1}{2}} = 23.54 \text{ minutes} \quad E_\gamma = 74.6 \text{ keV} \qquad (4.1)$$

The low energy of the emitted gamma ray requires that a planar, or thin-window, detector be used and also that it should be unshielded, by lead at least, because its energy coincides with a lead X-ray at ~74.5keV that would interfere with the true counts from uranium. This work used an EG&G Ortec portable low-energy gamma-ray detector, and was energy calibrated using ^{241}Am ($E\gamma$ = 59.57keV) and ^{57}Co ($E\gamma$ = 122.06keV) reference sources.

The potassium analysis depends on the following reaction

$$^{40}_{19}K \ (n,\gamma) \ ^{41}_{19}K \ (n,\gamma) \ ^{42}_{19}K \quad t_{\frac{1}{2}} = 12.36 \text{ hours} \quad E_\gamma = 1525 \text{ keV} \qquad (4.2)$$

In this case, the counting period (30mins) commenced after a cooling time of the order of 4-5hrs after the initial rabbit irradiation and uranium count, on a 25cc GeLi gamma detector (^{226}Ra calibration).

In order to activate the thorium to a sufficiently high level a considerably longer irradiation time was required. This had to be carried out in the CVS (Central Vertical Stringer) position since a six hour irradiation period was required and a maximum of one hour was available from the rabbit system. The CVS could accommodate a total of approximately 30 individual sample vials, contained in two aluminium cans. After activation a cooling period of about one week was followed by a 30 minute count on the 25cc GeLi detector, to measure the 312keV gamma ray from ^{233}Pa produced from:

$$^{232}_{90}Th \ (n,\gamma) \ ^{233}_{90}Pa \quad t_{\frac{1}{2}} = 26.95 \text{ days} \quad E_\gamma = 312 \text{ keV} \qquad (4.3)$$

ıe precision of this technique (approximately ± 10-15 % for U, ± 10-15 % ·10 % for K) is less than for the beta counter it does give information from small samples and provides an independent cross-check for quality assurance purposes.

4.3.3 Grain Preparation

The sedimentology literature (eg Tickell, 1965, Lindholm 1987 and McManus, 1988) was consulted for methods of grain size separation and analysis, but it was found that rather than performing actual separation of the different grain sizes the approach was a sampling strategy from which the grain size distribution was inferred. This was confirmed by a short series of experiments that showed that the "pipette method", in which a pipette is used to remove a sample of a sample of a suspension of sediment in a column of water at a particular depth and at a particular time after settling has commenced, produced not only a small yield but that the samples were also poorly sorted.

Some experiments were also made with a settling column but instead of having a closed end, like a measuring cylinder, the lower end was tapered and open. The reasons for this were two fold - firstly it was felt that the usual method of decanting of the liquid from grains that had settled at the bottom was likely to disturb them, either through over enthusiastic decanting and/or resuspension, so that the expected grain size fraction is not the one that is obtained. The effect of this could be reduced either by repetition of the procedure or, as envisaged here, by use of an open ended tube that could be stoppered and then briefly opened after the appropriate settling time to collect the required grain sizes.

Alternatively, the second approach, was to investigate the use of the open ended column in a "flowing" mode. Here, trimmed micro pipette heads were fitted to the outlet end of the column, thus reducing the flow rate, in an attempt to ascertain if a flow rate could be found that would allow faster separation of grain-sizes than the usual settling in a static column of water. It was found on microscopic examination of different separates that they were poorly sorted. Possible explanations were that the finer grains were being

dragged down by being caught in the paths of more rapidly descending larger grains, perhaps indicating overloading of the column. It was also noticed that some grains collected on the tapering sides of the column on reaching the bottom rather than flowing through the outlet. As a result, although an attractive method in principle, the use of a flowing column of water to separate different grain size fractions was not pursued further.

Dry sieving, using disposable nylon meshes (90μm, 60μm and 30μm) in a small plastic sieve set, was found to be inefficient. This may have been due to the sample becoming charged with static electricity as it was repeatedly rubbed against the nylon mesh, causing the grains to stick together and therefore inhibit passage through the sieve.

The approach that was eventually adopted was wet sieving for grains >30μm and settling in a static column of liquid acetone for the finer fractions. Deionised water was used to rinse the finer than 90μm grains through the sieve, the water plus <90μm grains being collected in a large beaker, until the water passing through the sieve was clear. This was taken to indicate that most <90μm grains had been washed through. The contents of the beaker were then washed through the next sieve (60μm), that which passed through being collected along with washings of fresh deionised water until it ran through clear. This was repeated for the 30μm sieve.

The grains retained by the meshes were dried by placing tissues on the underside of the sieve mesh to absorb as much excess water as possible. The meshes were then carefully removed from their holders and dried in a warm oven. The <30μm grains, suspended in a large volume of water, were transferred to centrifuge tubes and spun down to allow the water to be more easily decanted. These grains were then resuspended in beakers of acetone (for shorter settling times than in water). Beakers were used since this meant there was less likelihood of disturbing the settled grains when decanting than if a measuring cylinder was used. The settling procedures were repeated for each size fraction so as to improve the recovery of the desired grain size fraction. The grain size separates prepared as above were examined with the aid of a microscope and found to be well sorted, implying that the methods employed had been successful.

The separation of intermediate and fine grain sizes by settling in a static column of liquid is based on Stoke's Law, which can be conveniently expressed as:

$$t = \frac{18\eta_l h}{g(\rho_s - \rho_l)D^2} \qquad (4.4)$$

where

t = settling time (s)

η_l = viscosity of the liquid ($N.s.m.^{-3}$)

h = height of liquid column (m)

g = acceleration due to gravity ($9.80 m.s^{-2}$)

ρ_s = density of mineral grain ($kg.m^{-3}$)

ρ_l = density of liquid ($kg.m^{-3}$)

D = diameter of grain (m)

Viscosity and density values were obtained from standard scientific data textbooks (CRC Handbook of Chemistry and Physics) from which settling times were calculated for mineral grains in water. These results were in very good agreement with values published in geological literature. As a further exercise the settling times (in acetone) quoted by Zimmerman (1971) to obtain grains in the size range of 1 to 8μm were recalculated.

There was some disagreement between the two sets of values, so further calculations were performed for different grain densities in an attempt to clarify the situation. Correspondence with Questiaux is gratefully acknowledged. These are presented graphically, in Figure 4.2.

Once prepared, the fine grains were deposited onto 0.25 mm stainless steel discs by evaporation from an acetone column in a similar manner to that originally described by Zimmerman (1971).

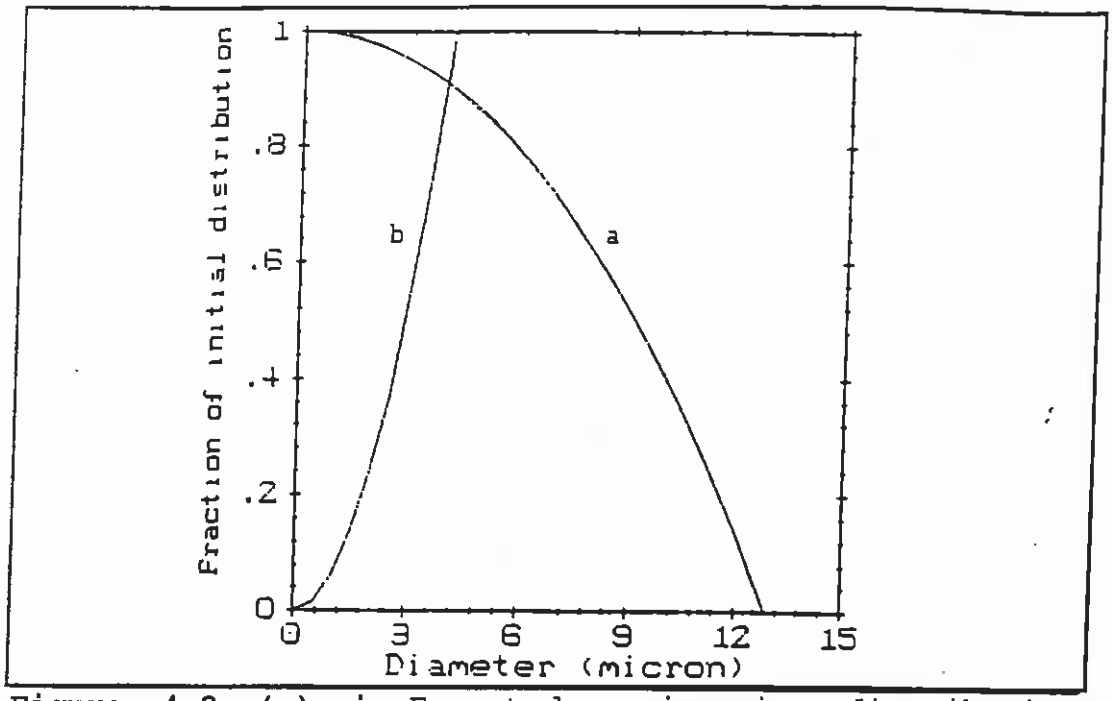

Figure 4.2 (a) i Expected grain size distribution calculated from Stoke's Law. Curve a shows the fraction of grains left in suspension after 2 minutes. Curve b shows the fraction of grains that settle out in 20 minutes.

Grain density = 2.65 g.cm^{-3}

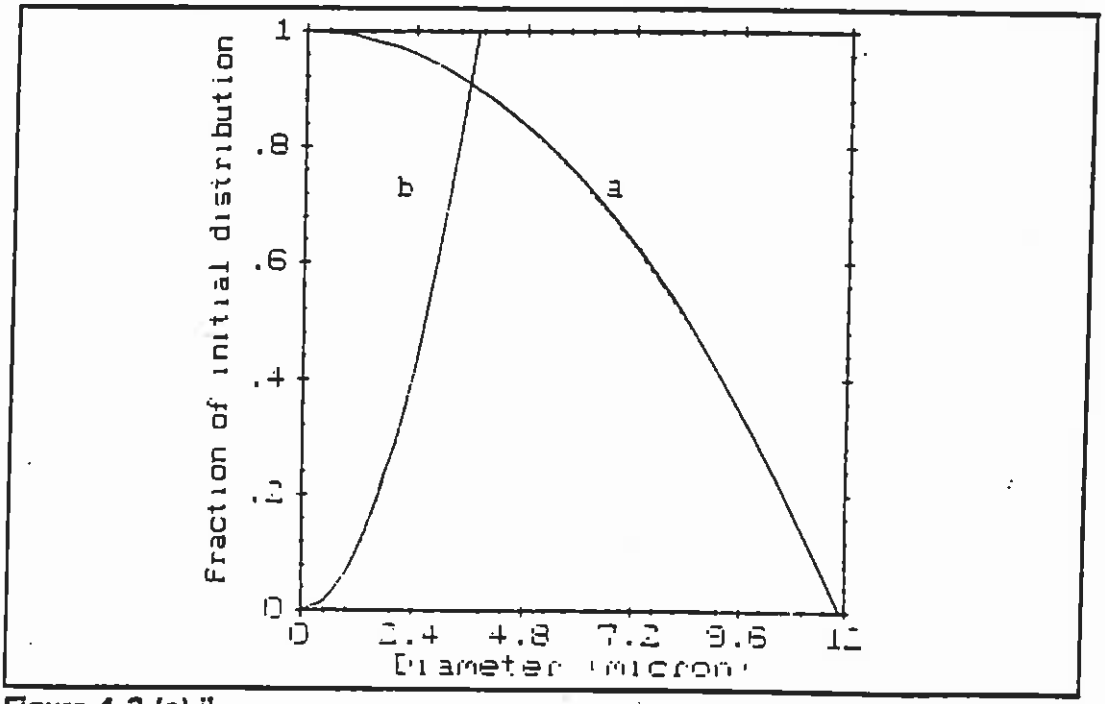

Figure 4.2 (a) ii

Grain density = 3 g.cm^{-3}

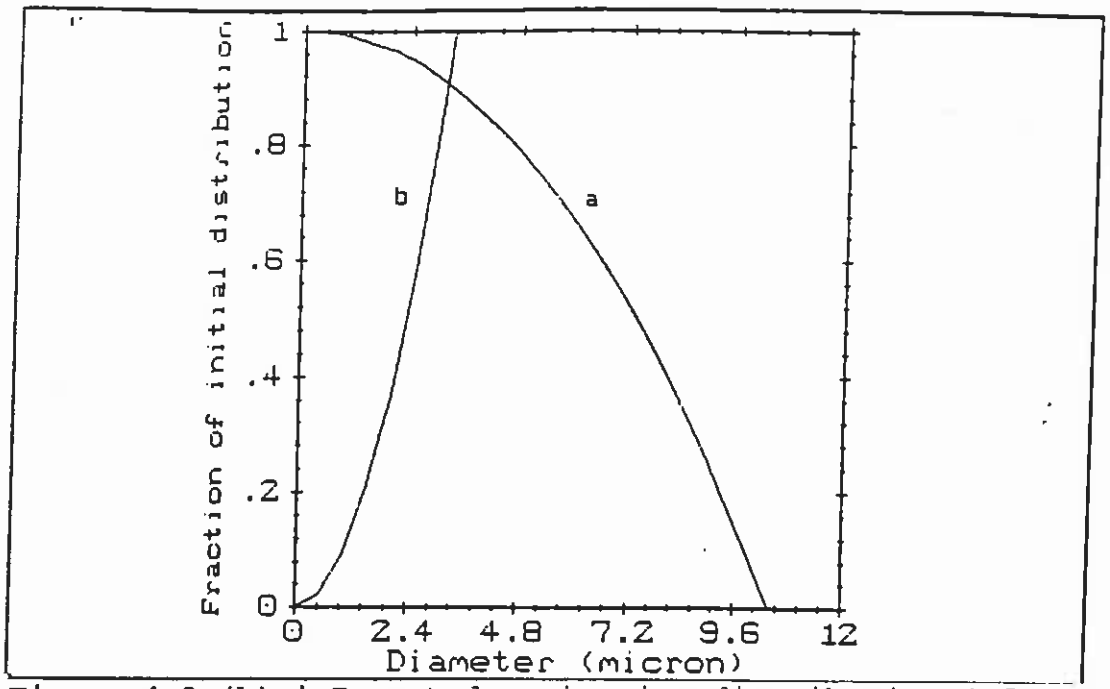

Figure 4.2 (b) i Expected grain size distribution (after Zimmerman, 1971). Grain density = 2.65 g.cm^{-3}

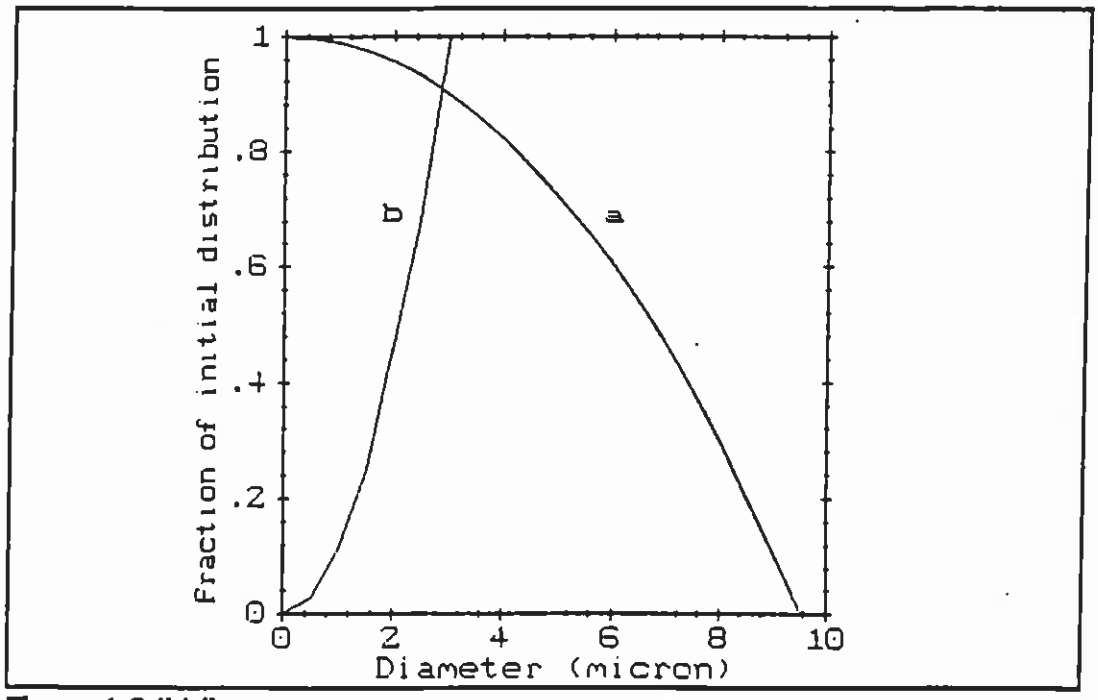

Figure 4.2 (b) ii

Grain density = 3 g.cm^{-3}.

e Calibration Experiments

An initial set of experiments, using the microcline (MC1) feldspar, was designed to confirm the working calibration of a six-source ^{241}Am vacuum alpha irradiator facility' purchased from the Littlemore Scientific Engineering Company. Prepared microcline fine grains were irradiated in the Oxford University Research Laboratory for Archaeology, flown back to East Kilbride, and used to cross-compare the East Kilbride source. An investigation into the effect of variation of sample mass, and a preliminary study of variation of apparent alpha efficiency with grain size was undertaken to examine the feasibility of using coarse grain alpha irradiations to estimate alpha efficiency during isochron construction. The cross-calibration check was designed so as to minimise the effects of short term fading, by matching delays between irradiation and glowing, and also the effects of sensitivity changes due to repeated irradiation/glowing cycles. The results were very acceptable: the measured alpha efficiency of a microcline feldspar sample (from the same mineral extract as that used for the microcline/model matrix experiments) was $0.114 \pm 6.2 \times 10^{-3} (\sigma n^{-1})$ (se 1.65×10^{-3}) using the East Kilbride source compared $0.116 \pm 5.8 \times 10^{-3}$ (σn^{-1}) (se 1.55×10^{-3}) from the Oxford source. These results were calculated as mean values for 16 discs over a temperature range of 260°-380°C. They are not statistically different and confirm the validity of the previous working calibration. The possibility of sensitivity change during glowing was examined, using EK alpha irradiation and glow cycles before and after the Oxford cycle. The effect was negligible, the mean ratio of EKα2/EKα1 for the same set of discs was 0.998 ± 0.03 (σn^{-1}).

The variation of TL output versus sample mass (and therefore also sample thickness) was investigated in response to consideration of the short range of alpha particles. The results are presented in Figures 4.3, 4.4 and 4.5.

The fact that the form of the graph is very similar for alpha, beta and gamma irradiation implies that the effect is not primarily due to a property of alpha radiation. The linear response up to ~2.5mg of sample, corresponding to a sample thickness of ~12μm, suggests that beyond this thickness there is an optical effect relating to the formation of multiple layers of grains which may attenuate the light output. There is also some

evidence that the alpha efficiency is independent of disc loading (except perhaps at low sample masses of <1mg, see Figure 4.6, where low signal levels would result in larger errors anyway). This may result from the fact that the light detected originates from the top layer of grains.

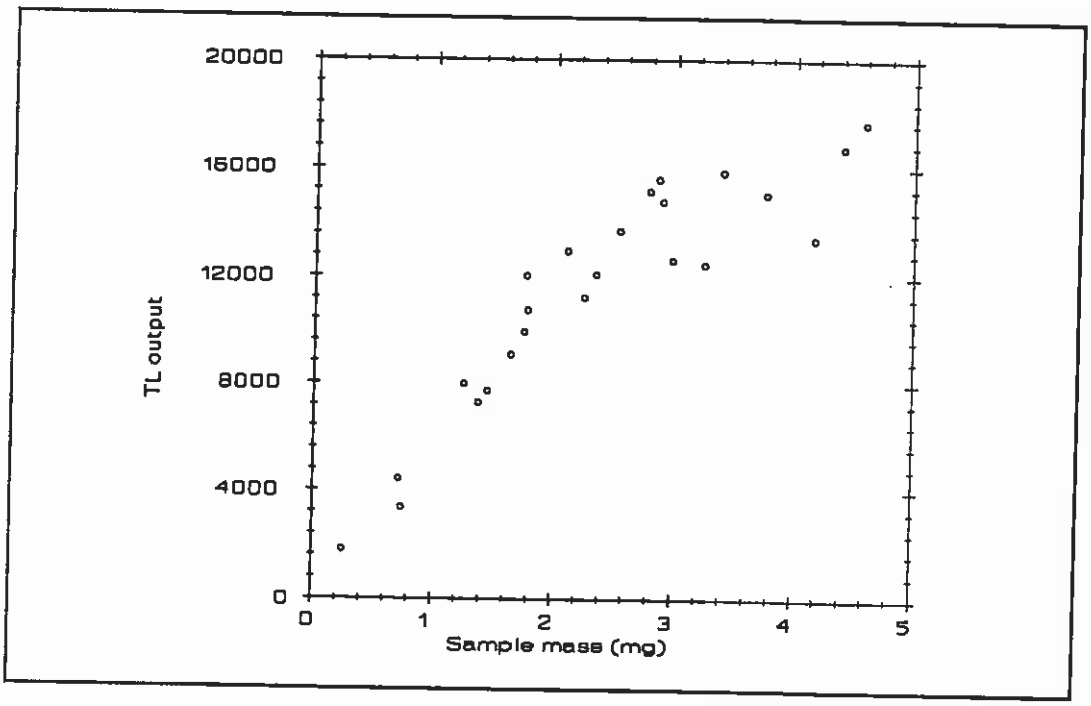

FIGURE 4.3 TL OUTPUT VERSUS SAMPLE MASS FOR ALPHA RADIATION.

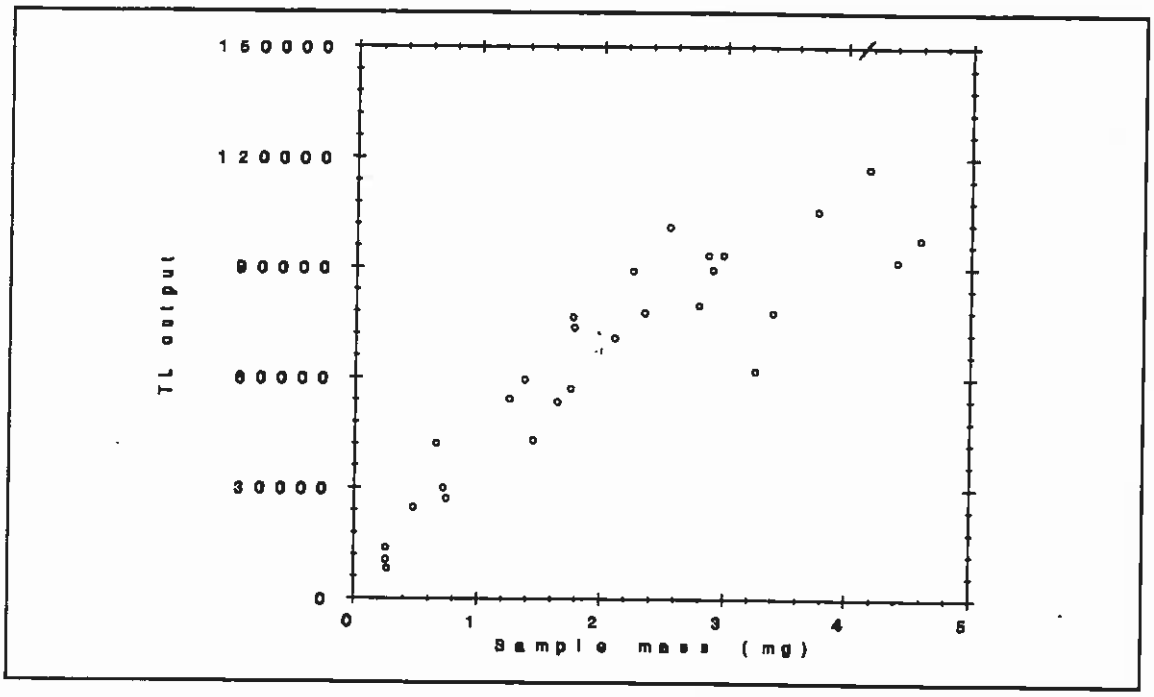

FIGURE 4.4 TL OUTPUT VERSUS SAMPLE MASS FOR BETA RADIATION.

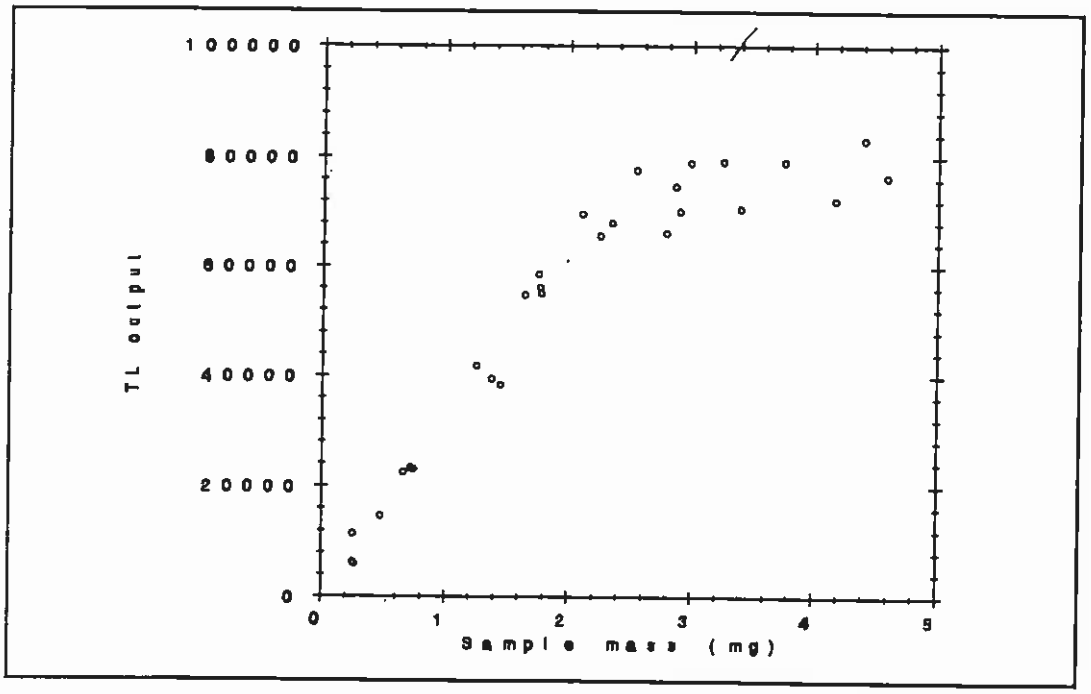

FIGURE 4.5 TL OUTPUT VERSUS SAMPLE MASS FOR GAMMA RADIATION.

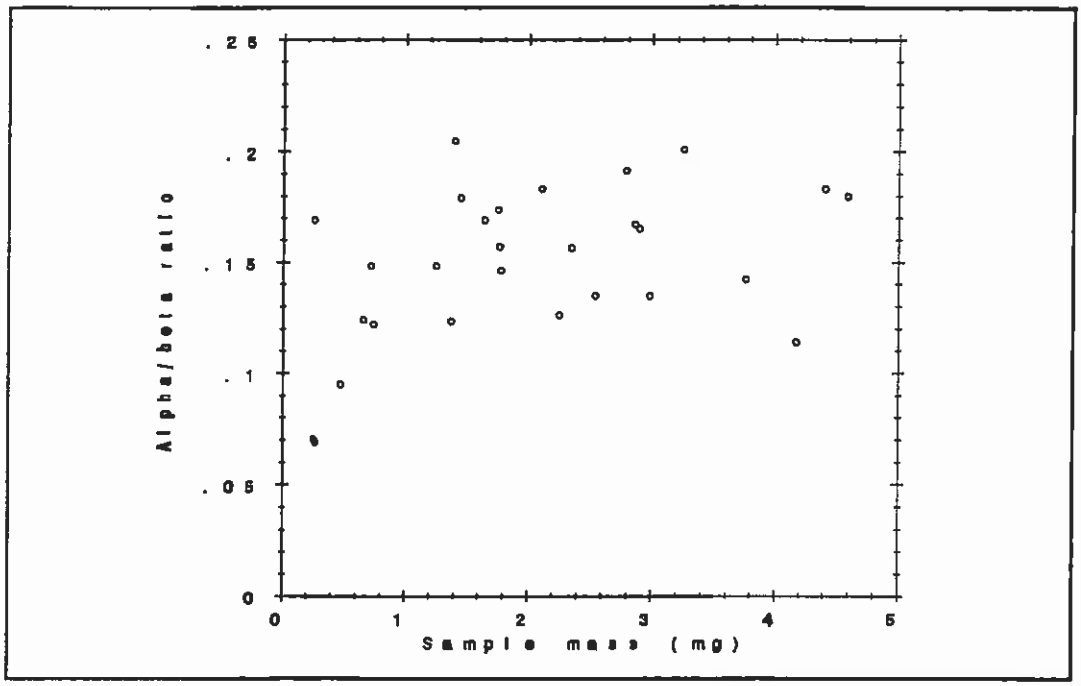

FIGURE 4.6 ALPHA EFFICIENCY VERSUS SAMPLE MASS.

A preliminary investigation of the variation of apparent alpha efficiency with grain size was carried out. The expected trend of reduced apparent efficiency with increasing grain size was readily apparent.

4.4 MODEL MATRIX I: MICROCLINE GRAIN SIZE ISOCHRON

4.4.1 Experimental Plans

In the first model matrix experiment microcline feldspar grains were introduced to a matrix of known radioactivity for a fixed exposure period, and allowed to accumulate a radiation dose. Measurements of the stored doses from grains of varying size were compared with estimates of the expected doses to examine the isochron model. It was important to assess the practical and safety aspects of each stage of the experiment - for example the handling of high concentration uranium and thorium ores in powder form, whilst minimising health risks, and to incorporate quality assurance checks on the procedures employed.

4.4.2 Materials

The planned matrix for the microcline feldspar grains was to be composed of 40% RGU-1, 40% RGTh-1, 15%S16 and 5% BL3, by mass. This corresponds to the overall matrix composition and expected dose rates as given in Section 4.2.5. The procedure for mixing the individual components together was the same as given in Section 4.3.2, for preparing the secondary beta standard, with the added precaution of wearing a face mask to further reduce the risk of inhalation. Disposable vinyl gloves were worn during the handling of these materials as standard laboratory practice. The actual matrix composition was 40.009g RGU-1, 40.00g RGTh-1, 15.03g S16 and 5.00g BL3, which corresponds to:

		Dα	Dβ	Dγ	Total
U	739.40ppm	(2054.79)	108.02	84.96	
Th	2845.04ppm	(2102.48)	81.37	146.23	
K	$8x10^{-3}$%	-	Neg	Neg	
	TOTAL	(4157.27)	189.39	231.19	1044.17
			(18%)	(22%)	

TABLE 4.6 ACTUAL COMPOSITION OF MODEL MATRIX I

NB $\bar{D}$ values are given in $mGy.a^{-1}$.

As described earlier, (section 4.3.2) beta-counting and NAA were used as quality assurance measures. The results are presented in Tables 4.7 and 4.8.

	Dβ	Dβ meas/Dβ calc
Calculated	189.39	-
Initial	182.39 ± 1.79	0.963
After Anneal	128.50 ± 1.76	0.678
After Storage	163.70 ± 2.41	0.864

TABLE 4.7 BETA DOSE RATES FOR MODEL MATRIX I COMPARED AT DIFFERENT STAGES OF THE EXPERIMENT

(NB D values are in $mGy.a^{-1}$)

Mean Values, determined by NAA	% of expected value
Uppm = 724.22 ± 27.9	97.5%
Thppm = 2711.80 ± 92.1	95.32%
*K% = 0.744 ± 0.11	-

TABLE 4.8 RADIONUCLIDE CONCENTRATIONS OF MODEL MATRIX I, MEASURED BY NAA

K% by NAA is ~2 orders of magnitude higher than the expected value, probably due to the presence of potassium as an unreported component in the general composition of the ore. In this context the discrepancy is not significant since the beta dose rate from the measured K content is small compared with the U and Th contribution.

The source material for the grains for this model matrix was the pre-separated microcline feldspar (MC1) with an initial grain size range of 160-210 microns. A small agate pestle and mortar were used to crush this material to produce grain sizes below 160 microns. The potassium content was determined as 10.18 ± 0.51% by elemental weight using neutron activation analysis of two 50mg sub-samples and the methods outlined in Section 4.3.2 . Uranium and thorium were not detected.

4.4.3 Exposure Details

To ensure that the microcline grains could be thoroughly mixed, first with each other and then with the matrix, they were put into an oven at 50°C for approximately 2 hours, to remove surface moisture that would cause the grains to stick together. This was successful in that the grains were noticeably easier to mix after this treatment. All mixing-operations involving the matrix were carried out with the added precaution of wearing a face mask (3.219g of microcline grains were added to 100g of matrix).

The microcline/matrix mixture was then placed in a silica tube, one end previously flame sealed length 20cm, diameter ~3cm, so that when laid down there was an airspace along the length of the tube. This precaution was taken to minimise the possibility of contaminating the oven by some of the matrix material in the event of it being pushed out by trapped air, within the tube, expanding on heating. The silica tube was placed inside a brass tube to improve thermal conduction to the matrix, and placed in an oven for approximately one hour at a mean temperature of 575°C. This was not only to ensure that the microcline grains started the experiment with zero TL but also to remove the TL signal from the material making the bulk of the matrix - since the TL signal from previously non-zeroed matrix grains present in a microcline separate being measured would dominate the light output. However, by zeroing both matrix and grains at the same time means that they will have the same TL age at the time of measurement and so a degree of "contamination" could be tolerated.
After cooling, in dark room conditions, a 20g sub sample of the matrix was taken for beta-counting.

The mixture of matrix and grains was split into two equal parts to provide the opportunity for a two fold replication of the experiment, if required. The containers were as described in section 4.2.3 and after tightly screwing the lids on insulation tape was used to further inhibit the loss of radon. Several layers of black plastic were used to wrap the containers as a protective measure against exposure to daylight. There were then transferred to a lead-lined low-background cavity for storage during the exposure period (87 days).

4.4.4 Extraction of Grains

Once the exposure period had elapsed, one of the containers was removed from the low-background storage cavity and unwrapped in dark room conditions. To avoid the incorporation of material from the outer parts of the matrix that would have received a lower dose-rate, the top surface 2mm was removed with a spatula and then a film canister was carefully inserted to the matrix since this was fortuitously the right size to exclude the outer ~2mm of material. A small hole in the closed end of the film canister

allowed the air to escape during insertion without significantly disturbing the matrix. A 20g sub-sample of the "inner" matrix was beta-counted - the measured beta dose rate being 163.70 ± 2.41 $mGy.^{-1}$.

The approach towards extraction of the potassium feldspar phase of each grain size fraction was to first separate the larger grain sizes (ie between 90μm and 250μm) using an automatic (dry) sieve shaker. (This contrasts to the density separation followed by grain size approach towards the recovery of a fluorite grains, section 4.5.4). The 30-60-90μm separation was achieved as before by wet sieving through nylon meshes. This also had the advantage of reducing the risk of inhalation of dust particles of the matrix. This was also minimised for the dry sieving by allowing the sieves to stand for approximately 5 minutes after being agitated to let the dust settle before opening them. The 2-10-30μm fractions were also obtained as before using a settling technique in a static column of liquid.

As previously stated the separation of a polymineralic sample into particular enriched phases is based on the concepts originally introduced by Mejdahl (1983), but modified to use a non-toxic inorganic heavy liquid, and to incorporate centrifugation rather than settling funnels. Aqueous solutions of sodium polytungstate were made up to give a series of liquids with densities 2.51, 2.58, 2.62 and 2.74 $g.cm^{-3}$ using a volumetric flask and a four-figure balance. The sieved samples were sequentially centrifuged in the four liquids, forming layers of floating and sinking material which was decanted off, rinsed with deionised water, spun down, rewashed twice, rinsed in acetone and dried in a warm oven at 50°C overnight.

Obviously, longer centrifugation times were required for the smaller coarse grain sizes, compared to those employed for inclusions. The 2.51 -2.58 $g.cm^{-3}$ fraction, corresponding to microcline was chosen for measurement.

4.4.5 Measurement of Stored Dose

The separated grains from each of eight extracts were dispensed as monolayers onto a set of eight stainless steel discs (diameter 10mm, thickness 0.25mm) which had been sprayed with Electrolube Silicone Grease compound. The typical sample mass was ~3mg. The TL measurements were made using a computer-controlled automatic TL reader, designed and built "in-house" by D Sanderson and K Cairns, based on the Riso System (Botter-Jensen and Bundegaard, 1978; Botter-Jensen *et al*, 1983). The read out cycle was initial ramp (6.6°C.sec^{-1}) to 450°C followed by a second ramp to record the background signal, which was then automatically subtracted before the net spectrum is stored on disc. The stored dose was determined by direct comparison of the first (natural) and second (reirradiated) glows. The irradiation facility used to provide the known dose for the second glow was a nominal (April '87) one Curie ^{60}Co source housed in a "Pantatron" gamma radiographic unit, with remote control to enable operation at a safe distance. The samples to be irradiated were placed on an arc of equal dose rate that had been mapped out onto an aluminium platform for use in association with an environmental dosimetry project (Sanderson and Postlethwaite, in East, 1991). The sample discs were protected by placing them in small upturned plastic sample pot lids and then covered with an aluminium plate to act as a build-up layer to ensure charged particle equilibrium exists within the sample (Aitken, 1985). The gamma dose rate at the sample position had been determined to be 36.58 (±5%) μGy.s^{-1}, so the required 50mGy dose would be delivered in 22 min 46 seconds. This was obviously advantageous in that any slight timing errors would be negligible, but disadvantageous since the set up had to be supervised throughout the exposure period. A third glow was measured to record the response to alpha radiation, which for all but the fine-grains would not only reflect the lower efficiency of alpha radiation but also the attenuation of that alpha dose through the volume of the grain. The alpha doses were delivered from a six-seater ^{241}Am alpha-irradiation unit purchased from Littlemore Scientific, Oxford.

4.4.6 Results

A summary of the results obtained for the microcline/model matrix isochron experiment is presented in Table 4.9 and in graphical form in Figure 4.7. This figure also shows the expected isochron (based on the known age and the assumptions that the measured stored doses are correct and that the external gamma dose rate was zero).

Grain size (μm) 1	Stored Dose (mGy) 2	Error (mGy) 3	Dose Rate (mGy/a) 4	Error (mGy/a) 5
20	178.75	23.95	635.37	79.51
45	141.31	4.53	454.91	49.39
75	131.84	3.83	344.54	31.19
110	76.17	7.91	287.96	22.23
140	72.01	3.56	248.97	16.22
200	60.85	1.96	221.18	12.47

1. Taken to be the grain size at the middle of the range, eg 20μm from 10-30μm.
2. Calculated as the weighted mean.
3. Calculated as the standard error of the weighted mean.
4. Effective total dose rate from the matrix and grain.
5. Calculated from counting statistics (after Faires and Parks, 1973).

TABLE 4.9 SUMMARY OF RESULTS FROM MODEL MATRIX I EXPERIMENT

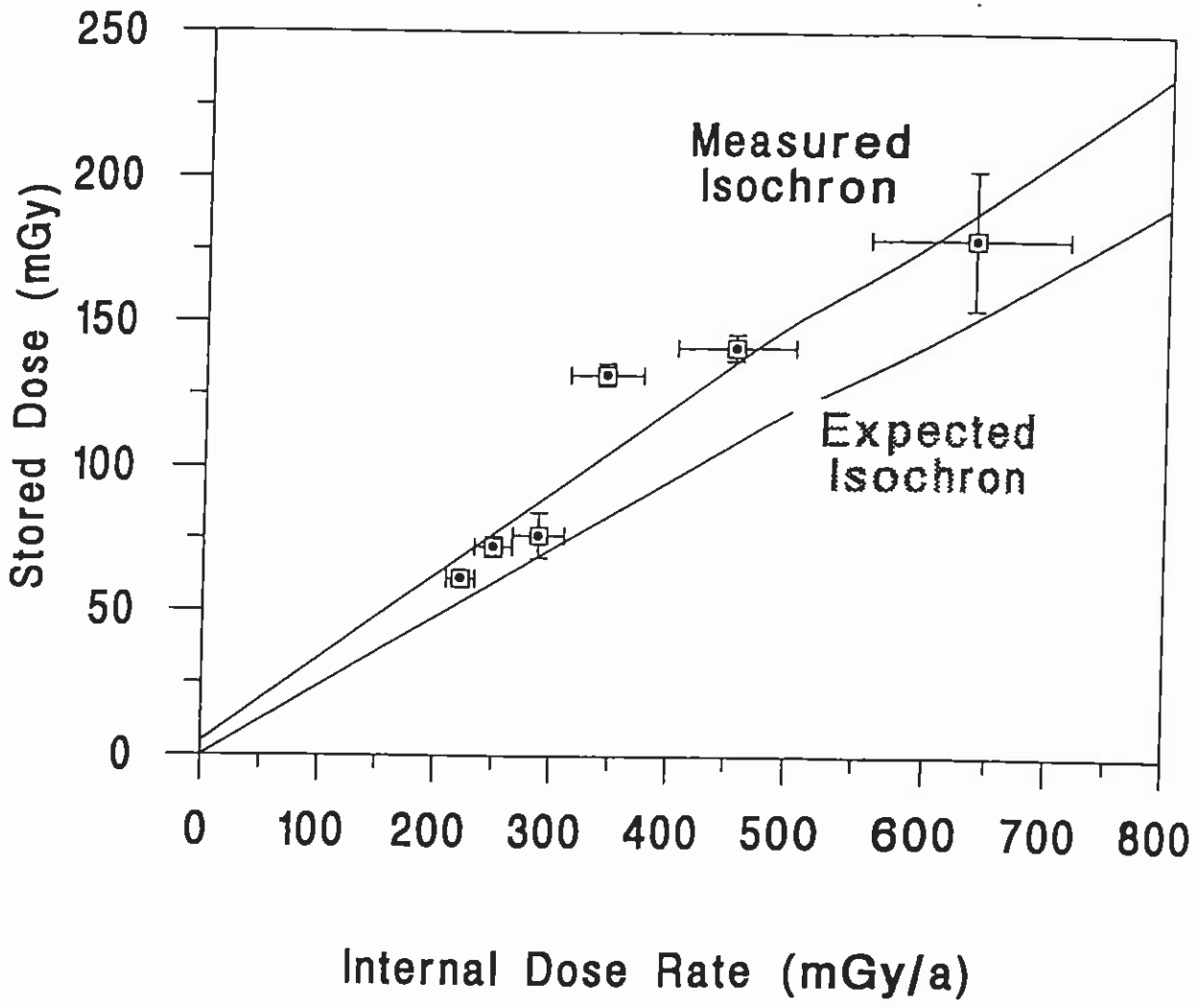

FIGURE 4.7 MODEL MATRIX I : ISOCHRON PLOT.

Linear regression analysis of this data set gave the following results :-

Measured values

Age estimate = 0.288 ± 0.047 a

External Dγ = 17 ± 65 mGy/a

compared to the expected age of 0.238 a and an external gamma dose rate of zero mGy/a. These results are extremely encouraging since the data not only exhibit the expected trend but also provide a very good age estimate. The gamma dose rate estimate, however, reflects the greater sensitivity of this parameter to scatter in the data. This reinforces the predictions of the error sensitivity of the model explored in section 3.6.

4.4.7 Analysis and Discussion

This experiment clearly demonstrated isochron behaviour. Overall the experimental confirmation of the predicted isochron behaviour of this sample, and its agreement, within two sigma, with the known storage period is very satisfactory. This is particularly encouraging given the practical difficulties of making high precision TL readings from natural feldspar systems at 50 - 150 mGy and the necessity of using an atypically high uranium series content, with its associated risk of radon leakage, as the irradiating matrix.

The stored dose was determined from the direct comparison of the natural (first glow) and reirradiated (second glow) signals. The ratio of first to second glow curves was found, and integrated over 250-350°C for each disc. This temperature range was chosen because it gave the best plateau and also helps to reduce the detrimental effect of low light levels and the interfering effect of black body radiation. Despite this precaution a number of discs had to be excluded from the data analysis due to poor glow shape. The weighted mean values were deemed appropriate since some grain size ranges exhibited more scatter than others. The fine-grain fraction, although separated from the matrix and measured, had so much scatter that the data were considered unreliable, and excluded from analysis; it is possible that this fraction included material within its

density band derived from the silicate matrix.

The internal dose rate values were calculated using the measured radionuclide concentrations, from neutron activation analysis, of the matrix and grains, and the isochron simulation programme (using the absorbed dose fractions and attenuation factors as described in section 3.4). This required knowledge of the alpha efficiency of the microcline (calculated here as α/γ ratio for the fine-grain fraction), a parameter that was of particular importance in this case due to the matrix radionuclide composition being solely U and Th so that an unusually high proportion of the dose rate was delivered by alpha radiation. The problem of poor data quality for the fine-grain size range meant that the alpha efficiency value carried an unfortunately large error term (~ ± 25%). This is reflected in the magnitude of the dose rate percentage error terms for the smaller grain sizes being approximately double that of the coarser fractions. The significance of the accuracy (and precision) to which the alpha efficiency is known can be illustrated by calculation of the internal dose rates for different values of the alpha efficiency. The reliability of the gamma dose rate estimate obtained from the regression results is more difficult to assess, since its value is sensitive to the regression line drawn through the measured points and it consequently has a large uncertainty associated with it. The background gamma dose rate in the lead-lined cavity used for the storage of the matrices had previously been measured as <0.3 mGy.a^{-1} by CaF_2 TLD - interpreted as the sum of self dose and hard cosmic ray dose rates. Measurements with a scintillation detector produced a value of 0.05 mGy a^{-1} without the model matrices present, excluding the hard cosmic component. This value however was later realised not to be applicable here because of the increased gamma dose rate due to the presence of the other matrix experiments within the cavity. A subsequent measurement with half the matrices present produced 0.17 mGy a^{-1}, implying that the combined gamma plus cosmic dose rate within the shielded cavity when all portions of the matrices were present would be of the order of 0.4 mGy a^{-1}. The absorbed dose fraction for a spherical rock sample of similar diameter to the cylindrical sample is approximately 0.1 (Mejdahl, 1983). Therefore there is probably an internal gamma ray dose rate of 23 mGy a^{-1} in this matrix; considerably in excess of the ambient gamma contribution. This contribution was treated as an external source in the analysis, which is justified here in that it represents a common

component to all grain fractions.

Another possible source of error was the effect of radon loss. This has previously been mentioned in connection with the variation of beta count rates obtained for the matrices at different stages of the experiment. The measured parent radionuclide concentrations (by NAA) were 724.22 ppm U, 2711.80 ppm Th and 0.744%K. Assuming no radon loss the expected beta dose rate from this matrix would be 183.99 $mGy.a^{-1}$. The initial measured beta dose rate was 182.39 $mGy.a^{-1}$ which agrees very well with the expected value. After annealing the matrix its measured beta dose rate was 128.50 $mGy.a^{-1}$ - suggesting that radon gas had been driven off. 100% radon loss would have resulted in a beta dose rate of 72.73 $mGy.a^{-1}$, the observed beta dose rate corresponding to 50% radon loss. The lower alpha efficiency lessens the impact of the reduced dose rate. Also, the effect of storing the matrix/grain mixture for 87 days, approximately 23 half-lives of radon, was to allow the gas to build up again. In any case, the effect of any radon loss would be to reduce the effective internal dose rate and increase the slope of the measured isochron and therefore also increase the age estimate derived from that slope.

It is concluded then, that any effects of radon loss did not contribute to the slight age overestimation observed here. It was noted, however, that even after the storage period the beta dose rate was some 10% lower that the initial measured value.

4.5 MODEL MATRIX II: CaF_2 GRAIN SIZE ISOCHRON

4.5.1 Experimental Plan

The previous section described an experiment in which a potassium feldspar (commonly found in ceramic matrices) was coupled with a matrix that provided a high dose rate but with a radionuclide composition ratio that was not representative of the relative proportions found in naturally occurring matrices.

Here, the approach was to prepare a model matrix with a radionuclide content in proportions as representative as possible of those found in archaeological ceramic and lithic matrices. This automatically limits the extent to which the dose rate can be scaled up due to the problem of ^{40}K enrichment. This in turn precluded the use of the usual TL minerals extracted from pottery on the grounds that they would not be sensitive enough to record measurable doses within the time available. Natural calcium fluoride (the mineral fluorite) is an extremely sensitive TL mineral and was therefore matched with this matrix.

4.5.2 Materials

The preparation of this matrix was more straightforward than the previous one for two main reasons. Firstly, there was less of a radiological hazard associated with preparation and handling since the constituents were less radioactive than those required for the microcline model matrix. Also, the secondary beta standard composition was suitable for this experiment and a further 100g was prepared as outlined in section 4.3.2.

The actual matrix composition was 76.2g RGK-1, 15.0g RGTh-1, 8.8g RGU-1, which corresponds to

		Dα	Dβ	Dγ	Total
U	36.15ppm	(100.46)	5.28	4.15	
Th	120.00ppm	(88.68)	3.43	6.17	
K	34.14%	-	28.34	8.23	
	Total	(189.14)	37.05	18.55	83.97

TABLE 4.10 ACTUAL COMPOSITION OF MODEL MATRIX II

The results of beta dose rate measurements are given below, in Table 4.11.

	Dβ	$D\beta_{meas}/D\beta_{calc}$
Calculated	37.05	
Initial	37.12 ± 0.47	1.002
After Anneal	27.60 ± 0.52	0.745
After Storage	35.18 ± 0.44	0.950

TABLE 4.11 BETA DOSE RATE FOR MODEL MATRIX II COMPARED AT DIFFERENT STAGES OF THE EXPERIMENT

(NB D values are in $mGy.a^{-1}$)

Mean Values, determined by NAA	% of expected value
Uppm = 29.53 ± 1.20	81.70%
Thppm = 113.31 ± 3.99	94.42%
K% = 32.62 ± 2.15	95.56%

TABLE 4.12 RADIONUCLIDE CONCENTRATIONS OF MODEL MATRIX II, MEASURED BY NAA

The source material for the grains required for this model matrix experiment was the laboratory stock of M.B.L.E. natural CaF_2. Approximately 5g was removed and given an initial annealing cycle of heating to ~600°C for 10 mins, in air, followed by rapid cooling. Aitken and Fleming (1972) state that this treatment should not cause any serious loss of TL sensitivity.

The plastic sieves and disposable nylon sieve meshes were not used here, so as to avoid the potential of residual fluorite contamination of the sieves. Therefore settling columns (open ended) were used to effect the separation into different grain sizes. The largest grains present in the CaF_2 "as received" were ~150μm so crushing with an agate pestle and mortar was required to produce the small grain size.

Great care was taken to avoid any contamination of the sample preparation laboratory, all bench surfaces were covered with large tissues that were dampened at the end of each day's CaF_2 handling operations and then folded into themselves to minimise the spread of any stray fluorite grains. All apparatus that had been in contact with fluorite

was marked as such. These measures appear to have been successful in that there was no subsequent evidence, whatsoever, of contamination.

Two 50mg samples of the fluorite were analysed by neutron activation. The thorium content was determined as 0.97 ± 0.26 ppm. Uranium and potassium were not detected. Therefore these will be taken as absent for the present purposes.

4.5.3 Exposure Details

The mixing of the CaF_2 grains with the matrix was carried out in the same manner as for the microcline grains (section 4.4.3). The total mass of fluorite added to the 100g of matrix was 3.728g. The fluorite/matrix mixture was also annealed, prior to packaging and storage, to remove TL signals from the matrix and any signal that may have been accumulated in the fluorite since its initial annealing step prior to crushing. The measured beta dose rate of a sample taken from the annealed matrix was 27.60 ± 0.52 mGy a^{-1}, which is 74% of the beta dose rate recorded after initial mixing of the matrix, again implying some radon loss. The exposure period of 70 days was spent in a lead-lined low-background cavity to reduce the effect of any external sources of radioactivity on doses stored in the fluorite grains.

4.5.4 Extraction Of Grains

The initial unwrapping and removal of the outer ~2 mm was carried out as for the microcline/model matrix. The portion removed for beta-counting gave a measured beta-dose rate of 35.18 ± 0.44 $mGya^{-1}$ (compared to 27.60 ± 0.52 $mGya^{-1}$ at start of experiment, ie just after annealing, and 37.12 ± 0.47 $mGya^{-1}$ after initial preparation of the matrix mixture).

The high density of fluorite, 3.18g.cm^{-3}, was exploited to facilitate efficient recovery of the grains from the matrix. A volume of approximately 200ml of a sodium polytungstate solution of density 2.74 g.cm^{-3} was prepared, the aim being to carry out a large sample density separation, under the force of gravity rather than centrifugation.

Several factors had to be considered, for example the volume of liquid had to be sufficiently large to be able to cope with a charge of the order of 40g, and with a density high enough to separate the fluorite from the less dense matrix. Conversely, care also had to be taken to aim to successfully perform the separation as fast as possible - since the extremely high TL sensitivity of the fluorite meant that extended periods spent out of the matrix, prior to measurement, could result in the addition of a non-matrix, environmental, dose being recorded. Therefore, the set up used was a necessary compromise between 'perfect' separation and "efficient" (near-perfect) separation.

The matrix was gradually added to the density liquid, using a spatula to mix and stir the two together. Despite this approach, a number of floating masses formed - probably the result of the outer parts becoming saturated with the liquid before the inner parts, thus trapping air and forming floating lumps. These were broken up as much as possible with the spatula before, and between, two fifteen minute periods of agitation in an ultrasonic bath - an approach that proved to be successful.

The settling period of approximately 3.6 days was spent in dark room conditions, away from any obvious sources of radioactivity, with the beaker covered with cling-film to avoid dust contamination and evaporation. Two distinct layers were observed, the floating one had a gelatinous appearance - reflecting its major composition of <38μm grains of quartz suspended in a high density liquid.

This top layer was 'spooned' off, leaving approximately 180ml of the liquid which would still contain some of the fine-grain CaF_2 in suspension. This was transferred to centrifuge tubes and diluted with deionised H_2O washings from the settling beaker, and then spun down. A further purification step, of centrifugation in a liquid of density $2.97 g.cm^{-3}$, was included and did remove lower density material from the CaF_2 concentrate. The fluorite grains were rinsed several times in deionised water with a centrifugation step between each. The rinsing was then repeated, using acetone instead of water, and the grains placed in an oven at 50°C to dry overnight. Assuming all the dense grains collected to be fluorite it was calculated that the amount recovered

represented 73% of the mass expected to be present.

The grains were separated out into their different grain size fractions in the same way as employed during their preparation. Seven different grain size fractions were prepared but whilst the two finest were still being separated, a test run of two discs of each of the five coarsest fractions was carried out.

4.5.5 Measurement of Stored Dose

The initial test run involved a total of ten discs, two from each of the five coarsest grain size fractions. These were prepared as for the microcline discs, but here the sample masses were much less, of the order of 0.5mg. The main runs, however, were composed of sets of eight discs for each grain size each of approximately 2-3mg sample mass.

All discs were glowed in a single sample reader in an atmosphere of oxygen free nitrogen. The heating cycle terminated at 400°C to reduce the possibility of causing sensitivity changes between first and second glows due to the pre-dose effect. The "natural" dose stored in the fluorite during exposure to the model matrix was evaluated by comparison of peak heights to those induced by a 5mGy gamma dose delivered by the ^{60}Co source as described in section 4.4.5. A third glow after an alpha irradiation was measured to investigate the variation of alpha response with grain size.

4.5.6 Results

The results from both test and full runs of this experiment are presented below. Table 4.13 gives a summary of the test run, which indicated a progressive change in stored dose with grain size fraction. The stored dose measurements from the full runs are presented in Table 4.14, and the corresponding internal dose rate values in Table 4.15. 65 of the 66 individual aliquots measured produced glow curves characteristic of CaF_2 both in shape and peak positions, indicating successful recovery from the matrix. The

other disc showed evidence of contamination and was excluded from the analysis.

Grain Size[1] (microns)	Stored Dose(mGy)	
	PII[2]	PIII[3]
150	11.5	10.9
150[4]	-	-
115	14.4	12.2
115	13.4	12.2
85	14.5	12.9
85	12.7	11.4
60	16.8	14.6
60	16.8	13.9
38	17.3	16.0
38	16.0	17.6

TABLE 4.13 RESULTS OF MODEL MATRIX II EXPERIMENT: TEST RUN

Notes

1. Grain size given is the middle value of the grain size range separated.
2. Calculated as $\frac{\text{PII height (Natural)}}{\text{PII height (5 mGy)}} \times 5\text{mGy}$
3. Calculated similarly but with PIII heights.
4. 2nd glow curve for this disc obviously contaminated.

Grain Size	Stored Dose (mGy)				Alpha/gamma ratio			
(micron)	PII	PII Error	PIII	PIII Error	PII	PII Error	PIII	PIII Error
150	12.59	0.27	11.06	0.24	0.026	$4x10^{-4}$	0.01	$3x10^{-4}$
115	14.88	0.32	13.17	0.28	0.034	$8x10^{-4}$	0.02	$6.5x10^{-4}$
85	16.42	0.58	13.94	0.53	0.042	$5x10^{-4}$	0.02	$2.5x10^{-4}$
60	18.61	0.38	15.79	0.27	0.055	$1x10^{-4}$	0.03	$6x10^{-4}$
38	21.44	0.46	17.60	0.41	0.070	$1.8x10^{-3}$	0.04	$1.1x10^{-3}$
20	21.23	0.31	17.71	0.37	0.099	$2.2x10^{-3}$	0.07	$1.4x10^{-3}$
10	25.60	0.41	20.05	0.41	0.135	$3.4x10^{-3}$	0.08	$2.4x10^{-3}$

TABLE 4.14 RESULTS OF MODEL MATRIX II EXPERIMENT: FULL RUN

Grain size (microns)	PII (mGy/a)	PII error (mGy/a)	PIII (mGy/a)	PIII error (mGy/a)
150	34.05	1.67	33.08	1.67
115	37.26	1.73	35.53	1.72
85	39.10	1.75	36.85	1.75
60	41.81	1.78	38.70	1.77
38	45.69	1.81	41.26	1.79
20	51.76	1.87	45.22	1.82
10	54.46	1.90	47.00	1.84

TABLE 4.15 DOSE RATE VALUES FOR MODEL MATRIX II

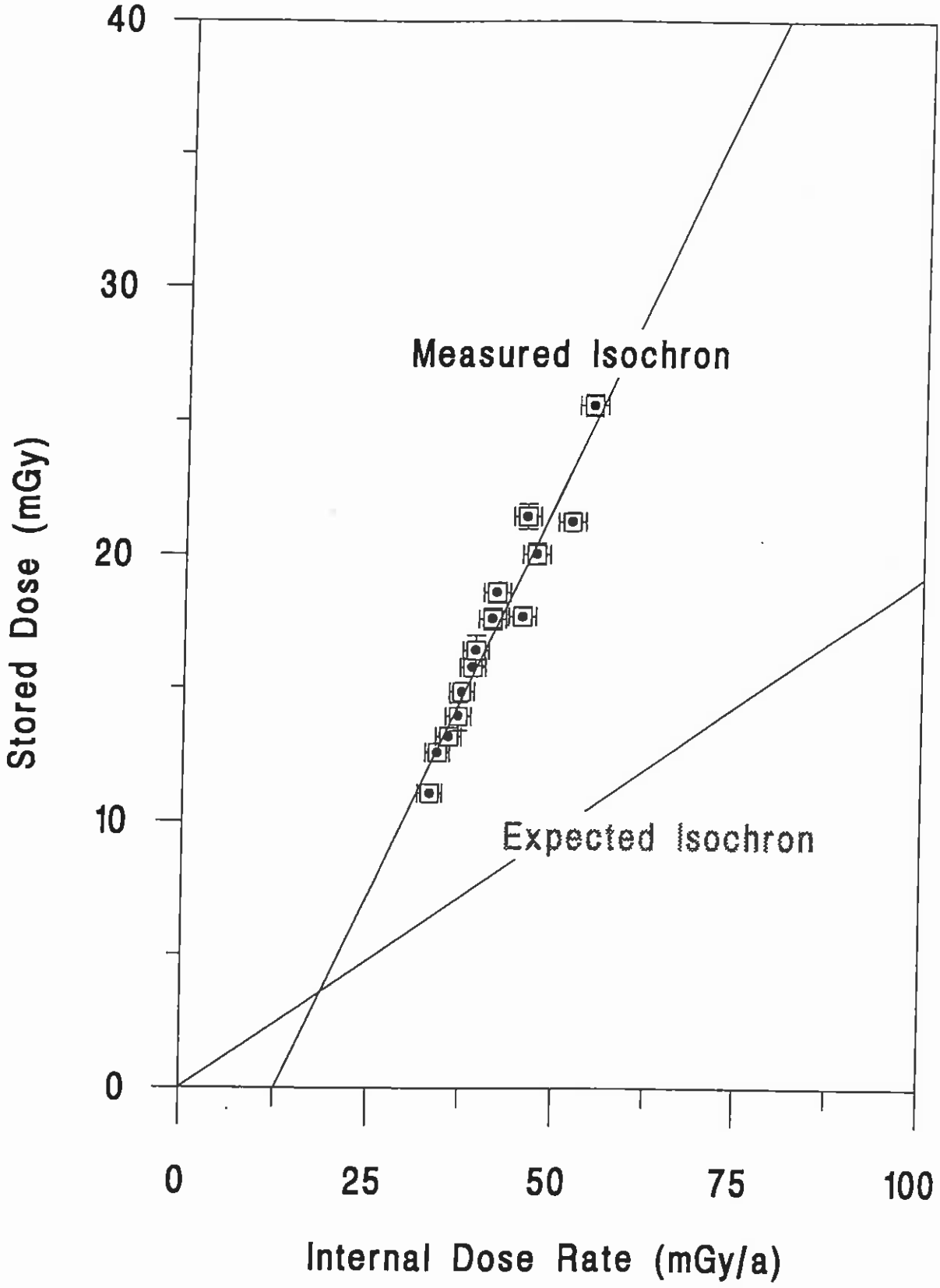

FIG.4.8. ISOCHRON PLOT ; FLUORITE/MODEL MATRIX

4.5.7 Analysis and Discussion

Both test and full runs showed clear indications of isochron behaviour. The isochron plot from the full run is shown in Figure 4.8. This figure also shows the expected isochron, based on the known age and the assumptions that the measured stored doses are correct and that the external gamma dose rate was zero.

However, both data sets produced systematic overestimates of the known exposure period of 0.192 years. Using linear regression analysis, the test run gave an age estimate of 0.536 ± 0.072 years, while the full run produced an age estimate of 0.594 ± 0.047 years.

There are a number of factors that could have influenced the results of this experiment. These include the estimation of dose rates, source calibrations, and stopping power variations. These are examined below.

4.5.7.1 Estimation of Dose Rates.

There was evidence in the reduced beta dose rate measurements taken after annealing the matrices of radon loss in both experiments followed by partial recovery during the exposure period. Dose rate conversion factors applicable to 100% radon loss, which considerably overestimate the possible effect within the matrix were taken from Aitken (1983), and used to calculate the expected dose rates for the microcline and fluorite model matrices. Since this involves a reduced dose rate it clearly cannot account for excess signals.

There was no evidence here for gamma cross-talk from the high to the low dose rate matrix as this would have effectively been an external dose rate component, and therefore should be apparent as a positive intercept on the y-axis of the isochron plot. There was no such intercept which suggests that if the observed discrepancy was due to excess dose rate, then this was present as an internal component.

The possibility of a gamma self-dose within this matrix can be considered. The infinite matrix gamma dose rate, calculated from the radionuclide concentrations, is approximately 17 mGy/a. However, the absorbed gamma dose fraction for an object of the dimensions and density (~1g/cm^3) used here is very small. The overall effect of an internal gamma dose rate component is therefore not likely to be significant.

The possibility of an excess internal dose rate component being derived through radon migration, from the high U/Th concentration matrix to the lower dose rate matrix containing the CaF_2 grains, is examined here.

Having calculated the expected dose rates (based on the measured radionuclide concentrations of the matrix, attenuation factors (as described in section 3.4) and alpha efficiency, taken here as the α/γ ratio for the fine-grain fraction) and knowing the age of the samples, if the measured stored doses are assumed to be correct, then it is possible to calculate the excess dose rate that would be required to give the known age. This is shown below in Table 4.16.

Grain size (μm)	Measured dose rate (mGy/a)	Required dose rate (mGy/a)	Excess dose rate required (mGy/a)
PII 10	54.46	133.47	79.01
20	51.77	110.69	58.92
38	45.68	111.78	66.10
60	41.82	97.03	55.21
85	39.10	85.61	46.51
115	37.26	77.58	40.32
150	34.04	65.64	31.60
PIII 10	47.00	104.54	57.54
20	45.21	92.34	47.13
38	41.26	91.76	50.50
60	38.70	82.33	43.62
85	36.85	72.68	35.83
115	35.53	68.67	33.14
150	33.08	57.66	24.58

TABLE 4.16 EXCESS INTERNAL DOSE RATE REQUIRED TO OBTAIN KNOWN AGE.

The next step is to calculate the maximum possible excess dose available. This would correspond to the situation where the high dose rate matrix suffers 100% radon loss - the available excess being the difference between full series and pre-radon dose rates.

MICROCLINE / MODEL MATRIX DOSE RATES			
(A) NO RADON LOSS			
U_{ALPHA}	Th_{ALPHA}	U_{BETA}	Th_{BETA}
2012.61 ± 77.45	2004.02 ± 68.07	105.74 ± 4.07	77.56 ± 2.63
(B) 100% RADON LOSS			
912.52 ± 35.12	837.95 ± 28.46	43.45 ± 1.67	27.12 ± 0.92
(C) DOSE RATE "LOST" [= (A)-(B)]			
1100.09 ± 42.33	1166.07 ± 39.61	62.28 ± 2.40	50.44 ± 1.71

TABLE 4.17 INFINITE MATRIX DOSE RATES CALCULATED FOR (A) NO RADON LOSS AND (B) 100% RADON LOSS FROM MICROCLINE/MATRIX

Using the appropriate attenuation factors to calculate the effective maximum possible dose rate to each grain size, it then possible to determine the excess dose rate required as a percentage of this value, as shown in Table 4.19.

Grain size (μm)	Measured dose rate (mGy/a)	Required dose rate (mGy/a)	Excess dose rate required (mGy/a)	Maximum excess dose rate available	(Required)/ (maximum) (%)
PII 10	54.46	133.47	79.01	375.16	21.06
20	51.77	110.69	58.92	339.78	17.34
38	45.68	111.78	66.10	259.48	25.48
60	41.82	97.03	55.21	209.14	26.40
85	39.10	85.61	46.51	175.32	26.53
115	37.26	77.58	40.32	154.12	26.16
150	34.04	65.64	31.60	121.17	26.08
PIII 10	47.00	104.54	57.54	273.21	21.06
20	45.21	92.34	47.13	250.26	18.83
38	41.26	91.76	50.50	198.81	25.40
60	38.70	82.33	43.62	166.45	26.21
85	36.85	72.68	35.83	144.46	24.80
115	35.53	68.67	33.14	130.39	25.40
150	33.08	57.66	24.58	107.88	22.79
				Mean	23.82
				Std. Dev.	3.07

TABLE 4.19 CALCULATED EXCESS DOSE RATES REQUIRED

The results presented in Table 4.19 suggest that the stored doses measured in the fluorite grains might be explained if approximately 24% of the available excess dose rate (assuming radon loss from the microcline/model matrix experiment) were able to migrate to the fluorite/matrix system. Despite the fact that measures had been taken to prevent, or at least limit, radon loss, the beta dose rate of the microcline/model matrix measured (thick source beta counting) at the end of the exposure period was lower than the initial (prior to annealing) value.

Expected beta dose rate	= 183.9 mGy/a
(based on measured (NAA) radionuclide concentrations, no radon loss)	
Measured beta dose rate (initial)	= 182.4 mGy/a
Expected beta dose rate "lost" (if 100% radon loss)	= 112.7 mGy/a
24% of expected beta dose rate "lost" (if 100% radon loss)	= 26.9 mGy/a
If the microcline/model matrix beta dose rate had equilibriated at approximately 24%	
down then the expected measured value would be 182.4 - 26.9	= 155.5 mGy/a
Actual measured value at the end of the exposure period	= 163.7 mGy/a

Although these figures do not provide conclusive evidence that this was the case, they are perhaps indicative that the situation may have contributed to the observed results. However, if this were the case one might expect a corresponding increase in the measured beta dose rate of the fluorite/model matrix. Table 4.11 shows that this was not the case, although this could be explained if the delay between removing the matrix material from the container and starting the beta count was of the order of a few hours, during which time the excess beta activity could decay.

At present, there is no clear answer and it is felt that further experimentation would help clarify the situation, eg. immediate beta counting of the fluorite/model matrix on removal from containment after storage, followed by repeated counting to look for evidence of an excess beta dose fall off with time. Another approach could be to store a radioactively inert matrix, loaded with fluorite grains, in the same arrangement as has been described above. Measurement of the stored dose recorded in the fluorite would provide information regarding the presence, or otherwise, of an excess radiation dose rate.

The measured radionuclide concentrations in the fluorite were found using NAA. The thorium content was determined as 0.97 ± 0.26 ppm, uranium and potassium were not detected. Aitken (1969, 1985) states values of CaF_2 self dose ~0.1mGy.a^{-1} to a level which would not be significant here. Beta counting of a bulk sample of the fluorite source material was considered.

4.5.7.2 Source Calibrations.

The alpha source working calibration had been confirmed by a cross-comparison with the Oxford laboratory. The gamma source working calibration had been provided by Dr D Sanderson, from measurements made three months prior to its use for these experiments, decay-corrected to the irradiation date with a precision of ± 5%. The SURRC beta source was originally cross-calibrated to a source at Paisley which had been calibrated to both the Oxford and Riso sources to better than ± 2% precision in 1987. Subsequent experiments at SURRC cross-compared the beta source with a 200 TBq gamma source by TLD which was also calibrated by National Physical Laboratory traceable photochromic plastics (Harwell red perspex dosimeters). Both of these measurements agreed to within 0.8% (Ward, 1988). These have been well traced to national and international standards; furthermore coherent TL dates have been obtained from known-aged Roman samples and from a number of well-characterised archaeological sites where radiocarbon evidence is also available. Additional confidence in the source calibrations is provided by the observation that the measured fine-grain alpha efficiencies agree well with published values.

4.5.7.3 Effect of Stopping Power Variations.

The use of potassium sulphate as the main matrix component introduces the possibility of error in absorbed dose fractions. To evaluate the possible implications the beta stopping power contrast between this matrix and typical silicates was estimates as below: Beta stopping power is proportional to Z, as calculated from

$$\bar{Z} = \frac{\sum N_i Z_i^2}{\sum N_i Z_i} \quad (4.5)$$

where Ni is the relative number of nuclei of charge Zi (the theoretical basis for this choice of $\bar{Z}$ is given in Cross (1968) (NB $\bar{Z}$ for an element = Z.)

Calculated values of $\bar{Z}$

Si	14
SiO_2	10.80
K_2SO_4	14.35
CaF_2	14.79

Stopping powers for compounds and mixtures are additive, in terms of the weight fractions f_{zi} of elements of atomic number Z_i then

$$S_{comp} = f_{Z1}\,(S_{Z1}) + f_{Z2}\,(S_{Z2}) + f_{Zi}\,(S_{Zi})$$

(From Attix 1986 p 178)

It can be calculated that the β stopping power of a K_2SO_4 matrix is 5% lower than a silicate matrix. However, dose rate is inversely proportional to the stopping power ratio so the β-dose rate will be 5% higher.

CaF_2/K_2SO_4 mean β stopping power ratio = 0.99

CaF_2/SiO_2 mean β stopping power ratio = 0.94.

Therefore the dose recorded by fluorite grains will be ~ 6% higher than for quartz grains in a silicate matrix. In a potassium sulphate matrix however the use of CaF_2 matches matrix properties within 1%. Neither effect is sufficiently pronounced to account for the gross excess age estimates.

Alpha particle range is approximately proportional to $A^{\frac{1}{2}}$ (Bragg-Kleeman rule) where A = atomic weight of the material (for compounds and mixtures) the effective A can be found from:

$$A^{1/2} = \frac{\sum n_i A_i}{\sum n_i A_i^{1/2}} \qquad (4.6)$$

where n_i is the atomic fraction of the element A_i

K_2SO_4 A eff = 26.01

CaF_2 A eff = 26.92

α stopping powers can be found from interpolation of values given in data tables eg Northcliffe and Schilling.

Al (A = 26.98)

Ne (A = 20.18)

The alpha stopping power of a K_2SO_4 matrix is 14% lower than a silicate matrix. This implies that the K_2SO_4 matrix will have an alpha dose rate that is 16% higher than a silicate matrix.

The alpha stopping power ratio of CaF_2: Quartz = 0.598/0.667 = 0.8966 . Therefore the alpha dose recorded in fluorite grains will be ~ 10% less than for quartz grains. This implies an overall increase of ~ 6% in the effective alpha dose rate for fluorite grains in a potassium sulphate matrix. This in itself is insufficient to explain the experimental results obtained.

4.5.7.4 Other considerations

Another potential variable is the possibility of non-uniform distribution of grain sizes within a particular specified range, eg 10-30μm treated as 20μm may contain more "finer" grains or vice versa than expected. The effect of this would be greater for the small grain size ranges with the result being essentially to pivot the isochron line. The direction of the pivoting action would depend on whether the grain size distribution was biased to the finer or coarser end of the range. The possibility that the crushing action either generated a higher than expected surface to volume ratio, or preferential defect structures on grain surfaces, leading to high alpha efficiency was considered briefly. Although further experimental work would be needed to specifically exclude this possibility, it was noted that the measured alpha efficiencies, by external radiation

followed a similar grain-size dependence to that described by Aitken (1985), implying that these effects were not dramatic.

4.6 SUMMARY

This chapter has described the use of model matrices to evaluate the validity of the isochron predictions of Chapter 3. This required the identification of suitable combinations of materials from which to prepare the two proposed grain/matrix mixtures. The development of grain size and mineral phase separation techniques to include intermediate grain sizes has been described. The preparation and execution of the model matrix experiments have been described in detail.

Isochron behaviour was clearly observed in both experiments. The microcline feldspar experiment produced an acceptable age estimate from a high dose rate matrix, despite having an atypical U, Th, K mix. The fluorite experiment also produced clear evidence of an isochron with good precision. These age estimates were, however, systematically greater than the known age by a factor of approximately 3. Having considered the magnitude of numerous possible systematic error terms it was concluded that the sample was probably inadvertently exposed to an additional internal radiation source, most likely the consequence of unexpected radon migration from the adjacent higher activity source. Nevertheless these results show the potential of model experiments, and also suggest improvements that could be made in the experimental design for further investigation and subsequent studies of real samples.

5.DISCUSSION AND CONCLUSIONS

5.1 SUMMARY

This work has aimed to contribute to the solution of a problem relevant to archaeology and microdosimetry, namely the TL dating of destratified archaeological ceramics. The background to this problem has been presented within the context of the historical development of thermoluminescence dating (Chapter 1) and of dosimetry concepts (Chapter 2). It was noted that much valuable archaeological material, including many ceramics from important sites excavated during the early part of this century, and having an influential role in the establishment of archaeological chronologies and sequences, exists in museums. Absolute dating of this corpus of material would be extremely valuable to archaeology in allowing historic hypotheses to be tested. However, this is not possible using conventional approaches to thermoluminescence dating since these require full solution of the TL age equation for individual mineral phases. This in turn requires knowledge of the external radiation dose rate during burial; comprised of gamma and cosmic radiation. In the case of 'fine grain' dating the external component provides a variable fraction of the total dose rate, perhaps typically some 25%; for 'inclusions' this proportion may be larger, perhaps 30% or more. To maintain dating precision of 5% overall, it is necessary to estimate the external component within a precision of some ± 20%. Where direct in-situ measurements on the excavation site are not feasible, or where representative samples of the burial media are unavailable an alternative approach is needed.

Previously proposed strategies (for example the 'subtraction' method which combines fine grain and inclusion approaches, the use of large inclusions with varying beta attenuation, zircon dating) were considered, and reviewed critically. It was shown in Chapter 3 that these approaches were simply special cases of a general model for the TL age equation whereby the age can be extracted, independently from the external radiation dose rate, using an isochron approach. The isochron model was developed explicitly and theoretical simulation used to explore different microdosimetric systems. Two main isochron solutions were identified, the grain size (or alpha-beta attenuation) and alpha efficiency isochrons. The simulations could be used to advantage by indicating the most promising experimental strategy for a given sample matrix and

mineralogy, eg. for a matrix containing a high potassium concentration there would be the potential to exploit grain size effects resulting from beta attenuation. However, for a low potassium matrix these effects would be less pronounced and so the alpha dose rate component becomes more significant, thus increasing the possible benefits of any variations in alpha efficiency that may be apparent.

Given the constraints of materials and time an experimental approach using two model matrices was employed (Chapter 4) to evaluate the validity of the grain size isochron predictions. Isochron behaviour was clearly observed in both cases. The microcline feldspar experiment produced a consistent age estimate from a high dose rate matrix. It should be noted that the microcline grains used here are of the sort of grains one would realistically find in archaeological samples. This, coupled with the fact that the low stored doses encountered in this experiment limit precision, make the result obtained (measured age estimate = 0.29 ± 0.05a, expected age = 0.238a) very encouraging and supportive of the isochron model. The fluorite experiment was expected to provide high precision verification of the isochron model. It did produce a highly coherent data set consistent with the expected sensitivity and reproducibility of CaF_2. However, the age estimate obtained was greater that the expected value by a factor of approximately 3. This result proved difficult to explain and a number of possible reasons were examined. It was eventually concluded that the possibility of radon migration from the microcline matrix into the fluorite matrix may have resulted in an unexpected alpha and beta dose contribution to this second matrix, due to the decay of radon daughters. This radon migration hypothesis could be tested in various ways, eg. by measuring the beta countrate of the fluorite matrix immediately after removal from storage and then subsequently to monitor for an initial excess countrate followed decay to a constant value, or by storing a blank (radioactively inert) matrix, loaded with fluorite grains, in a similar geometry to that used for the model matrix experiments described in Chapter 4. The test for radon migration would be positive if, after storage, the measured stored dose in the fluorite was found to be greater than the combined effect of cosmic and self dose rate components. Alternatively, the high and low dose rate matrices could have been isolated physically, by storing them in separate low-background lead-lined shields, or temporally, by conducting the experiments at different times.

5.2 FUTURE DEVELOPMENTS

The most obvious area for immediate further work has been highlighted above, ie. the need to resolve the discrepancies observed in the experimental results obtained from controlled systems. To achieve the ultimate aim of this work - to obtain TL isochron age estimates from archaeological material - an important, if not essential, intermediate stage would be to test the method on known age material.

The transition from controlled systems to real samples introduces some challenging variables, eg. a ceramic fragment will contain a finite assemblage of grain sizes and mineral types that will exhibit a range of TL characteristics. The optimisation of separation techniques for different grain sizes and mineral types should be straightforward to achieve through the development of current methods.

The use of complementary techniques to measure radionuclide concentrations of the mineral separates (eg ICP-MS, although it involves a more complex preparation stage) would provide a useful check on NAA results. Fission track mapping of the uranium and thorium distribution may also be usefully introduced to provide information relevant to alpha dosimetry.

In terms of the large number of measurements required to produce an isochron plot, the use of automated readout and irradiation facilities would not only reduce the number of man-hours spent making these measurements but could also improve precision through measurement of greater numbers of discs per sample. The availability of a gamma source of a suitable dose rate would be an advantage in cases where very coarse grains (and therefore very useful isochron data points) are present in the sample being dated, since the problem of attenuation of the dose from a laboratory beta source does not apply.

Recent developments in luminescence dating, particularly the use of light to release the trapped charge, may have much to offer isochron methods. The potential of being able to carry out rapid high precision ED measurements has obvious advantages. However,

it is also apparent that it may be possible to use different stimulation wavelengths that are mineral specific eg. exposure to green light will stimulate luminescence from quartz and feldspar, whereas infrared wavelengths stimulate luminescence from feldspars. It may, therefore, be possible to reduce the level of mineral separation that is currently required. Development of spatial imaging techniques, eg. imaging photon detectors, may provide sufficient resolution to image individual grains, perhaps as small as fine grains, and so eliminate the need for grain size separation of a sample.

5.3 CONCLUSIONS

The need for an archaeological solution to the problem of dating destratified samples has been clearly demonstrated. It has been shown that isochron methods provide a general solution to the problem of eliminating the unquantifiable external dose components from TL dating. By simulation it has been demonstrated that measurable contrasts in stored dose between extractable phases from many ceramic samples are predicted using the standard dosimetric models that form the basis of TL dating. Experiments with model matrices have confirmed the general behaviour. The results from a microcline loaded matrix of high U/Th contents were highly satisfactory, and provide support for the isochron approach. The results from another experimental simulation using CaF_2 appear to have identified a pitfall, in the form of unexpected radon crosstalk, which must be investigated further and taken into account in future experimental work.

Archaeological samples will present a more variable system. However, there are grounds for believing that these obstacles are not insurmountable. Developments in automation of TL dose estimation, eg. the use of photostimulation, and in single grain imaging techniques may significantly enhance the practicability of isochron approaches to TL dating. It is also possible that detailed studies will lead to improved models for the microdosimetry of TL dating. It remains to be seen whether isochron methods will become standard approaches to archaeological dating. However, it is clear that they offer a potential solution to the problem of dating destratified samples.

6. ADDENDUM

Having carried out the experimental investigation of the isochron model as described in this thesis, the results from the fluorite matrix remained problematical to explain in a satisfactory manner. It was therefore decided to take advantage of having prepared and stored two portions of each matrix. The assistance of Dr. Sanderson in carrying out this work is acknowledged here. Two approaches were followed; firstly, the measurement of the beta countrate from the fluorite matrix from the time of removal, to look for a possible excess countrate that might indicate the effect of radon crosstalk from the microcline matrix, with continued counting to monitor any subsequent decay of the countrate. The results are given below, with the values from the first portion for comparison.

	$D\beta$	$D\beta_{meas}/D\beta_{calc}$
Calculated	37.05	
Initial	37.12 ± 0.47	1.002
After Anneal	27.60 ± 0.52	0.745
After Storage	35.18 ± 0.44	0.950
Second portion (approx. 5min after opening)	35.75 ± 0.42	
Second portion (approx. 20hr after opening)	35.21 ± 0.42	

TABLE 6.1 BETA DOSE RATE FOR MODEL MATRIX II COMPARED AT DIFFERENT STAGES OF THE EXPERIMENT
(NB D values are in $mGy.a^{-1}$)

The conclusion drawn from these results was that there did not appear to be any evidence for radon crosstalk.

The second approach was to dry sieve this material to obtain some ~100 micron fluorite grains. These were washed, dried and then two discs were prepared. The predicted stored dose in these grains, assuming no excess dose rate, was calculated as shown

below.

	Inf. matrix dose rate mGy/a	Attenuation factor(1-ϕ)	Effective dose rate PII α eff 0.135	Effective dose rate PIII α eff 0.085
U α	100.46	0.215	2.92	1.84
Th α	88.68	0.248	2.97	1.87
U β	5.28	0.904	4.77	4.77
Th β	3.43	0.857	2.94	2.94
K β	28.34	0.965	27.35	27.35
TOTAL			40.95	38.77

TABLE 6.2 CALCULATED EFFECTIVE DOSE RATE FOR 100 MICRON FLUORITE GRAINS.

(Infinite matrix dose rate data from Table 4.10, attenuation factors derived from Tables 3.1 and 3.2, alpha efficiency as measured previously from fine-grain fraction).

Having calculated the expected dose rates, as shown above, and knowing the exposure period (4.25 years), the expected stored doses can also be calculated;-

PII : 174 mGy

PIII : 165 mGy

The natural TL was glowed out and then a beta dose of approximately 168 mGy was delivered from a Sr^{90} source. The dose rate of the source, 28 mGy/sec, means that the six second exposure time obviously would have some timing error associated with it. This was considered acceptable given the aims of the experiment.

RESULTS

Disc 1	Natural signal	Signal after 168 mGy dose	Stored dose mGy
PII	186939	156273	201
PIII	856712	760407	189
Disc 2			
PII	42166	39939	177
PIII	263540	254144	174

TABLE 6.3 STORED DOSE EVALUATIONS

(Disc 1 is thought to have a larger timing error associated with its beta dose than disc 2).

6.1 CONCLUSIONS

It is evident from the above that (a) this matrix was receiving the same dose rate as had been predicted for the first portion examined in Chapter 4 (b) there was no evidence of radon crosstalk between the second pair of matrices and (c) after a 4.25 year exposure period the results from these 100 micron grains are within experimental error of the predicted values.

Although, at this stage, the reasons for the anomalous results obtained from first portion of this matrix remain unclear, it would appear that the original experimental design and method were valid. It is expected that a more detailed analysis of the residual material would resolve the problem, and the isochron approach does indeed deserve further investigation.

REFERENCES

Aitken, M. J. (1968) Thermoluminescent Dating in Archaeology. Introductory Review. In: *Thermoluminescence of Geological Materials. Ed.* D. J. McDougall, pp. 369-387, Academic Press, New York.

Aitken, M. J. (1969) Thermoluminescent dosimetry of environmental radiation on archaeological sites. *Archaeometry* **11,** 109-114.

Aitken, M. J. (1974) *Physics in Archaeology.* Clarendon Press, Oxford.

Aitken, M. J. (1978a) Dose-rate evaluation. *PACT* **2,** 18-33.

Aitken, M. J. (1978b) Radon loss evaluation by alpha counting. *PACT* **2,** 104-117.

Aitken, M. J. (1979) Pre-dose dating: predictions from the model. *PACT* **3,** 319-324.

Aitken, M. J. (1985a) Alpha particle effectiveness: numerical relationship between systems. *Ancient TL* **3** (3), 22-25.

Aitken, M. J. (1985b) *Thermoluminescence dating.* Academic Press, London.

Aitken, M. J. (1990) *Science-based dating in archaeology.* Longman, London.

Aitken, M. J., Fleming, S. J., Reid, J. and Tite, M. S. (1968) Elimination of Spurious Thermoluminescence. In: *Thermoluminescence of Geological Materials. Ed.* D. J. McDougall, pp. 133-142. Academic Press, New York.

Aitken, M. J. and Murray, A. S. (1976) The pre-dose technique: radiation quenching. The Edinburgh Symposium on Archaeometry and Archaeological Prospection, Extended Abstracts, HMSO.

Aitken, M. J., Tite, M. S. and Reid, J. (1963) Thermoluminescent Dating: Progress Report. *Archaeometry* **6,** 65-75.

Aitken, M. J., Zimmerman, D. W. and Fleming, S. J. (1968) Thermoluminescent Dating of Ancient Pottery. *Nature* **219,** 442-445.

Aitken, M. J., et al. (1985) Beta and gamma gradients. *Nucl. Tracks,* Vol. **10** Nos 4-6, 647-653.

Bailiff, I. K. (1976) Use of phototransfer for the anomalous fading of thermoluminescence. *Nature* **264,** 531-533.

Bailiff, I. K. (1982) Beta-TLD apparatus for small samples. *PACT* **6,** 72-75.

Bailiff, I. K. (1983a) Sensitization of R-traps? *PACT* **9,** 207-214.

Bailiff, I. K. (1983b) Pre-dose dating of Iron-Age pottery from northern Britain. *PACT* **9,** 219-225.

Bailiff, I. (1988) Principles of TL dating, in course notes, from SERC short course on the Application of TL dating, Durham University, 4-8 January, 1988.

Bailiff, I. K. and Aitken, M. J. (1980) Use of thermoluminescence dosimetry for evaluation of internal beta dose-rate in archaeological dating. *Nucl. Instrum. Methods* **173,** 423-429.

Bell, W. T. (1976) The assessment of the radiation dose-rate for thermoluminescence dating. *Archaeometry* **18,** 107-111.

Bell, W. T. (1976a) Thermoluminescence dating dose rate data. *Archaeometry* **21,** 243-245.

Bell, W. T. (1976b) Attenuation factors for the absorbed radiation dose in quartz grains for thermoluminescence dating. *Ancient TL* **8,** 2-13.

Bell, W. T. (1977) Thermoluminescence dating: revised dose rate data. *Archaeometry* **19,** 99-100.

Bell, W. T. (1980) Alpha dose attenuation in quartz grains for thermoluminescence dating. *Ancient TL* **12,** 4-8.

Berger, M. J. (1971) Distribution of absorbed dose around point sources of electrons and beta particles in water and other media. *Journal of Nuclear Medicine (Supp.)* **5,** 5-23.

Berger, M. J. (1973) Improved point kernels for electron and beta ray dosimetry *NBSIR* 73-107. National Bureau of Standards, Washington, DC.

Bintliff, J. L. (ed) (1984) *European Social Evolution. Archaeological Perspectives.* Pub. Uni. of Bradford. Chanctonbury Press Ltd.

Botter-Jensen, L., Bundegaard, J. and Mejdahl, V. (1983) An HP-85 microcomputer controlled automated reader system for TL dating. *PACT* **9,** 343-349.

Bowman, S. G. E. (1979) Phototransferred thermoluminescence in quartz and its potential use in dating. *PACT* **3,** 381-400.

Bowman, S. G. E. and Huntley, D. J. (1984) A new proposal for the expression of alpha efficiency in TL dating. *Ancient TL* **2,** 6-11.

Boyle, R. (1664) Experiments and considerations upon colours with observation on a diamond that shines in the dark. Henry Herringham, London.

Charalambous, S. and Michael, C. (1976) A new method of dating pottery by thermoluminescence. *Nucl. Instrum. Methods* **137,** 565-567.

Clark, P. A. and Templer, R. H. (1988) Thermoluminescence dating of materials which exhibit anomalous fading. *Archaeometry* **30** (1), 19-36.

Cross, W. G. (1968) Variation of beta dose attenuation in different media. *Physics in Medicine and Biology* **13,** 611-618.

Daniels, F., Boyd, C. A. and Saunders, D. F. (1953) Thermoluminescence as a research tool. *Science* **117,** 343-349.

East, B. W. (1991) Environmental behaviour of radionuclides in an urban environment. *DOE Report* **No: DOE/HMIP/RR/91/026.**

Faires, R. A. and Parks, B. H. (1973) *Radioisotope laboratory techniques.* Butterworths, London.

Fieschi, R. and Scaramelli, P. (1968) Photostimulated thermoluminescence in alkali halid crystals. In: *Thermoluminescence of geological materials. Ed.* D. J. McDougall, 291-308.

Filberth, E. W., Rowe, M. W. and Shaefer, H. J. (1980) Uranium in Hueco and Guadalupe Mountain Indian Ceramics. *Archaeometry* **22** (1), 107-110.

Fleming, S. J. (1966) Study of Thermoluminescence of crystalline extracts from pottery. *Archaeometry* **9,** 170-173.

Fleming, S. J. (1970) Thermoluminescence dating: refinement of the quartz inclusion method. *Archaeometry* **12,** 135-146.

Fleming, S. J. (1973) The pre-dose technique: a new thermoluminescence dating method. *Archaeometry* **15** 13-30.

Fleming, S. J. (1979) *Thermoluminescence techniques in archaeology.* Clarendon Press, Oxford.

Fleming, S. J. and Thompson, J. (1970) Quartz as a heat resistant dosimeter. *Health Physics* **18,** 567-568.

Fleming, S. J. and Stoneham, D. (1973) The subtraction technique of thermoluminescence dating. *Archaeometry* **15** (2), 229-238.

Fremlin, J. H. (1968) Effects of Non-uniformity of material on the thermoluminescent method of dating. In: *Thermoluminescence of Geological Materials. Ed.* D. J. McDougall, pp. 419-425. Academic Press, New York.

Fremlin, J. H. and Srirath, S. (1964) Thermoluminescent dating: examples of non-uniformity of luminescence. *Archaeometry* **7,** 58-62.

Goedicke, C. (1985) TL dating: a novel form of differential dating. *Nuclear Tracks and Radiation Measurements* **10,** 811-816.

Greening, J. R. (1985) *Fundamentals of radiation dosimetry.*

Greison, K. (1942) The intensities of the hard and soft components of cosmic rays as functions of altitude and zenith angle. *Physics Review* **61,** 212.

Guerin, G. and Valladas, G. (1980) Thermoluminescence dating of volcanic plagioclases. *Nature* **286,** 697-699.

Horowitz, Y. S. (1984) *Thermoluminescence and Thermoluminescent Dosimetry.* CRC Press, Florida.

Huntley, D. J., Godfrey-Smith, D. I. and Thewalt, M. L. W. (1985) Optical dating of sediments. *Nature* **313,** 105-107.

Hutt, G., Smirnov, A. and Tale, I. (1979) On the application of thermoluminescence of natural quartz to the study of geochronology of sedimentary deposits. *PACT* **3**

Katz, L. and Penfold, A. S. (1952) Range-energy relations for electrons and the determination of beta end-point energies by absorption. *Reviews of Modern Physics* **Vol. 24** (1), 28-44.

Kennedy, G. C. and Knopff, L. (1960) Dating by thermoluminescence. *Archaeology* **13,** 147-148.

Grogler, N, Houtermans, F. G. and Stauffer, H. (1960) Über die Datierung von Keramik und Ziegel durch Thermolumineszenz. *Helvetica Physica Acta* **33,** 595-596.

Langouet, L., Roman, A. and Gonzales, R. (1980) Datation de poteries anciennes par la méthode D.A.T.E., 1976. Symp. on Archaeometry and Archaeological Prospection, National Museums of Antiquities of Scotland, Edinburgh, 312-320.

Lewis, D. R. (1968) Effect of grinding on thermoluminescence of dolomite, calcite and halite. In: *Thermoluminescence of Geological Materials. Ed.* D. J. Dougall, pp 125-132. Academic Press, New York.

Li, J-L., Pei, J-X., Wang, Z-Z. and Lu, Y-C. (1977) Kexue Tongbao (China) 22, 498-502.

Lovborg, L. and Kirkegaard, P. (1974) Response of 3" x 3" NaI(Tl) detectors to terrestrial gamma radiation. *Nuclear Instruments and Methods* **121,** 239-251.

Malik, S. R., Durrani, S. A. and Fremlin, J. J. (1973) A comparative study of the spatial distribution of uranium and of TL-producing minerals in archaeological materials. *Archaeometry* **15** (2), 249-253.

Mangini, A., Pernicka, E. and Wagner, G. A. (1983) Dose-rate determination by radiochemical analysis. *PACT* **9** (1), 49-56.

McKeever, S. W. S. (1985) *Thermoluminescence of solids*. Cambridge University Press.

McKerrell, H. and Mejdahl, V. (1981) Progress and problems with automated TL dating. Proc. 16th Int. Symp. Archaeometry and Archaeological Prospection, Riso-M-2265, Riso National Laboratory, Roskilde.

McManus, J. (1988) Grain size determination and interpretation. In: *Techniques in Sedimentology. Ed.* M. Tucker, Blackwell Scientific Publications.

Meakins, R. L., Dickson, B. L. and Kelly, J. C. (1979) Gamma ray analysis of K, U and Th for dose rate estimation in thermoluminescent dating, *Archaeometry* **21** (1), 79-86.

Mejdahl, V. (1972) Progress in TL dating at Riso. *Archaeometry* **14** (2), 245-256.

Mejdahl, V. (1979) Thermoluminescence dating: beta dose attenuation in quartz grains. *Archaeometry* **21** (1), 61-72.

Mejdahl, V. (1983) Feldspar inclusion dating of ceramics and burnt stones. *PACT* **9**, 351-366.

Mejdahl, V. and Wintle, A. G. (1984) Thermoluminescence applied to age determination in archaeology and geology. In: *Thermoluminescence and Thermoluminescent Dosimetry, Volume III. Ed.* Y. S. Horowitz, C.R.C. Press.

Mejdahl, V. and Winther-Nielsen, M. (1982) TL dating based on feldspar inclusions. *PACT* **6**, 426-437.

Michels, J. W. (1973) *Dating methods in Archaeology*. Seminar Press, New York.

Miller, J. A. (1970) Dating by the potassium - argon method- some advances in technique. In *Science and Archaeology, edited* by D. Brothwell and E. Higgs, Thames and Hudson.

Moorehead, F. F. and Daniels, F. (1957) *J. Chem. Phys.* **27**, 1318-1324.

Morozov, G. V. (1986) The Dating of Quaternary Ukranian Sediments by Thermoluminescence XIIIth INQUA Congr. Kiev.

Murray, A. S. and Aitken, M. J. (1982) The measurement and importance of radioactive disequilibria in TL samples. *PACT* **6**, 155-169.

Murray, A. S. and Aitken, M. J. (1988) Analysis of low-level natural radioactivity in small mineral samples for use in thermoluminescence dating using high resolution gamma spectroscopy. *Applied Radioactive Isotopes* **Vol 39** (2), 145-158.

Nambi, K. S. V. and Aitken, M. J. (1986) Annual dose conversion factors for TL and ESR dating. *Archaeometry* **28** (2), 202-205.

Plachy, A. L. and Sutton, S. R. (1982) Determination of the dose rate to quartz in granite. *PACT* **6**, 188-194.

Poolton, N. J. and Bailiff, I. K. (1989) The use of LED's as an excitation source for photoluminescence dating of sediments. *Ancient TL* **Vol 7** (1), 18-20.

Prescott, J. R. and Stephan, L. G. (1982) Contribution of Cosmic radiation to environmental dose. *PACT* **6**, 17-25.

Randall, J. T., and Wilkins, M. H. F. (1945) Phosphorescence and electron traps. Proceedings of the Royal Society of London, A. 184, 366-407.

Rendell, H. M., (1985) The precision of water content estimates in thermoluminescence

dating of loess from Northern Pakistan. *Nucl. Tracks.* Vol. **10,** Nos 4-6, 763-768.

Sanderson, D. C. W. (1987) Thermoluminescence dating of Scottish vitrified forts. Unpublished PhD thesis, Department of Physics, Paisley College of Technology.

Sanderson, D. C. W. (1988) Thick source beta counting (TSBC): a rapid method for measuring beta dose rates. *Nuclear Tracks and Radiation Measurements.* **Vol 14** Nos 1/2, 203-207.

Sanderson, D. C. W. and Clark, P. A. (1987) Recent progress in TL dating of Scottish ceramics and burned stones. (Abstract) Science and Archaeology, Glasgow 1987. *BAR* **196** (ii), 623.

Sanderson, D. C. W., Placido, F. and Tate, J. O. (1988) Scottish Vitrified Forts: TL Results from Six Study Sites. *Nuclear Tracks and Radiation Measurements* **Vol 14** Nos. 1/2, 307-316.

Sanderson, D. C. W., et al. (1989) in Long and short range limits in luminescence dating. Research Laboratory for Archaeology, Oxford, Occasional publication no. 9.

Schlesinger, M. (1965) *J. Phys. Chem. Solids* **26,** 761.

Shelkoplyas, V. N. (1971) In: *Chronology of the Glacial Age,* 155-6a.

Sutton, S. R. and Zimmerman, D. W. (1976) Thermoluminescent dating using zircon grains from archaeological ceramics. *Archaeometry* **18** (2), 125-134.

Sutton, S. R. and Zimmerman, D. W. (1979) The zircon natural method: initial results and low level TL measurement. *PACT* **3,** 465.

Srirath, S., and Fremlin, J. H. (1968) Non-uniformity in the thermoluminescence of

"Pot-boilers". In: *Thermoluminescence of Geological Materials. Ed.* D. J. Dougall, pp. 427-429. Academic Press, New York.

Templer, R. H,, (1985) The dating of zircons by auto-regenerated TL at low temperatures. *Nucl. Tracks.* Vol. **10**, Nos 4-6, 789-798.

Templer, R. H. and Walton, A. (1985) Zoning in zircons. *Nuclear Tracks and Radiation Measurements* **10** Nos 4-6, 683-692.

Tickel, F. G. (1965) Developments in Sedimentology 4: The Techniquess of Sedimentary Mineralogy. Elsevier Publishing Company.

Tite, M. S. (1966) Thermoluminescent dating of ancient ceramics: a reassessment. *Archaeometry* **9**, 155-169.

Tite, M. S. (1968) Some complicating factors in thermoluminescent dating and their implications. In: *Thermoluminescence of Geological Materials. Ed.* D. J. McDougall, pp. 389-405. Academic Press, New York.

Tite, M. S. and Waine, J. (1962) Thermoluminescent dating: a re-appraisal. *Archaeometry* **5**, 53-79.

Turner, R. C., Radley, J. M. and Mayneord, W. V. (1958) The alpha-ray activity of human tissues. *British Journal of Radiology* **31**, 397-402.

Tyler, A. N., (1992) personal communication.

Urbach, F. (1930) sitzber Akad Wiss Wein Math naturn K1, Abt. IIa **139**, 363.

Valladas, H. and Valladas, G. (1982) Effet de l'irradiation et sur des grains de quartz. *PACT* **6**, 171-178.

Ward, S. (1988) An investigation of thermoluminescence of glass discs of a potential

high dose dosimeter. B.Sc Honours Dissertation. SURRC/ Department of Physics, Strathclyde University.

Warren, S. E. (1978) Thermoluminescence dating pottery: an assessment of the dose rate from rubidium. *Archaeometry* **20** (1), 71-72.

Wintle, A. G. (1973) Anomalous fading of thermoluminescence in mineral samples. *Nature* **245,** 143-144.

Wintle, A. G. (1980) Thermoluminescence dating: a review of recent applications to non-pottery materials. *Archaeometry* **22** (2), 113-122.

Wintle, A. G. and Huntley, D. J. (1979) Thermoluminescence dating of a deep sea sediment core. *Nature* **279,** 710-712.

Zimmerman, D. W. (1967) Thermoluminescence from fine grains from ancient pottery. *Archaeometry* **10,** 26-28.

Zimmerman, D. W. (1971) Thermoluminescent dating using fine grains from pottery. *Archaeometry* **13,** 29-52.

Zimmerman, D. W. (1971) Uranium distributions in archaeological ceramics: dating of radioactive inclusions. *Science* **174,** 818.

Zimmerman, D. W. (1972) Relative thermoluminescence effects of alpha- and beta-radiation. *Radiation Effects* **Vol 14,** 81-92.